ELECTRONICS FOR CRYOGENIC DETECTORS

Gianluigi Pessina
INFN di Milano-Bicocca
Università di Milano-Bicocca

pesina@mib.infn.it, https://pessina.mib.infn.it

ABSTRACT

Cryogenic detectors and their sensors span a wide range of characteristics. For most of them an overview of front-end readouts is provided.

PREAMBLE

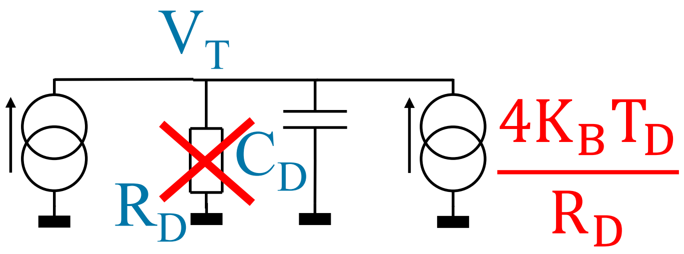

When T_D is room temperature thermal noise put always a limit, unless $R_D=\infty$: room temperature operated detectors shows almost all the time a capacitance impedance.

The detector temperature T_D of 10 mK is 30000 lower than that of 300 K: thermal noise is much less dominant and, as a result, great flexibility in choice is available.

DEEP CRYOGENIC DETECTORS

Operating temperatures below 100 mK or so are considered the range of calorimetric detectors. Almost always the pattern is as follows:

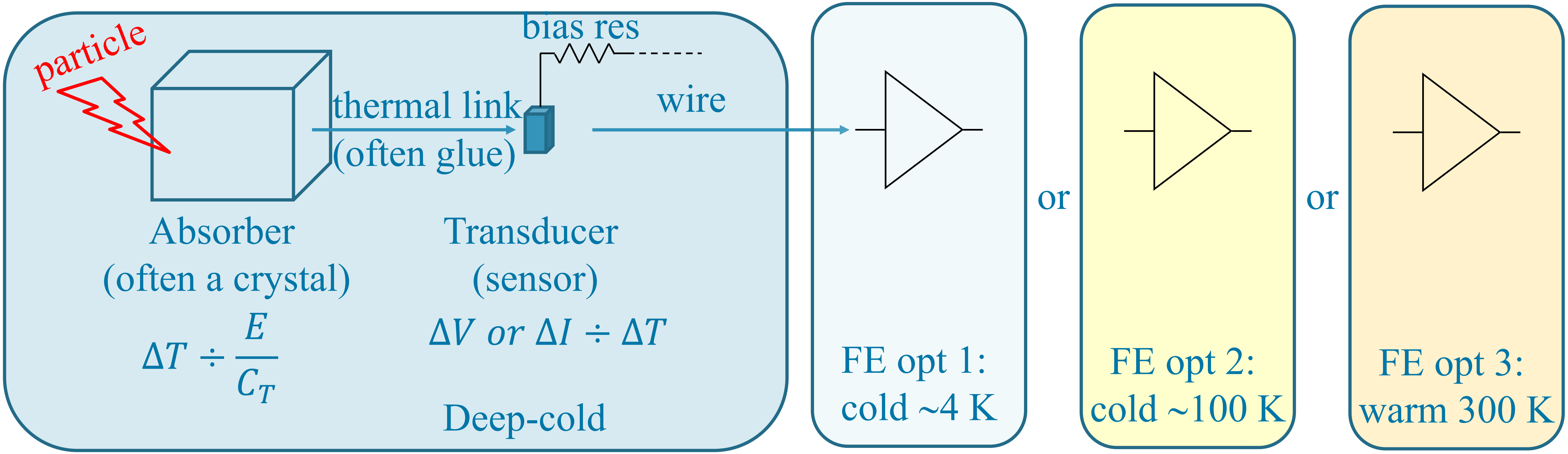

<u>REMEMBER</u>: Since the operating temperature is below 0.1 K the environment is a Dilution Refrigerator, wet (based on LHe) or dry (based on pulse tubes).

Deep cryogenic detectors 2

The reason why the detectors are pure calorimeters is easily understandable if one considers that at 0.1 K, for example, the average thermal energy of a phonon, $K_B T$, is less than 10 μeV!

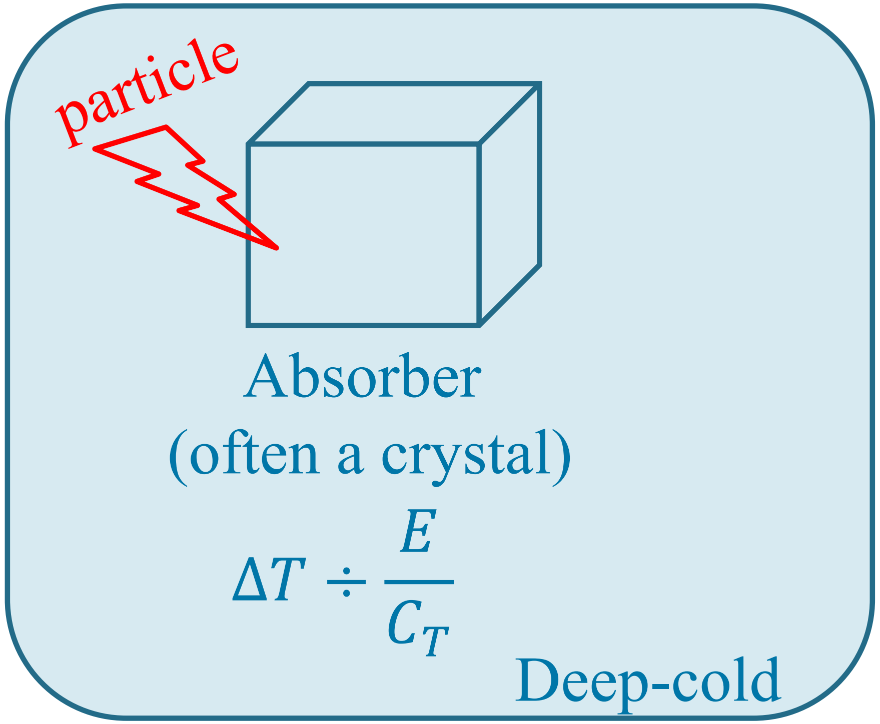

The impinging particle generates phonons (*) and the energy fluctuation should be:

$$\sigma = \sqrt{E_{particle}\, K_B T}$$

Thus, for a particle energy of 1 KeV we expect σ=0.1 eV_{RMS}.

The fluctuation in the crystal's energy content is larger. For example, a medium-sized crystal with a heat capacity of 100 pJ/K has a fluctuation of:

$$\sigma = \sqrt{C_T T K_B T} \approx 25\ eV_{RMS}$$

Much lower fluctuations are obtained at lower temperatures, 10 mK or so.

(*) prompt athermal, prompt, phonons that degrade in thermal phonons.

Deep cryogenic detectors 3

The signal generation mechanism inside the absorber is thermal, and the speed of sound is the limiting factor. We expect that the greater the mass of the absorber (larger volume), the slower the thermalization process.

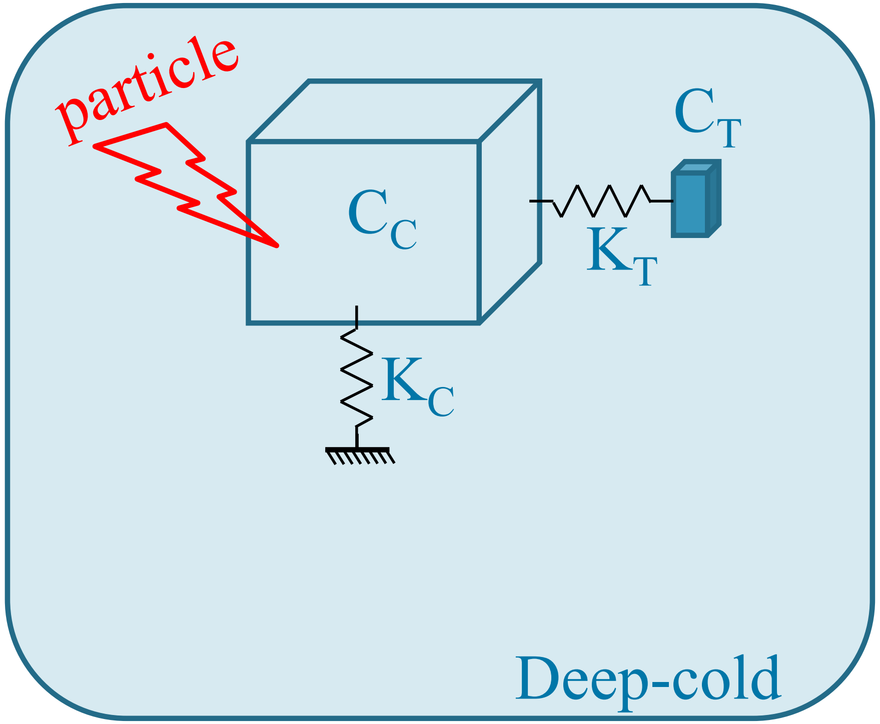

Another factor affecting speed are the thermal time constants derived from the heat capacity of the absorber and its thermal conductance to the heat sink and the heat capacity of the sensor and the thermal link between it and the absorber.

We must remember that thermal conductances vanish at deep temperatures such as T^3 in (diamagnetic) dielectrics and superconductors below the critical temperature and T in metals.

Deep cryogenic detectors 4

We have seen that the energy fluctuation of the absorber is negligible. The transducer introduces a first limitation. The choice for the transducer depends on the shape of the absorber, the temperature, the thermal contact that can be adopted and the signal range.

The bias impedance of the sensor, with its noise, can affect performance in different situations.

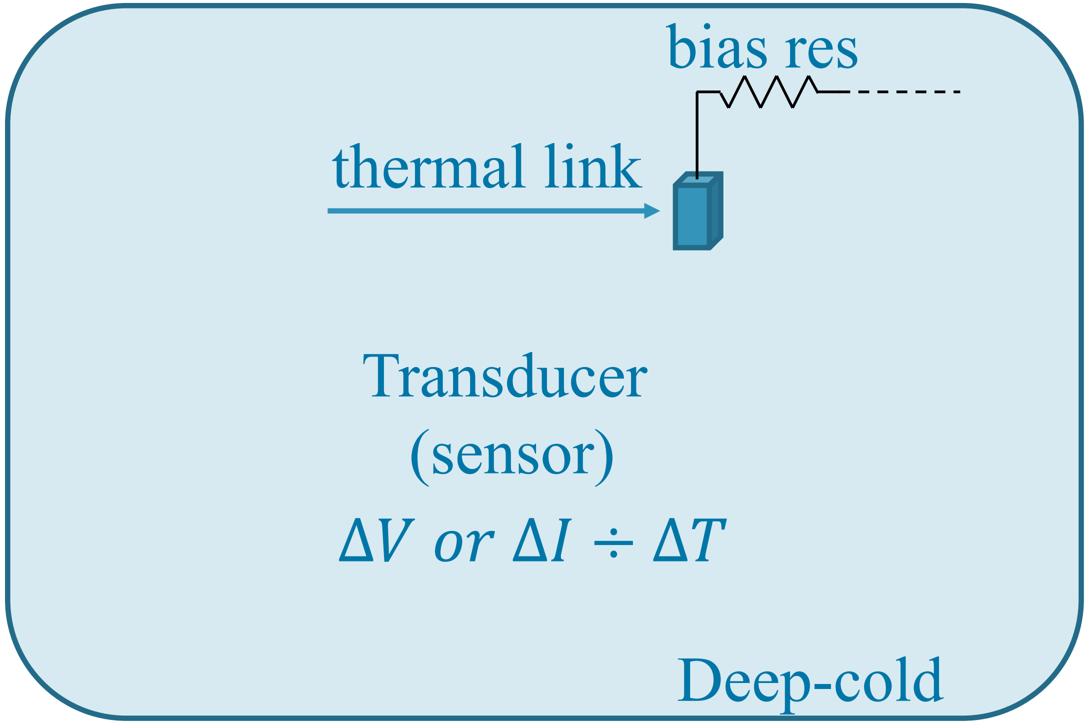

Some sensors types:

Very low impedance:
- Transition Edge Sensor, TES, (need SQUID);
- Metallic Magnetic Calorimeters, MMC (need SQUID);
- Microwave Kinetic Inductance Detector, MKID;

Medium impedance:
- Metallic thermistors.

High impedance:
- Semiconductor Thermistors;

The front-end is the second limiting factor for resolution.
As can be seen, there is flexibility on the location of the front-end. The criteria for choosing it depend on various application constraints…

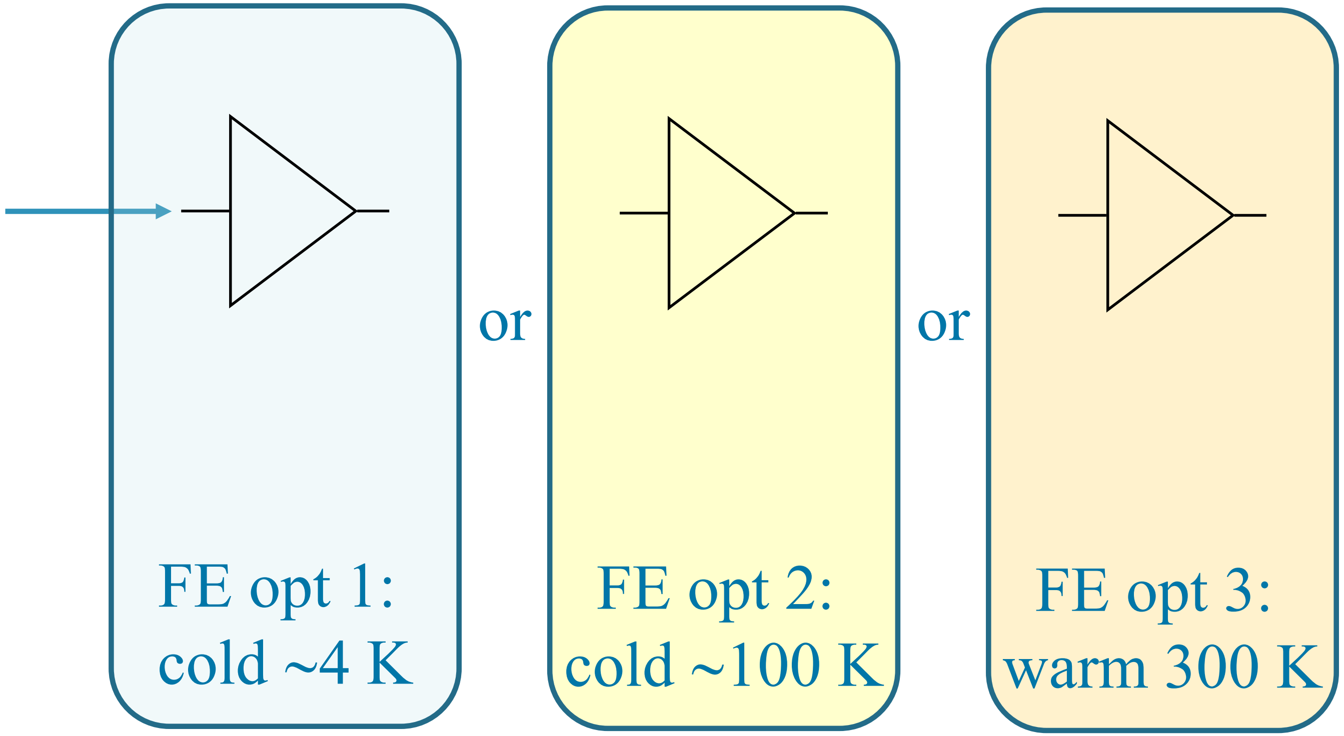

Deep cryogenic detectors 6

The topology and location of the very front-end can be based on:

- ✓ Sensor impedance;
- ✓ Signal bandwidth;
- ✓ Number of channels;
- ✓ Power budget
- ✓ Rate of events;
- ✓ Background contribution of material near the detector;
- ✓ …

Let's remember the noise sources of our preamplifier:

$$\boxed{\overline{e_A^2} = \overline{e_{White}^2} + \frac{A_f}{f}}$$

$$\boxed{\overline{i_A^2} = 2qI + \frac{I_f}{f}}$$

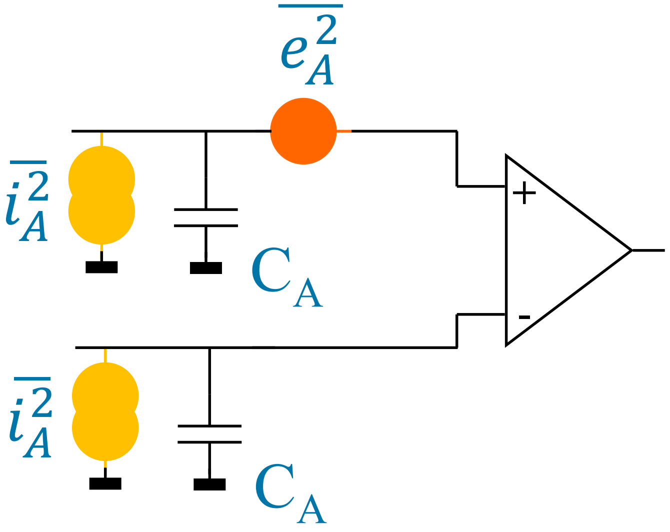

Very often the preamplifier is differential voltage input (helps in cross talk mitigation in arrays).

Low frequency noise, $\frac{A_f}{f}$, is never neglected.

It should not be forgotten that an important source of not negligible noise is the Dilution Refrigerator, wet or dry. This happens at least in cases where the signal bandwidth includes the range of mechanical vibrations.

wet-DR

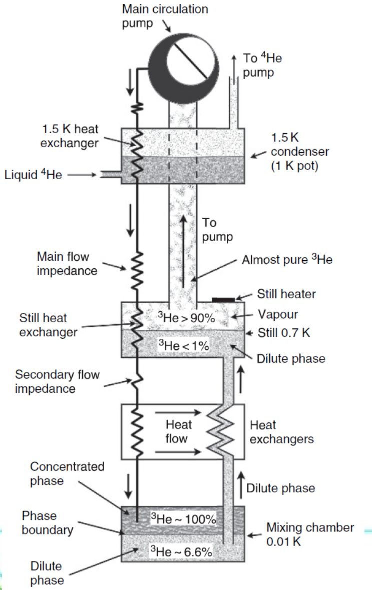

Fig. 6.5. Scheme of a 'classic' dilution refrigerator.

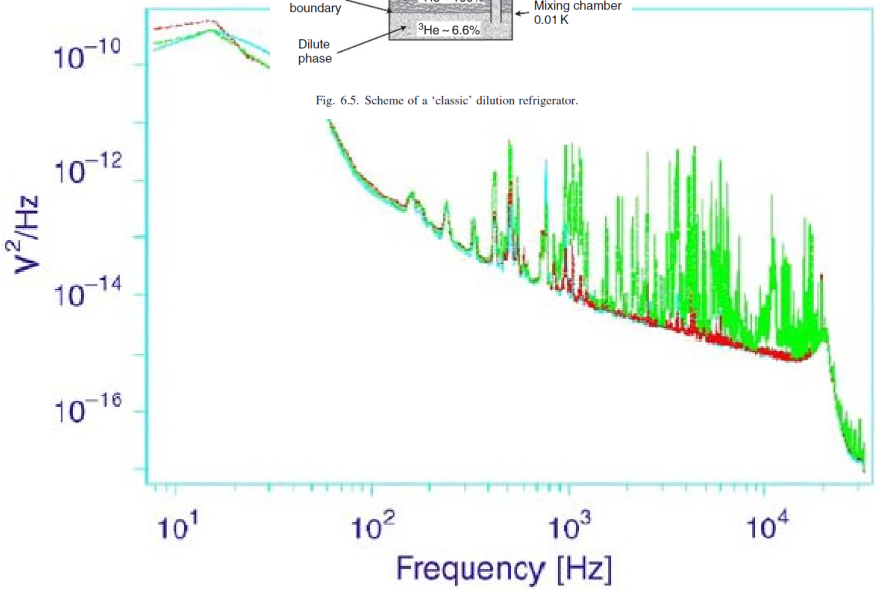

dry-DR

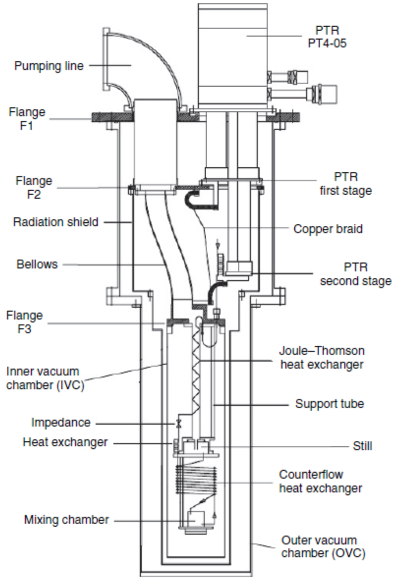

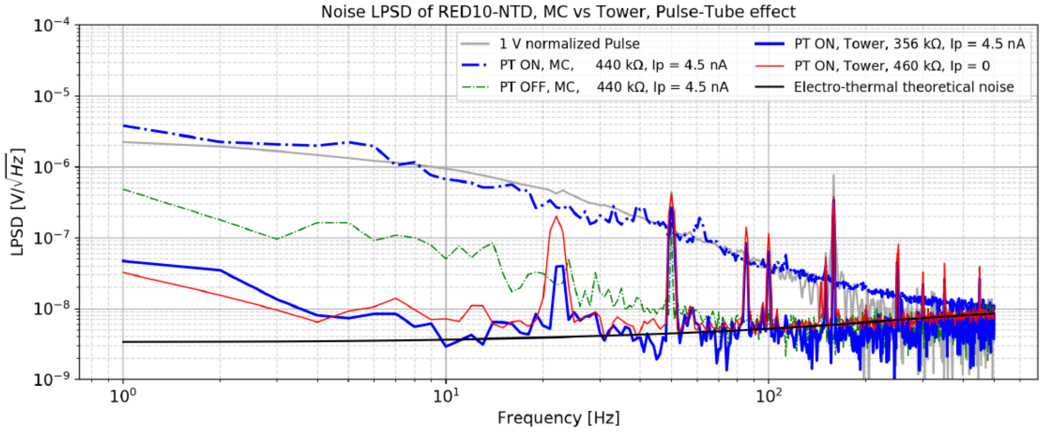

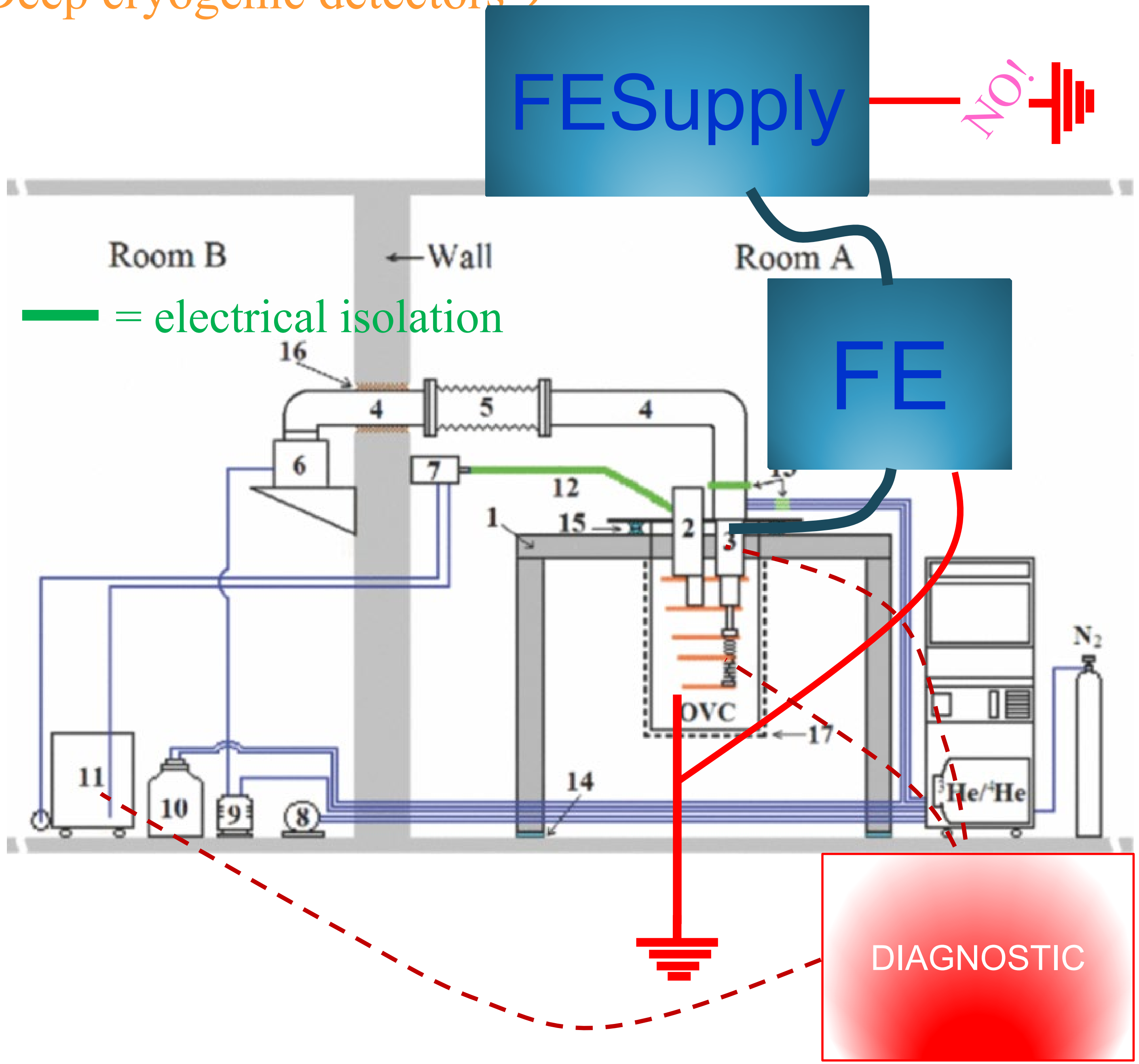

Finally, ground loops and EMI are another possible source of non-negligible noise.

Electrical connections embrace the frontend, the pumping system, and the diagnostics of the system.

The best condition is to isolate the pumping system from the refrigerator, taking care of the diagnostics.

The metal magnetic calorimeter, MMC, is a sensor employed with so-called μ-calorimeters, very small mass absorbers (often much less than a gram).

Metallic Magnetic Calorimeters, MMC

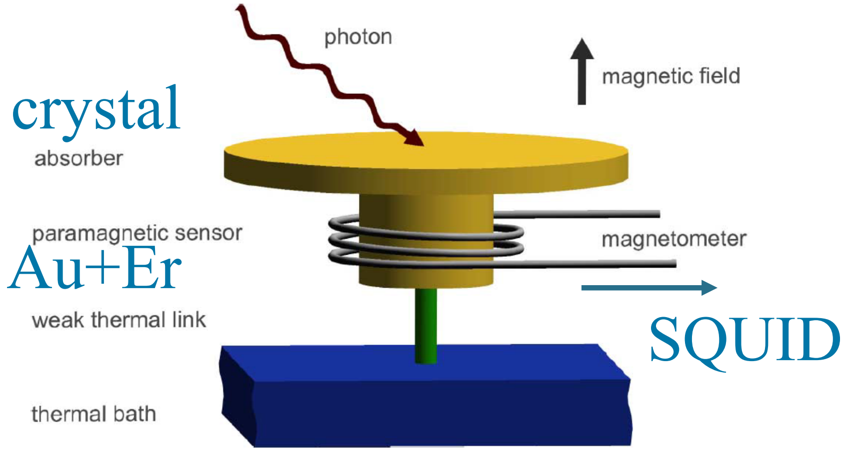

Fig. 1. Principle drawing of an MMC. The paramagnetic sensor is placed in a weak external magnetic field. The absorption of a particle increases the temperature and thus decreases the magnetization of the sensor. This change is read out by a low-noise high-bandwidth SQUID magnetometer.

The particle creates an increase in the temperature of the absorber and, consequently, of the paramagnetic sensor to which is glued.

The temperature change causes a change in the magnetic property of the paramagnetic sensor.

The detector is placed in a magnetic field that changes within the paramagnetic sensor as the temperature changes.

The pick-up coil reads the signal.

➡ *The impedance of the pick-up coil is very small, and the signal is also small due to the small bias. The S/N ratio is high, but signal pre-amplification is required through the use of a SQUID (see later).*

Deep cryogenic low impedance sensors 2

The Transition Edge Sensor, TES, is based on a very simple principle: a small sheet of superconducting metal (0 Ω) held at the edge of the superconducting-to-metal transition.

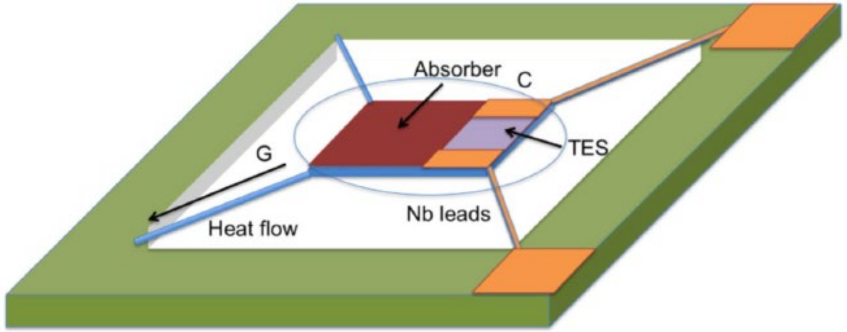

Again, the TES sensor is glued or synthetized on an absorber.

The TES is biased above the transition region where it achieves its maximum gain.

Resistance and the signal are very very small.

http://web.mit.edu/figueroagroup/ucal/ucal_tes/index.html

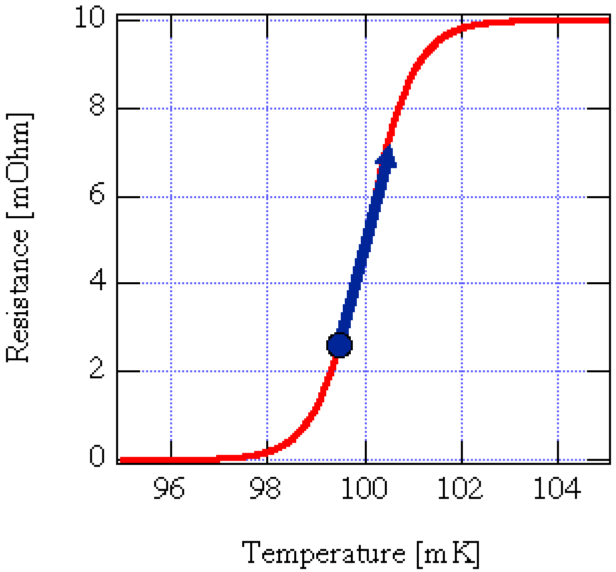

Note that when using a TES the temperature of operation must be set at that of the TES transition region.

The S/N ratio is high, but a pre-amplification of the signals is needed through the use of a SQUID (see later).

SQUID is for Superconducting Quantum Interference Device.

There are 2 types of SQUID:

dc-SQUID
rf-SQUID.

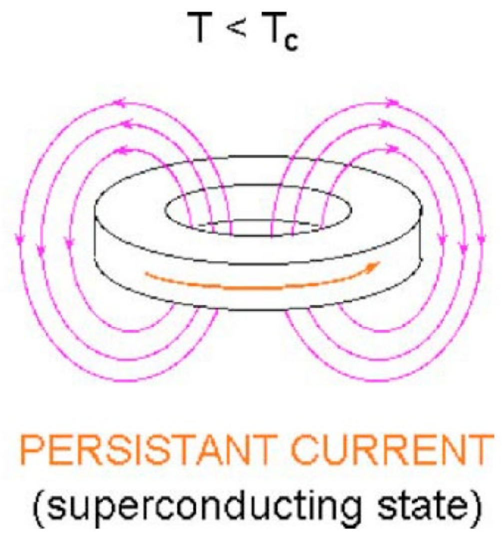

Suppose to consider a small superconductor ring held below its critical temperature T_C, the transition temperature between conductor and superconductor states.

In the superconducting state its resistance is zero, and each time a magnetic flux acts on it a current begins to circulate indefinitely and is added to all previous ones: there is no dissipation.

The flux is stored permanently.

The squid sensor 2

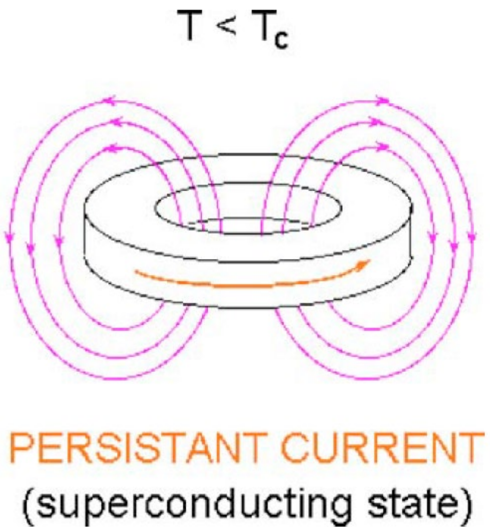

We are in a quantum flux regime.

It happens that every time a flux intercepts the coil it adds to the previous ones. It works as if in a charge-sensitive preamplifier the presence of the feedback resistor is omitted in parallel with the feedback capacitance, the output signals add up until the output is saturated.

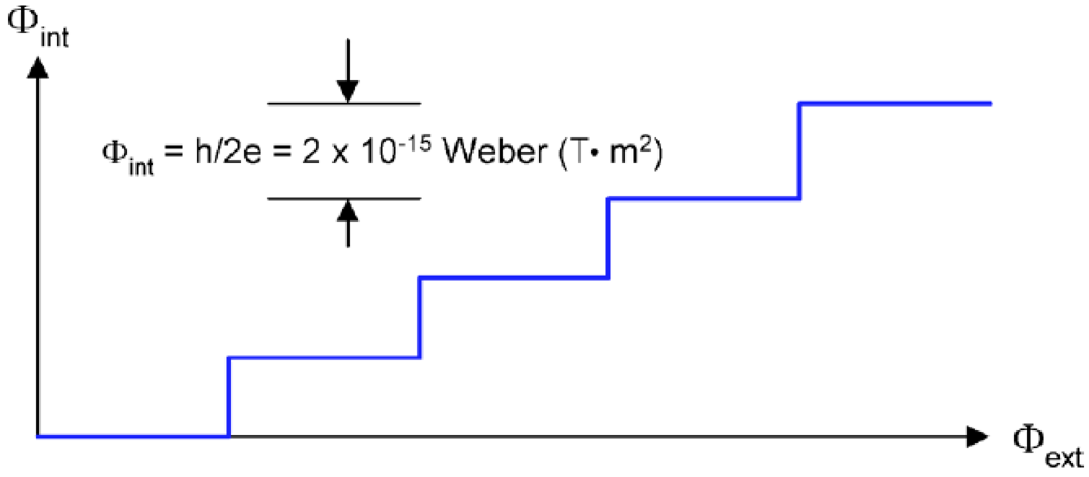

FIG. 3. (Color online) Flux quantization.

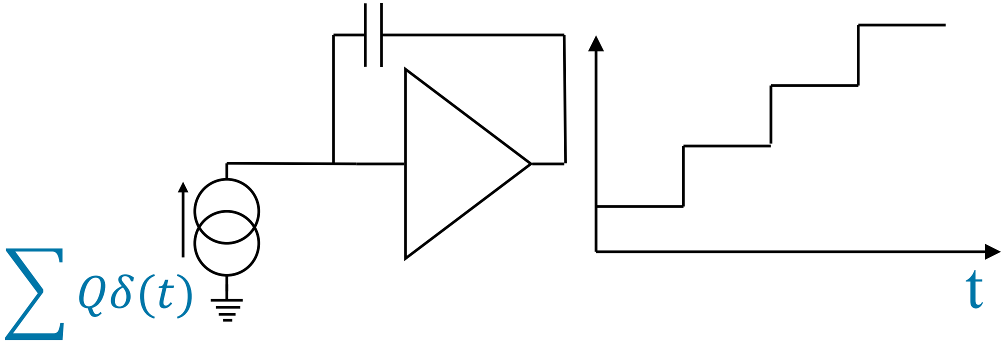

The squid sensor 3

By adding a feedback resistor to the charge-sensitive preamplifier, the accumulated charge on the feedback capacitance is discharged, once measured.

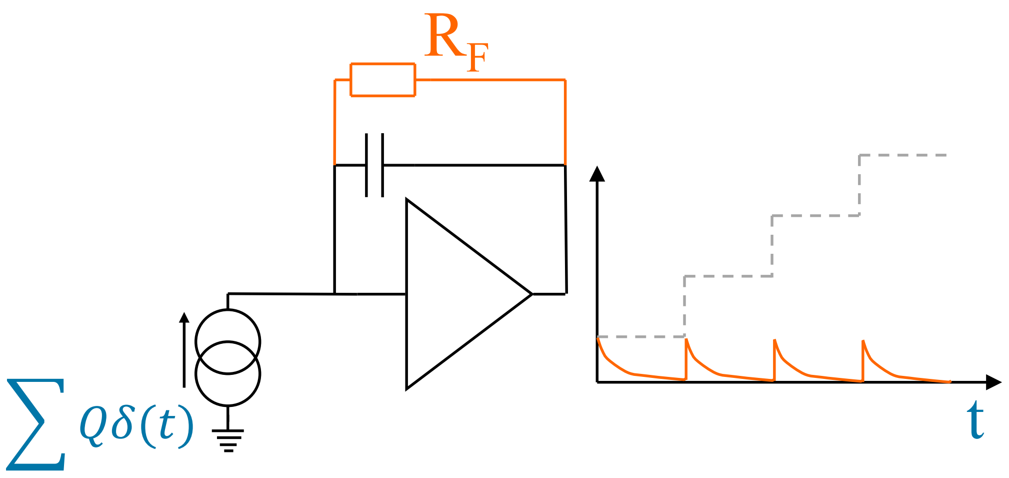

This similar concept is considered in the superconductor coil with the introduction of so-called weak links:

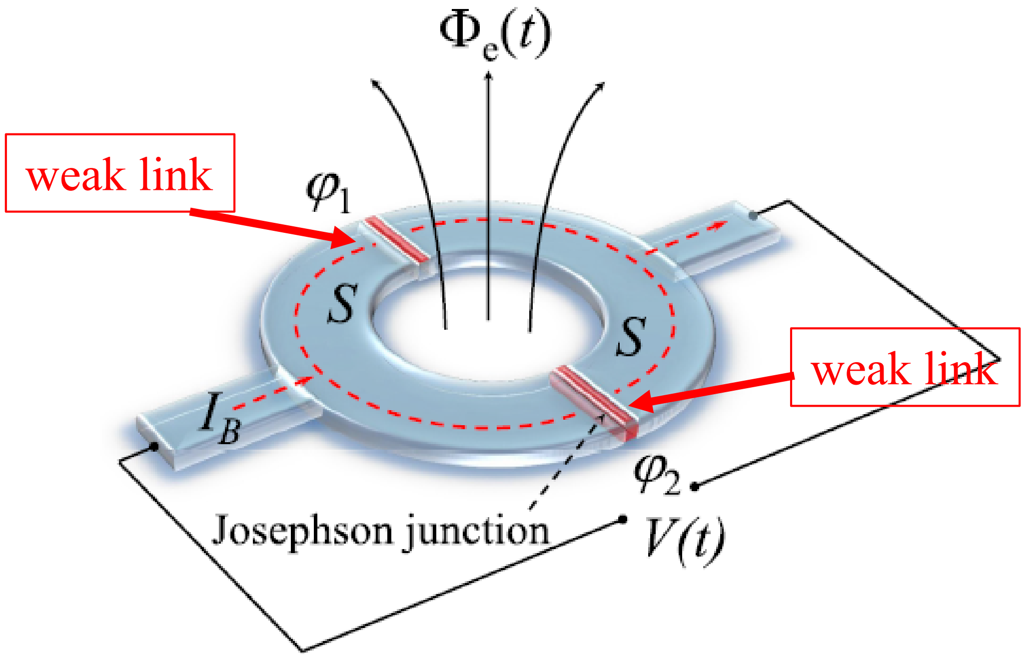

Weak links are usually made with insulating materials, creating what is called an SIS (Superconductor-Isolation-Superconductor) junction.

If the thickness of the weak links were large, no current could pass, and the voltage across the junction would be large if an I_B bias current were forced. In this case we say that the critical I_C current beyond which the supercurrent is destroyed is zero: you cannot have any supercurrent.

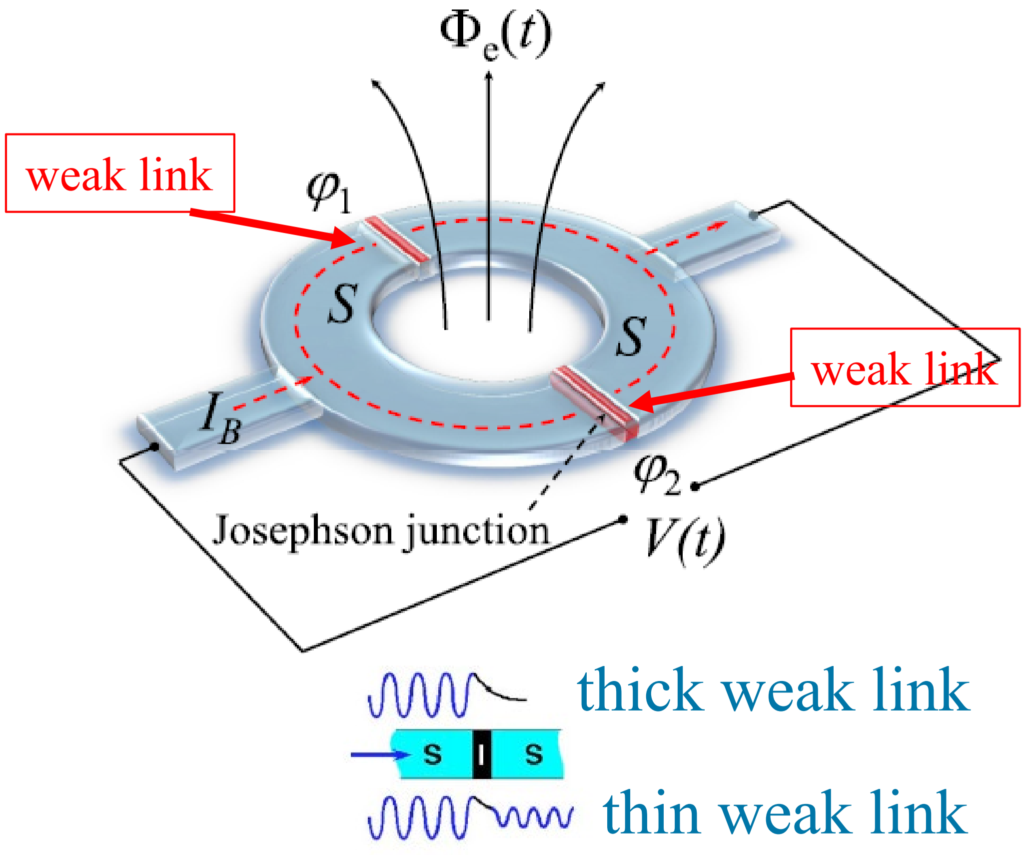

If the weak links are very thin, or thin enough, and this is usually the case with a thickness of about 100 nm, supercurrent is present up to an upper limit I_C, which, this time, is different from 0.

What happens is that the impedance of the weak links starts to dissipate around and above I_C.

The weak links are called Josephosn junctions and this is the dc-SQUID.

The dc-SQUID sensor 2

If the bias current I_B is within $(-I_C, I_C)$ the voltage across the junction is 0 whatever is the applied flux (the coil is in superconduditon state).

If I_B is close to I_C than a flux intersecting the junction is able to develop a voltage.

Due to quantum reason the voltage is periodic, with period h/2e, with respect to the input flux.

The sensitivity that can be obtained is very high, a very small fraction of h/2e.

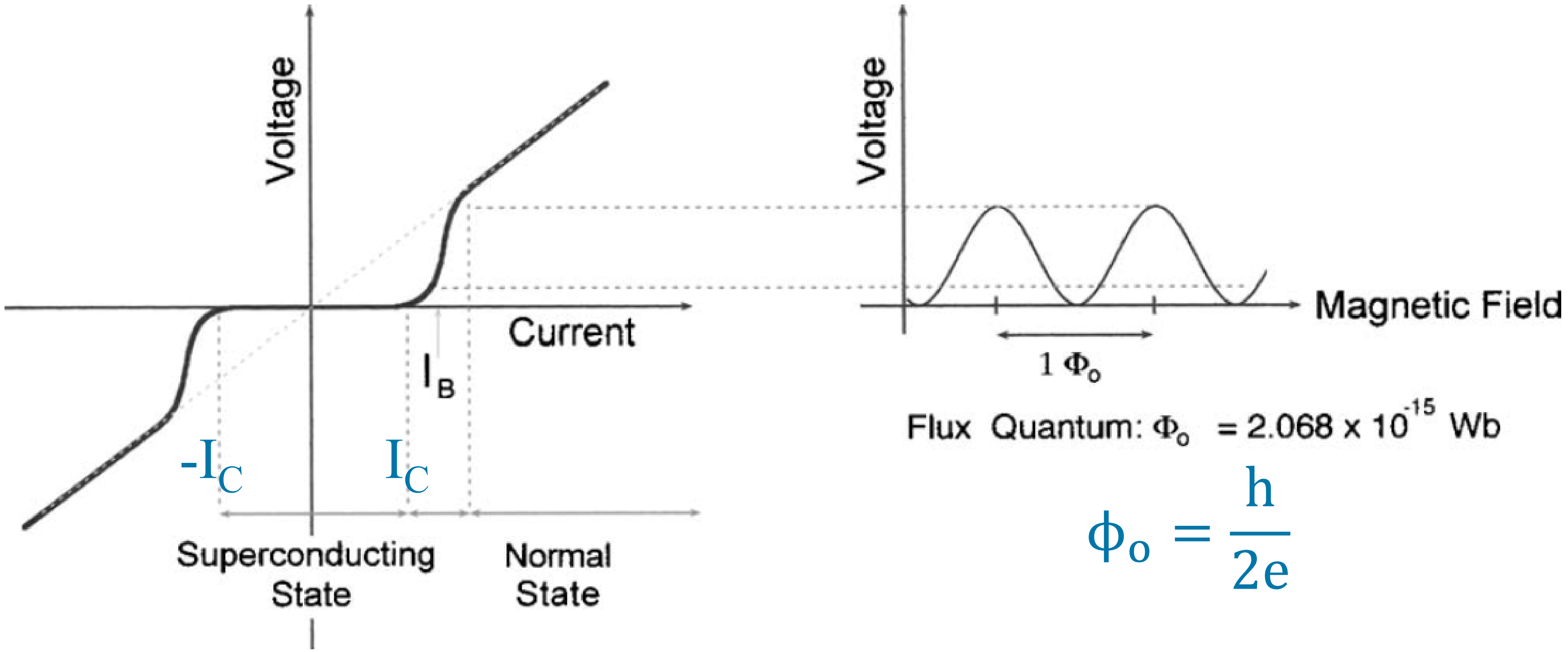

$$\phi_o = \frac{h}{2e}$$

When operating a dc-SQUID 3 steps must be taken: the first, as we have already seen, is to set the bias current I_B; the second is to lock the phase namely, to add a flux in order to set the phase at a good position (see later for this) and, third, is to linearize the response (see later also for this).

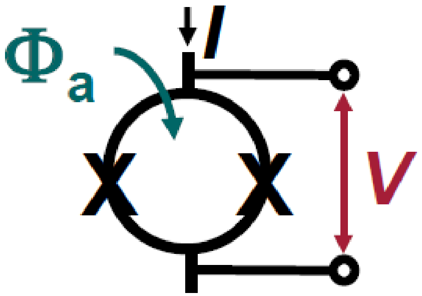

Step 1

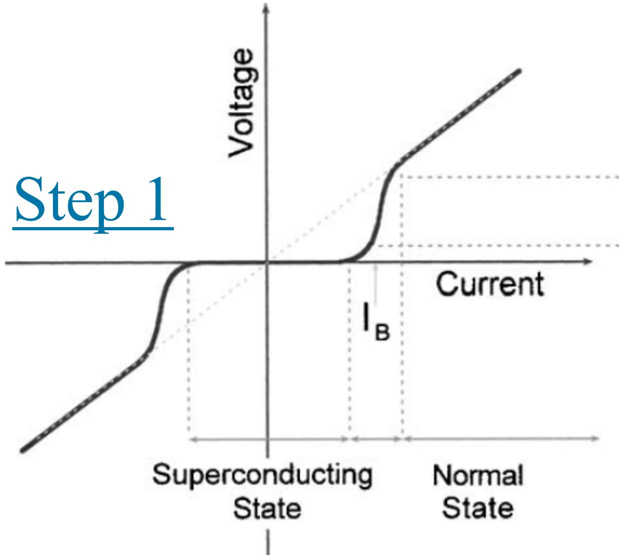

voltage vs applied flux $V(\Phi_a)$
(at I_B = const)

Step 2

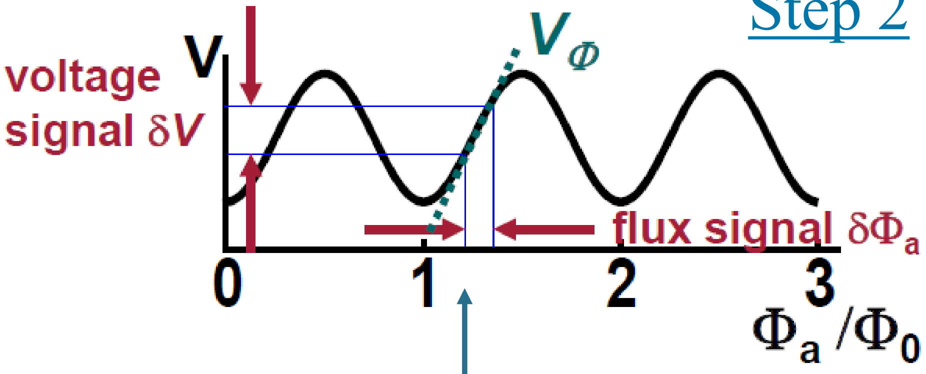

flux lock

https://nanocohybri.eu/wp-content/uploads/2019/01/Koelle_2.pdf

The way the SQUID senses the signal generated in the sensor, TES or MMC: a quantistic transformer.

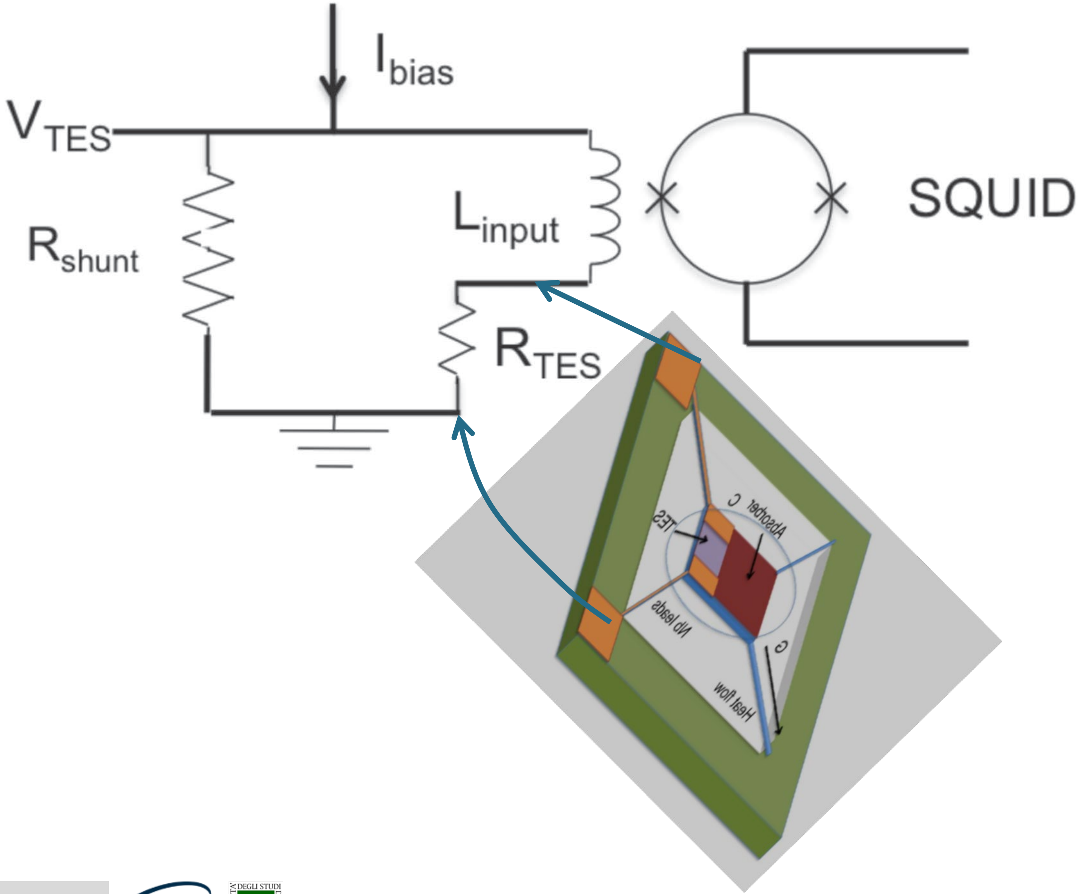

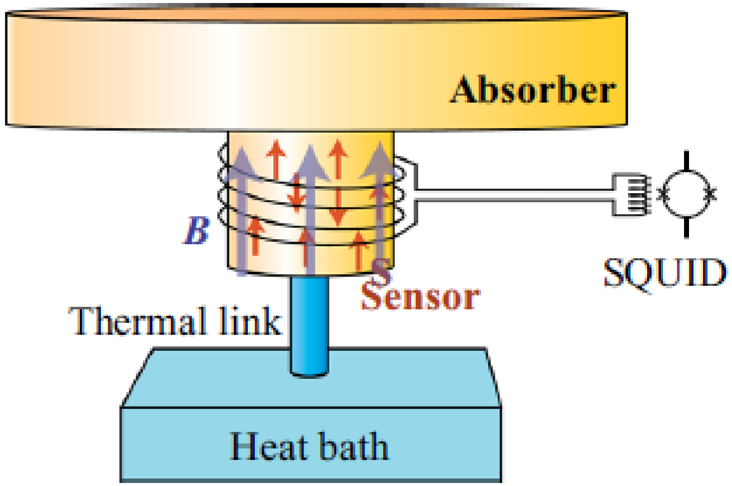

The dc-SQUID sensor 5

Let's get back to the dc-SQUID.

Step 1: the I_B bias current;

Step 2: phase locking.

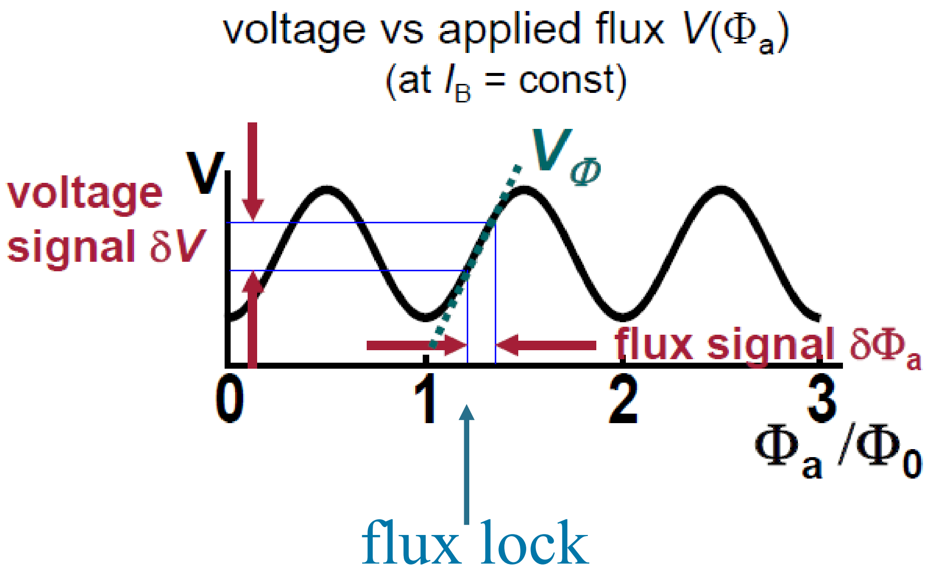

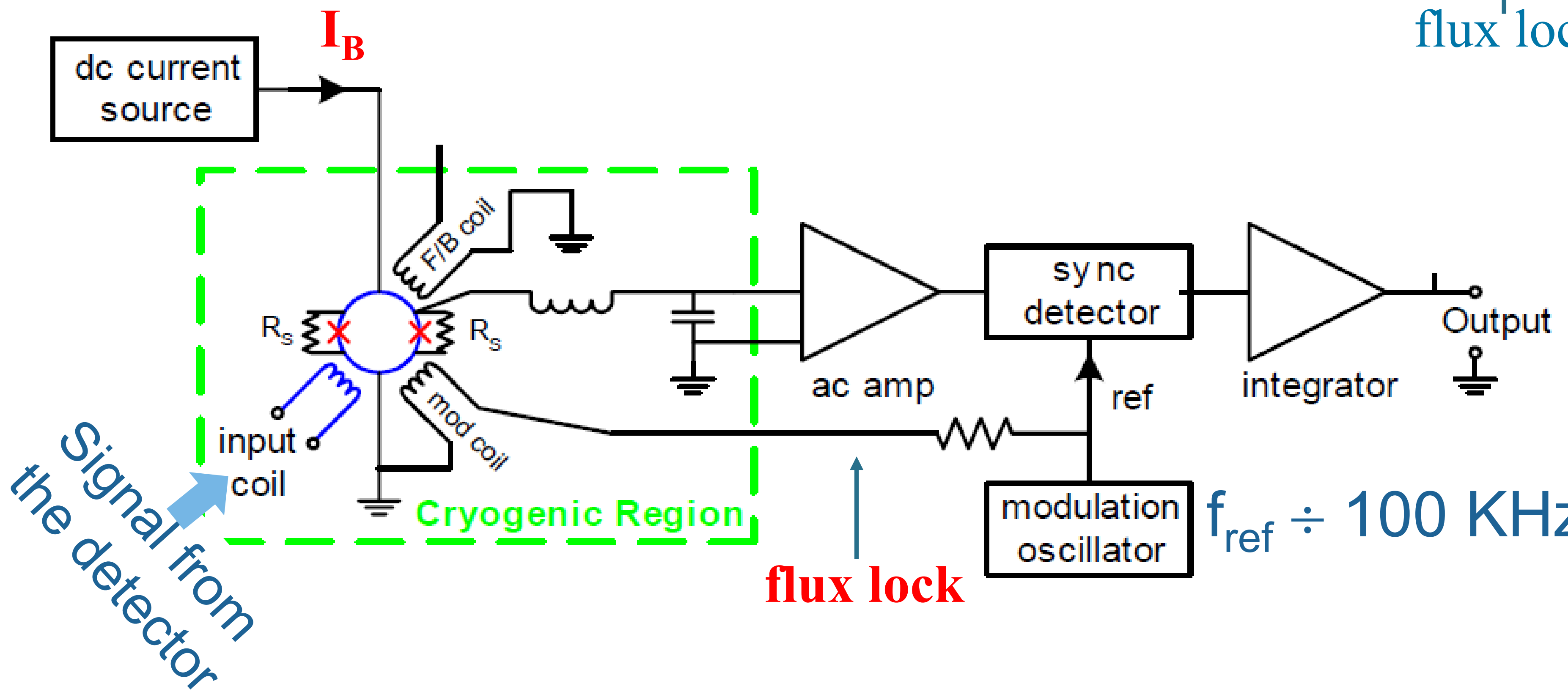

f_{ref} ÷ 100 KHz, few MHz

Now…

Step 3: Response linearization: a feedback coil is added through which the input signal into the SQUID is subtracted so as to keep the voltage excursion of the SQUID negligible.

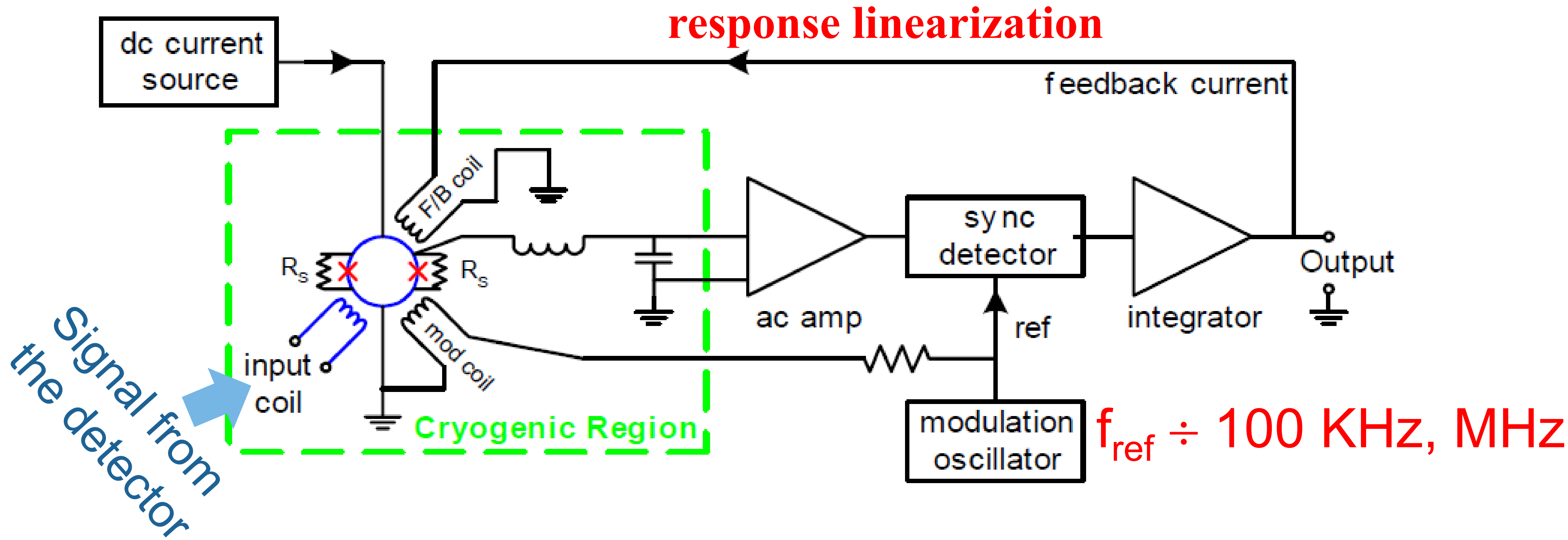

This technique is called **FLL, Flux Locked Loop**.

The dc-SQUID sensor 7

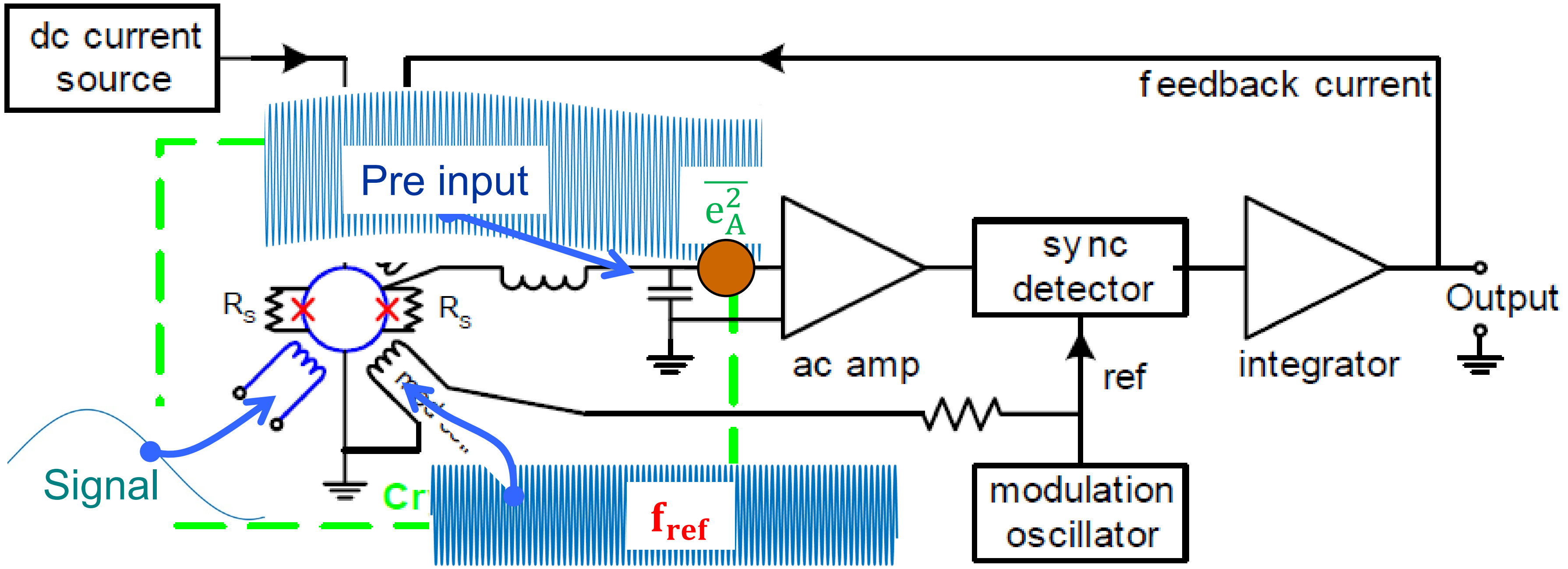

Modulation has another advantage: the reference modulation frequency is >> that of the detector signal, and the resulting preamplifier input is a modulation of the reference frequency.

The dc-SQUID sensor 8

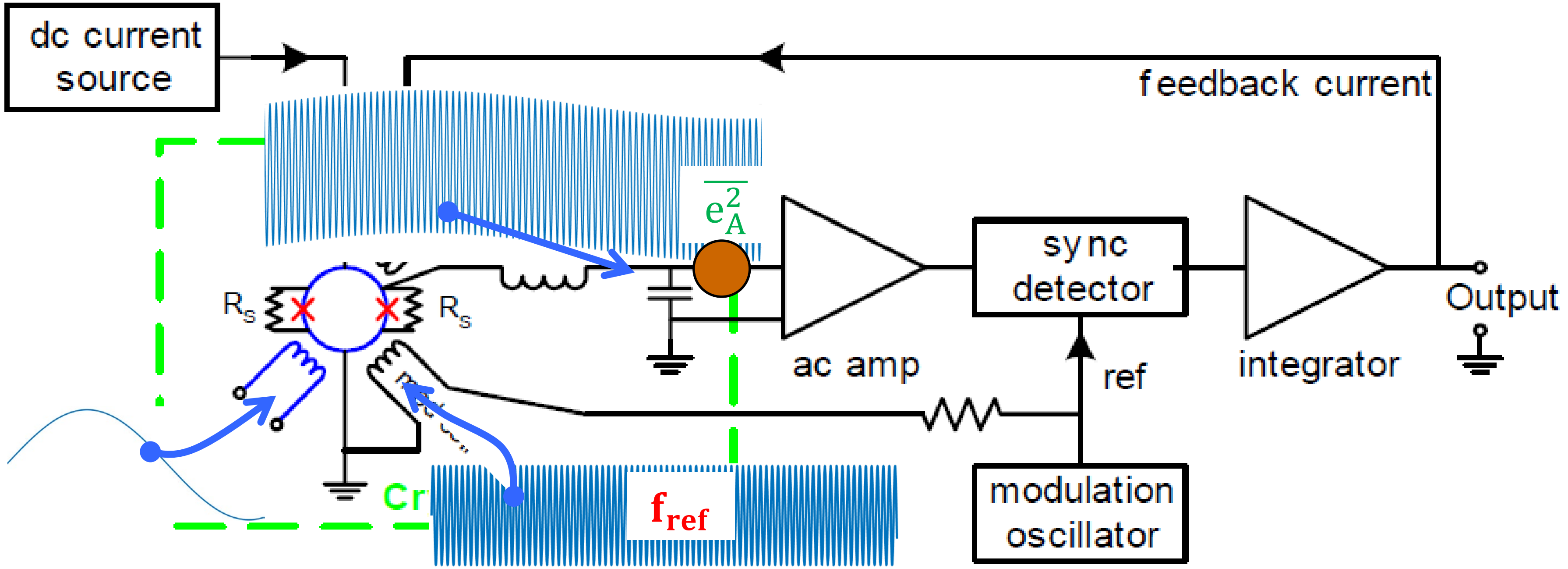

Preamplifier series noise is not modulated (shifted) and its contribution is that around f_{ref}: therefore, its low-frequency component, if present, is swept away:

PREAMBLE

TESs, MMCs and MKIDs, as well as SQUIDs, are all very low impedance devices.

The front-end noise source that must be kept small is the series noise. Parallel noise is less important:

$$\boxed{\overline{e_A^2} = \overline{e_{White}^2} + \frac{A_f}{f}}$$

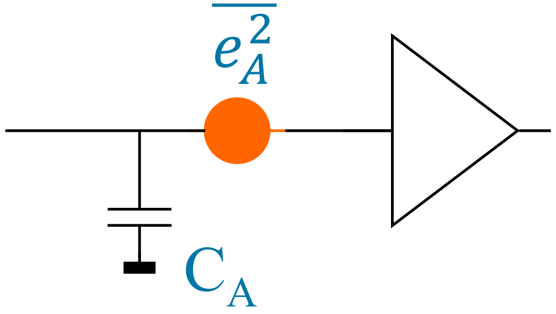

This class of sensors is generally coupled with small absorbing crystals. The signal bandwidth is relatively fast, up to 50 to 100 KHz as the maximum value.

DC-SQUID FRONTEND

The frequency at which the FLL operates is relatively small, from hundreds of KHz to a few MHz, and the of the front-end series noise is the more important: a front-end operating at room temperature is adopted as standard.

Front-end series noise is less than nV/√Hz and ranges from 0.1 nV/√Hz to 1 nV/√Hz. The parallel noise varies from negligible values, for the JFET input stage, to a few pA/√Hz, for the bipolar input stage, but is negligible because the impedance of the dc-SQUID is very small, ∝ Ω. Take care about the series impedance of the connecting wires to room temperature for both its thermal noise and voltage noise developed from the parallel noise.

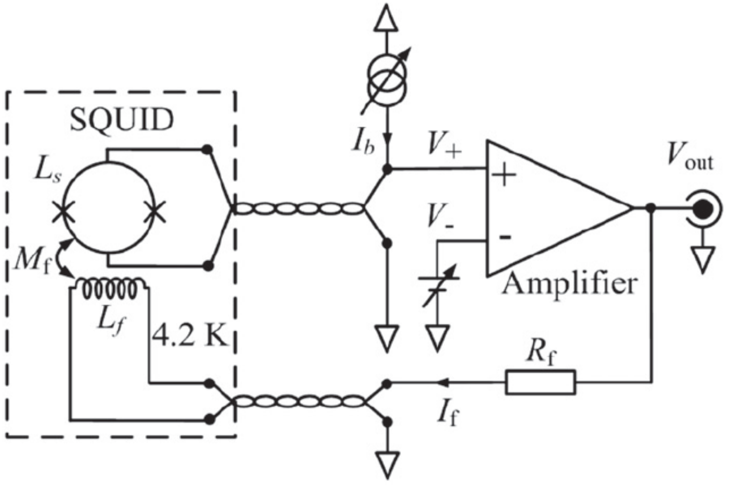

Figure 1. Equivalent circuit of SCRE with a current biased SQUID. The AD797 operational amplifier is employed in our case.

dc-squid frontend 2

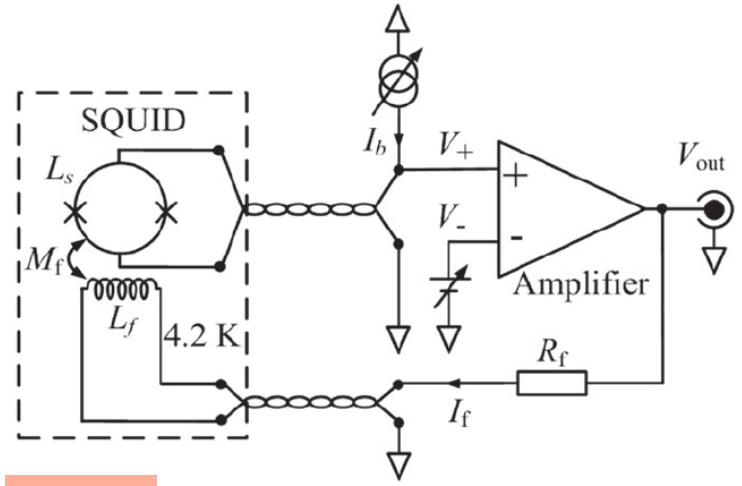

Figure 1. Equivalent circuit of SCRE with a current biased SQUID. The AD797 operational amplifier is employed in our case.

This is a simple solution, based on the use of a single well-known operational amplifier: the AD797 (*bipolar input*), which has a nominal value of 0.9 nV/√Hz and 2 pA/√Hz (above 1 KHz).

The authors state a transfer coefficient $\partial V/\partial \Phi_O$ of about 380 $\mu V/\Phi_O$, which translates into a contribution to preamplifier noise of less than 3 $\mu\Phi_O/\sqrt{Hz}$ (intrinsic squid noise should be a fraction of $\mu\Phi_O/\sqrt{Hz}$, $\Phi_O = h/(2e) \approx 2.07\times10^{-15}$ Vs, the quantum of magnetic flux).

dc-squid frontend 3

CRESST studies dark matter with an array of large-mass $CaWO_4$ (calcium tungsten oxide) scintillating crystals detected by TES.

The runs of CRESST are very long and the stability requirement is very stringent.

To keep the energy conversion gain constant, each detector in the array is equipped with a heater to which compensation power and periodic pulses are sent.

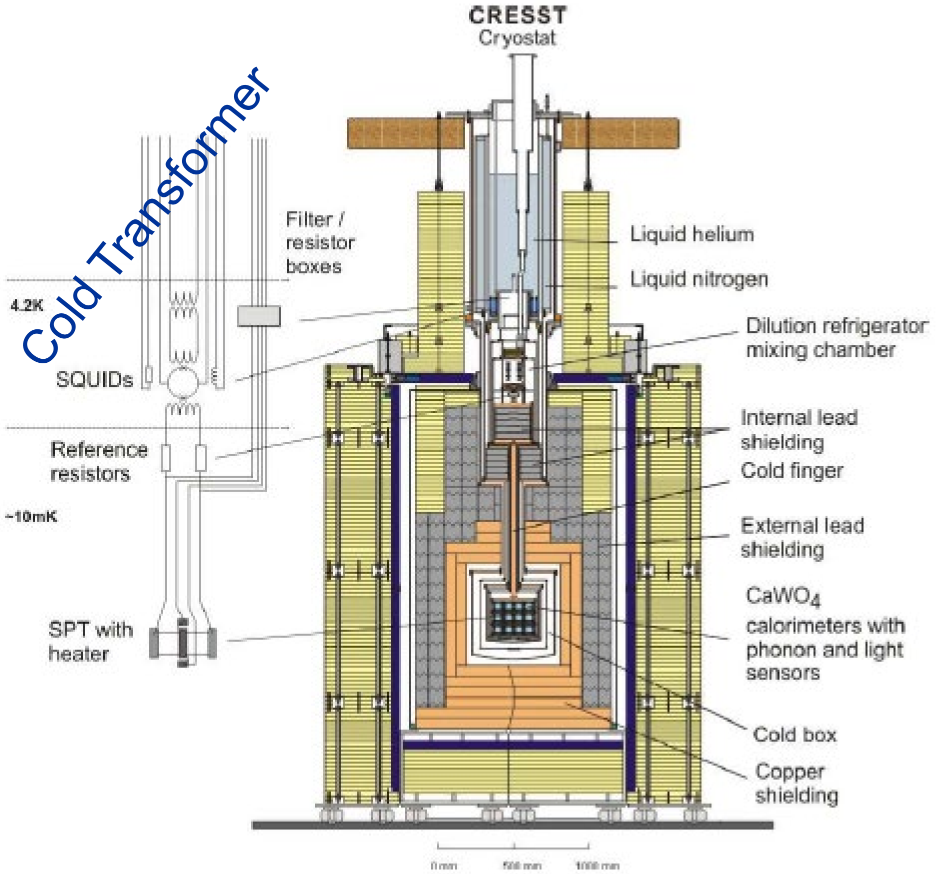

Kindly from Franz Pröbst

The reading is with DC squid + cold transformer (8:1) + room-T transformer (3:1) + room-T amplifier (JFET input, 2SK147, with a noise floor of 0.7 nV/√Hz).

A current noise close to that of the junction, 1.2 pA/√Hz, is claimed due to the large suppression of the amplifier noise resulting from the use of the 2 transformers in front of it.

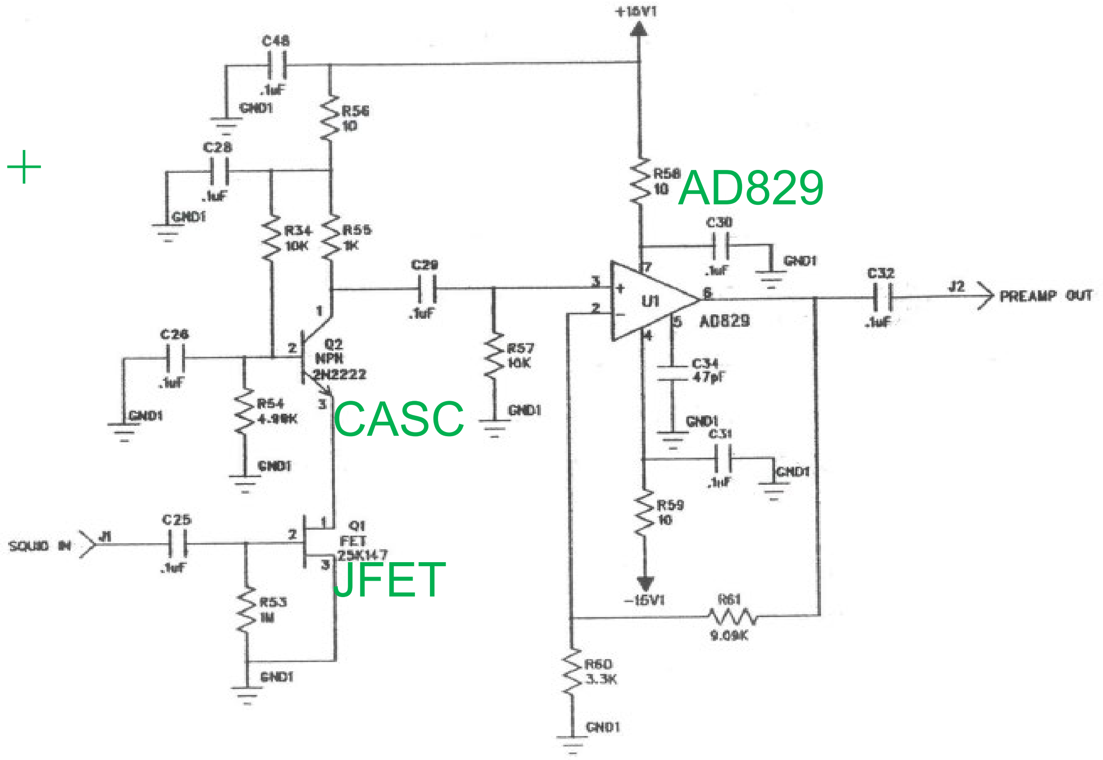

Kindly from Franz Pröbst

dc-squid frontend 5

SuperCDMS also studied dark matter, again TES for the phonon channel.

The reading is taken with a dc-squid array: a series of 100 dc-squids to mitigate the contribution of preamplifier noise. An amplifier at room temperature reads the array.

They claim a current noise close to about 10 pA/√Hz, with 1.2 nV /√Hz as the preamplifier's series noise.

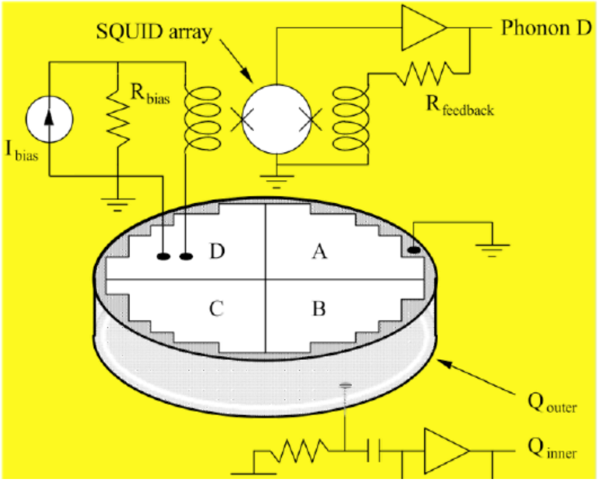

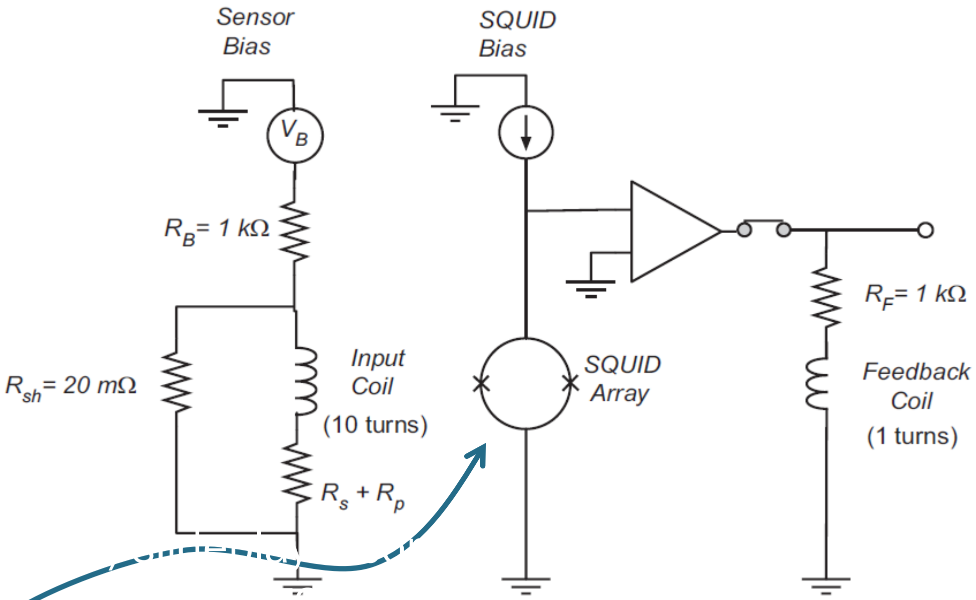

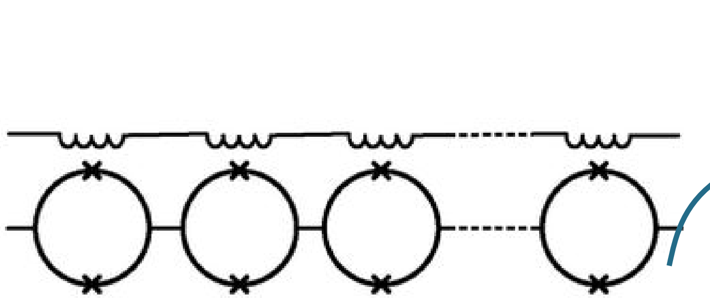

https://slideplayer.com/slide/12077675/

Here are other examples of amplifiers operating at room temperature: one with bipolar input (0,35 nV/√Hz)...

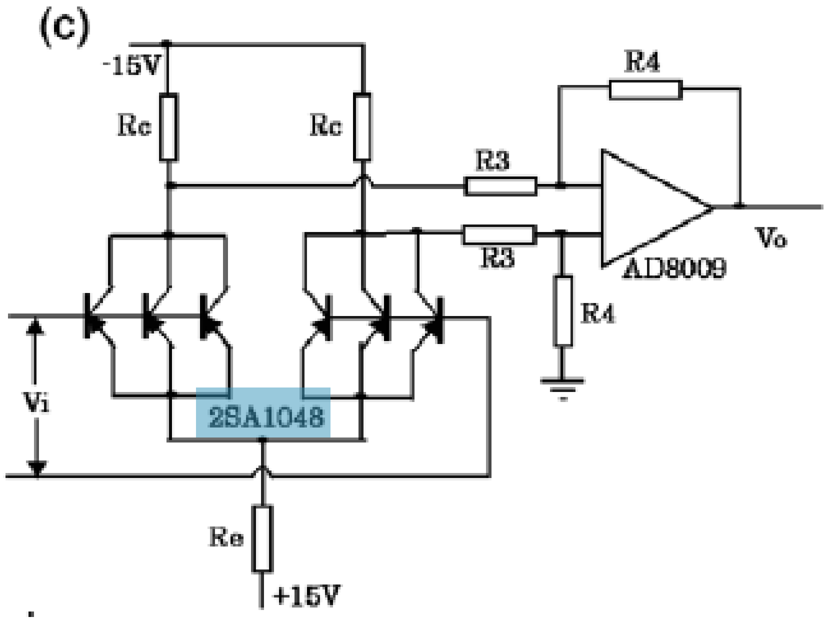

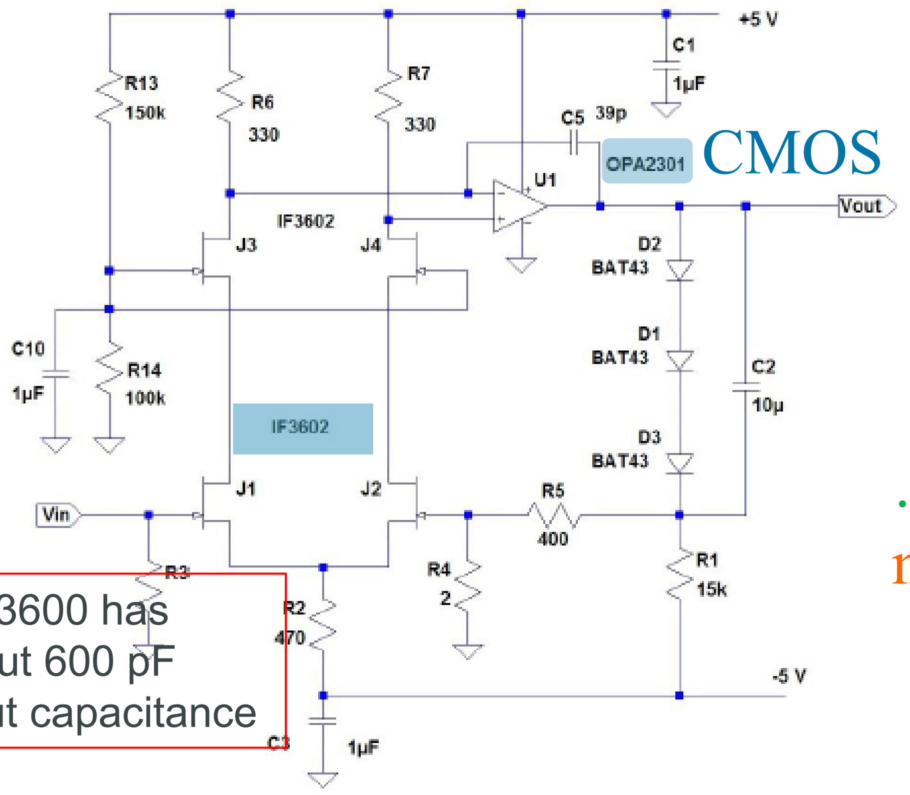

IFN3600 has about 600 pF input capacitance

…and an other with JFET input transistors (1 nV/√Hz @300 K, 0.6 nV/√Hz @ -100 °C).

dc-squid frontend 7

Here a preamplifier operating at both room temperature and 125 K with a performance of about 5 $\mu\Phi_O/\sqrt{Hz}$.

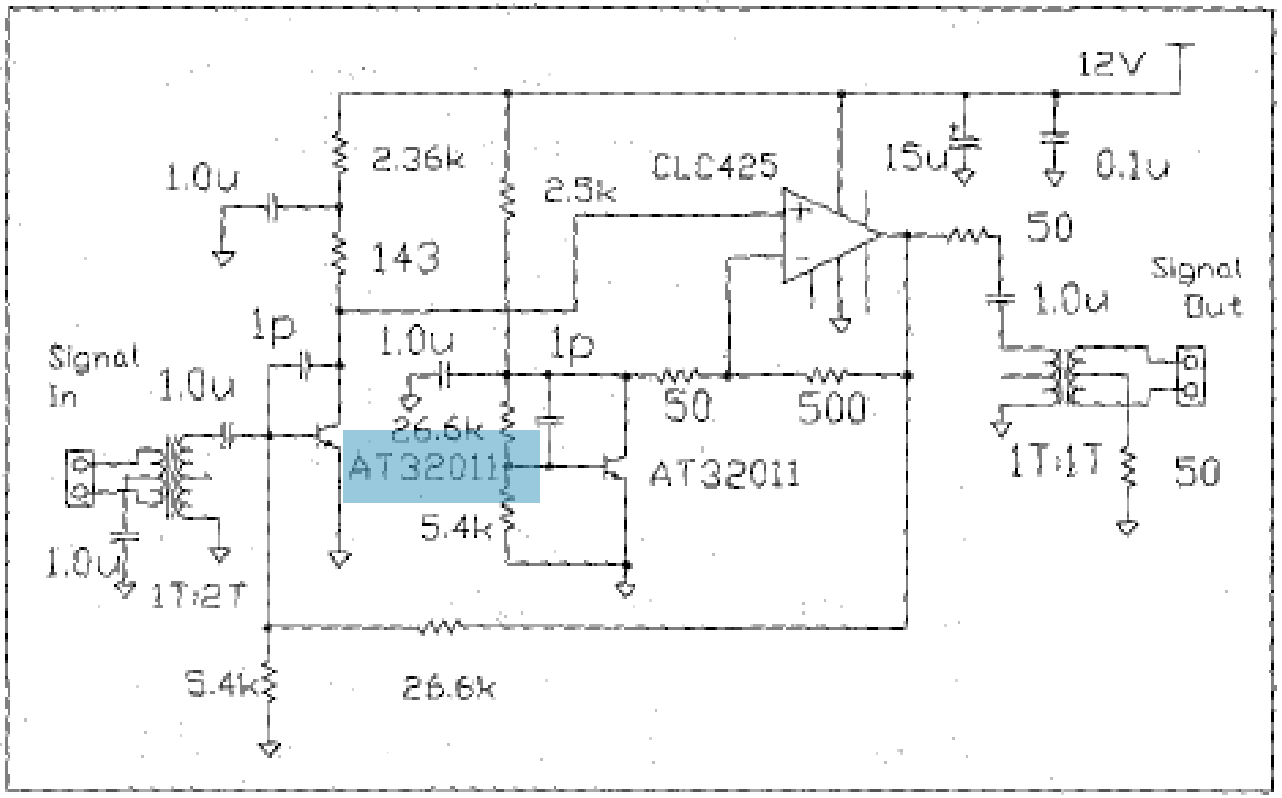

THE RF-SQUID SENSOR

The rf-SQUID differs from the dc-SQUID in having a single Josephson junction, or weak link.

Because the single junction is shorted by a superconductor, it cannot operate under DC conditions.

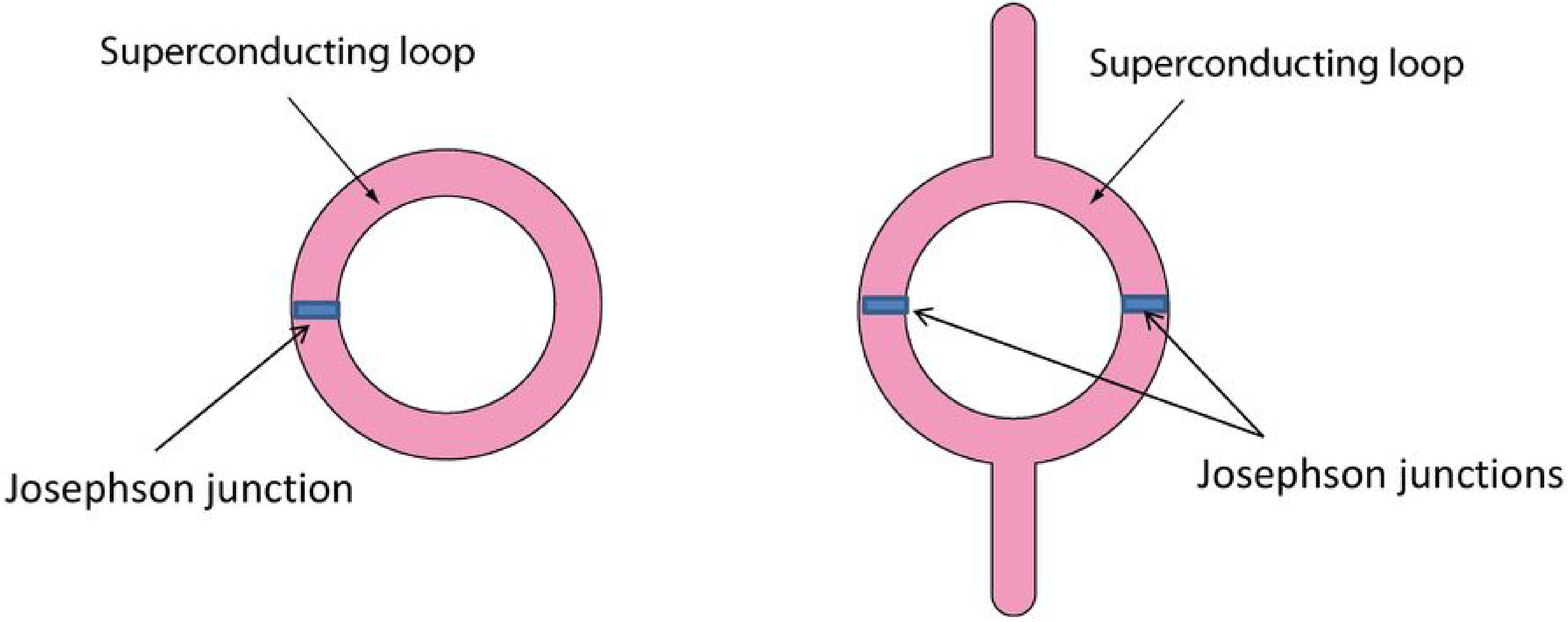

https://slideplayer.com/slide/12077675/

The rf-SQUID sensor 2

In order to operate an rf-SQUID must be coupled to a tank circuit consisting of an inductance and a capacitance tuned to it:

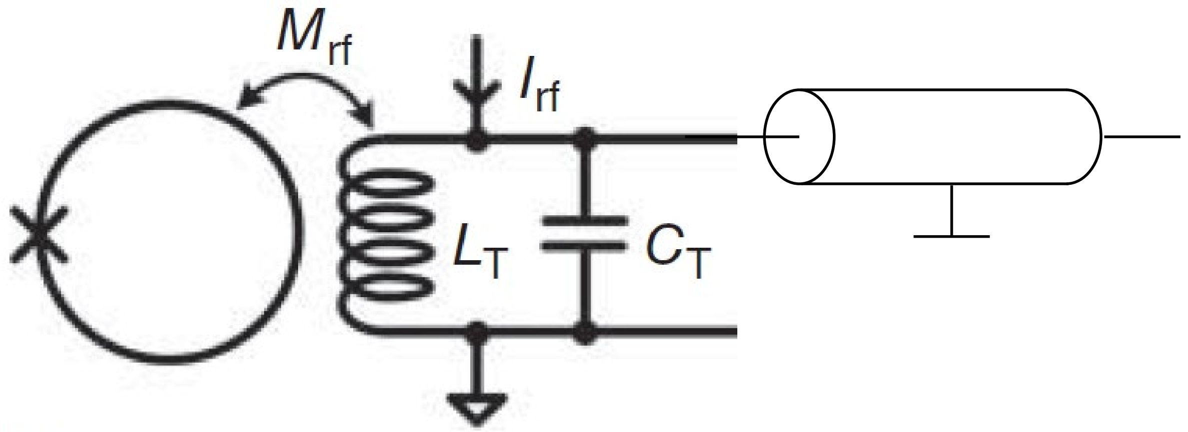

The connection to the amplifier cannot be longer than half the wavelength of the bias frequency, otherwise reflections may interfere negatively.

The rf-SQUID sensor 3

Large signals are obtained at large frequencies with large inductances and small capacitances, which conflict with the impedance matching requirements of the transmission line when the line is longer than $\lambda/2$.

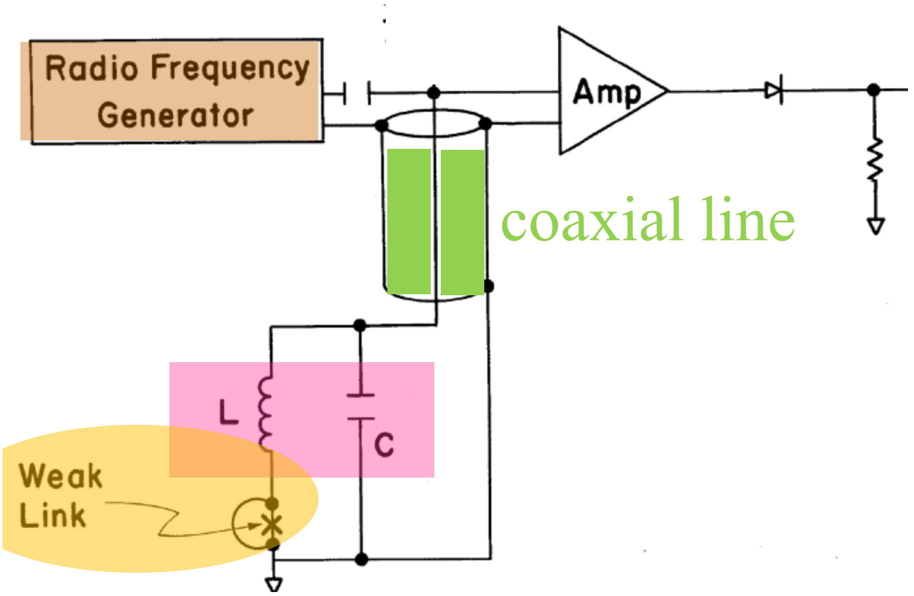

At 30 MHz the wavelength is a few meters, with no problems with front ends operating at room temperature; at 1 GHz the wavelength is a few centimeters: a cryogenic stage is needed.

A.H.Silver, Josephson Symp., 2012

The rf-SQUID sensor 4

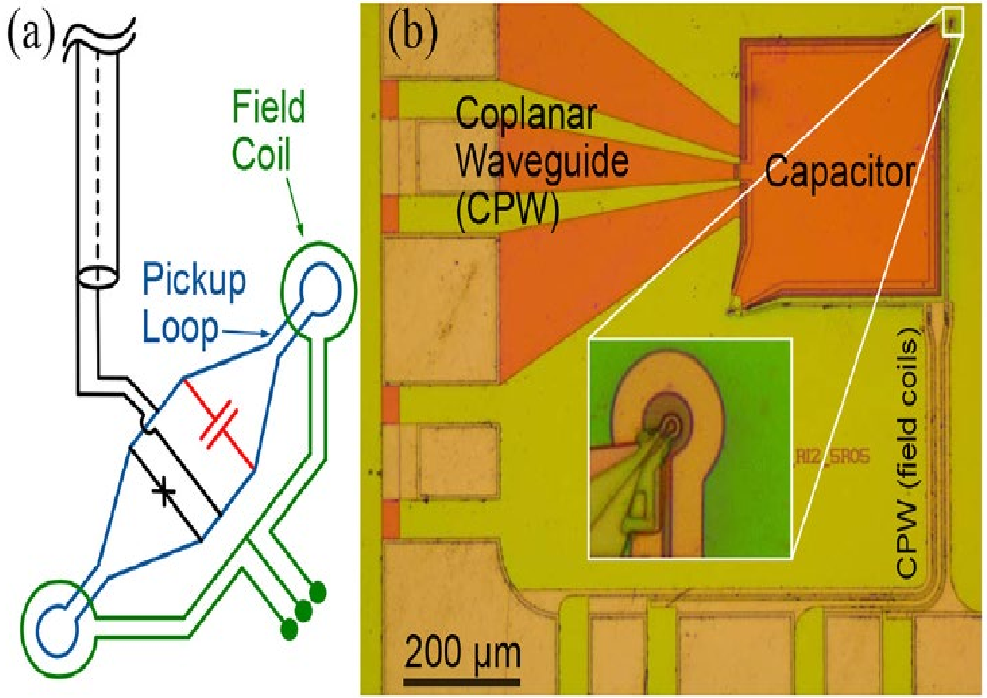

For resonant frequencies > GHz, the rf-SQUID and tank circuit are also implemented in a single chip.

The rf-SQUID sensor 4

The advantage of the rf-SQUID is multiplexing in arrays.

If the tuning main frequency, f_m, of the tank circuits can be set large, in an array each tank can be tuned with its own value f_m+f_k, with $f_k << f_m$, e.g. f_m=1 GHz, f_1=1 MHz, f_2=2 MHz, f_k=k MHz, …

In this way each tank can be connected to the same single line to which the sum of all tones are applied. A single cold preamplifier, called LNA, Low Noise Amplifier, can be then used for reading.

The tank circuit and the rf-SQUID can be side by side on the same chip.

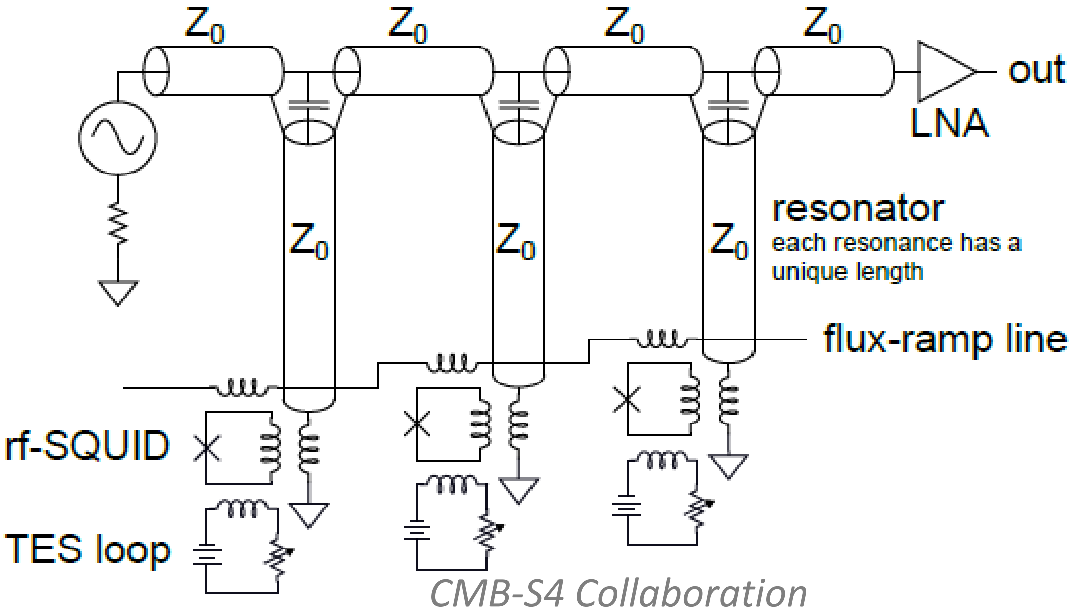

CMB-S4 Collaboration

Here TES sensors arrays can then be coupled to arrays of rf-squids …

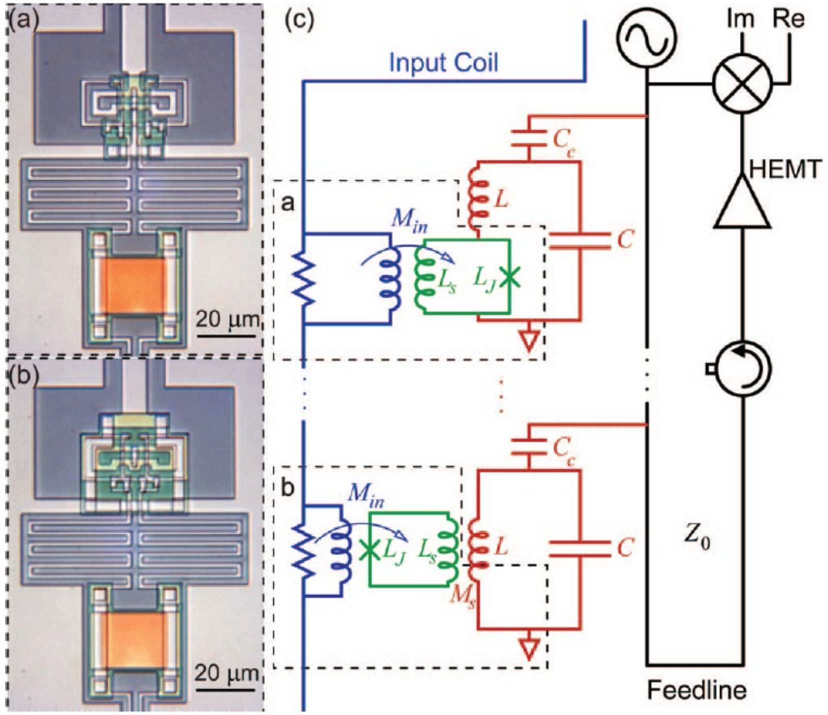

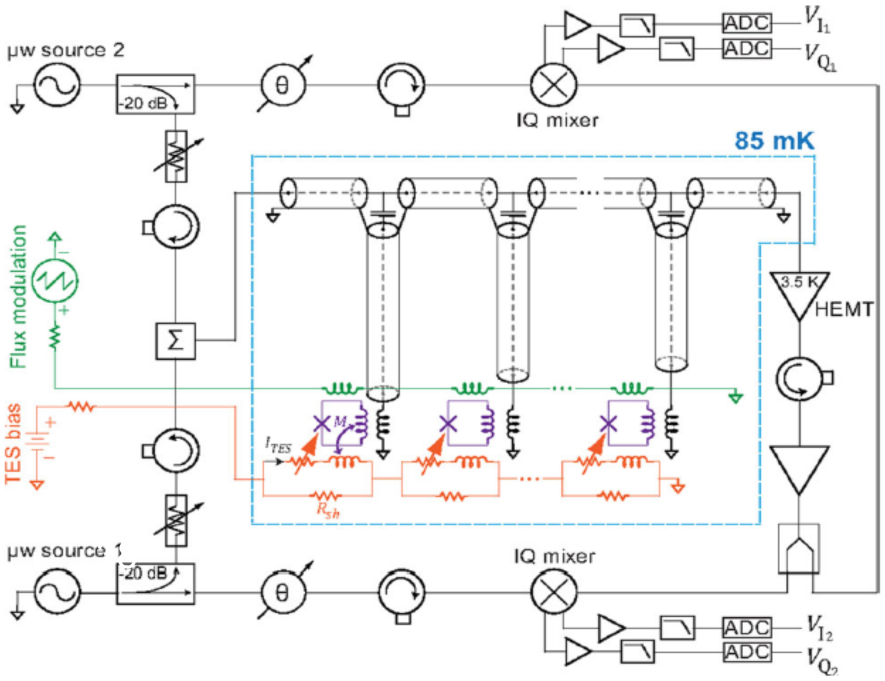

A sensor that can be readout and multiplexed without the need of a SQUID is the Microwave Kinetic Inductance Detector, MKID, a superconducting stub (its signals are larger than those of TES):

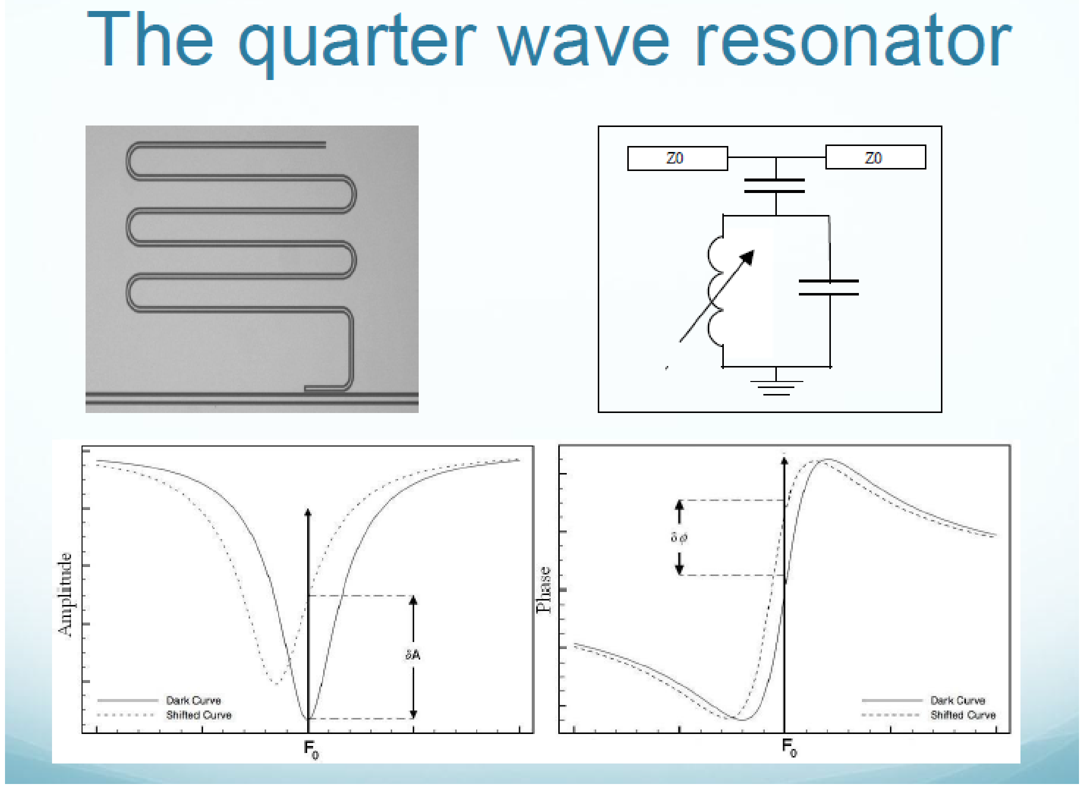

MKID 2

The MKID can be modeled with an inductance in parallel with a capacitance (a very small series resistance should also be considered). The composition material is a superconductor, so it has a small heat capacity and good electrical properties.

When radiation hits it, a small increase in its temperature slightly changes its superconductive state. As a result, its impedance changes.

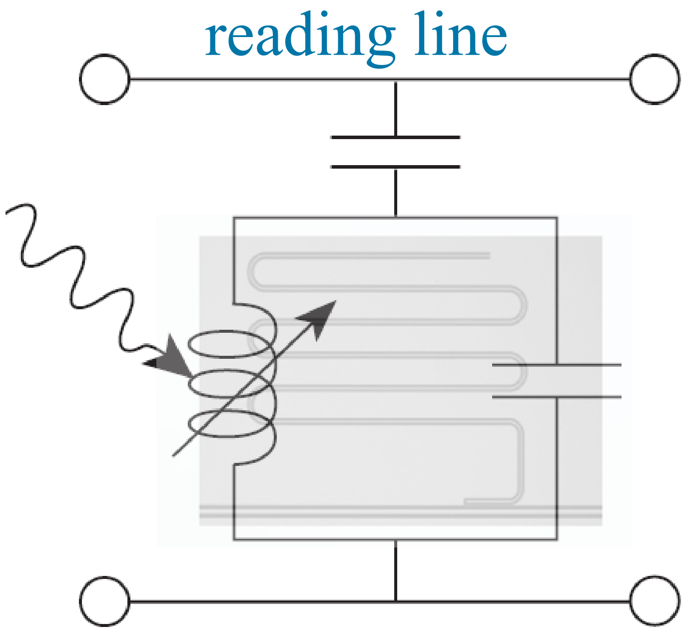

If the proper tuning frequency is applied to probe the resonator, the probe signal changes its amplitude and phase

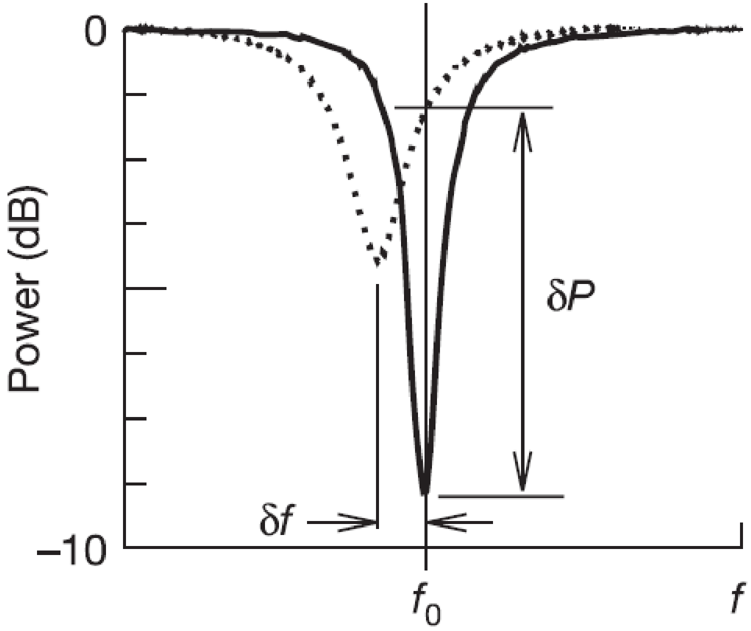

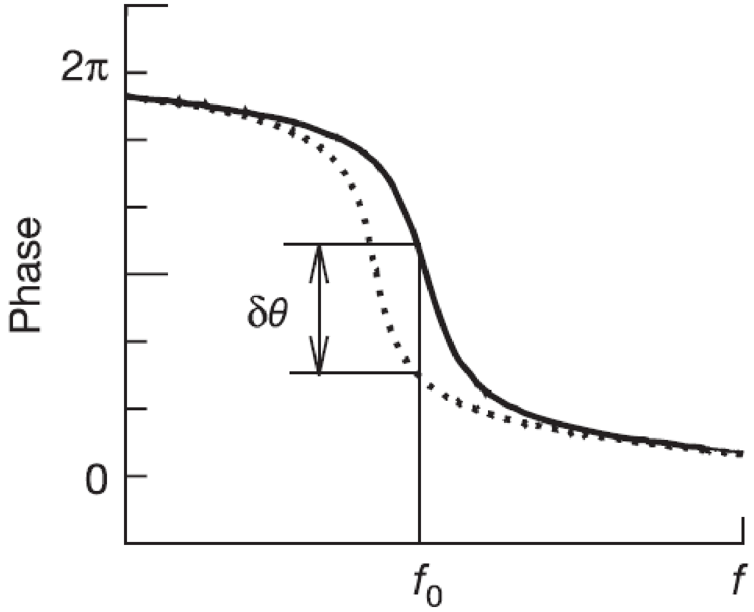

MKID 3

MKID can also be easily multiplexed with multitone biasing, as we have just seen with rf-SQUID.

NIKA2:
400 channels

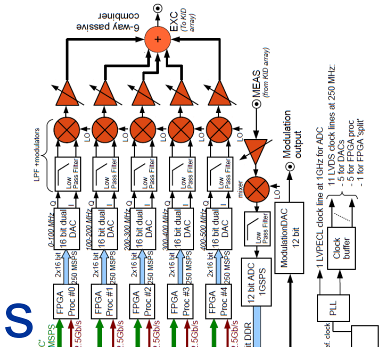

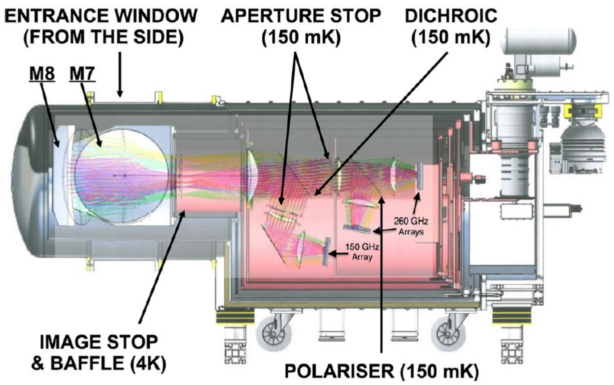

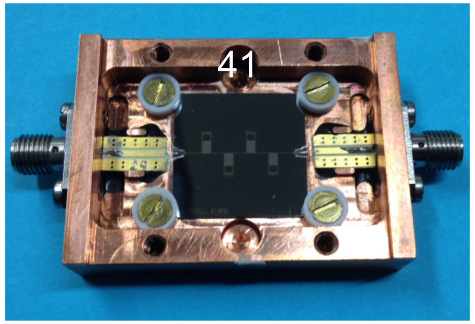

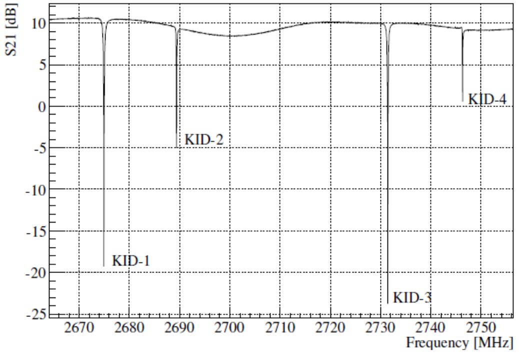

MKID arrays, like some rf-SCQUIDs, can be multiplexed through and only through the use of a single cryogenic low-noise microwave amplifier, LNA:

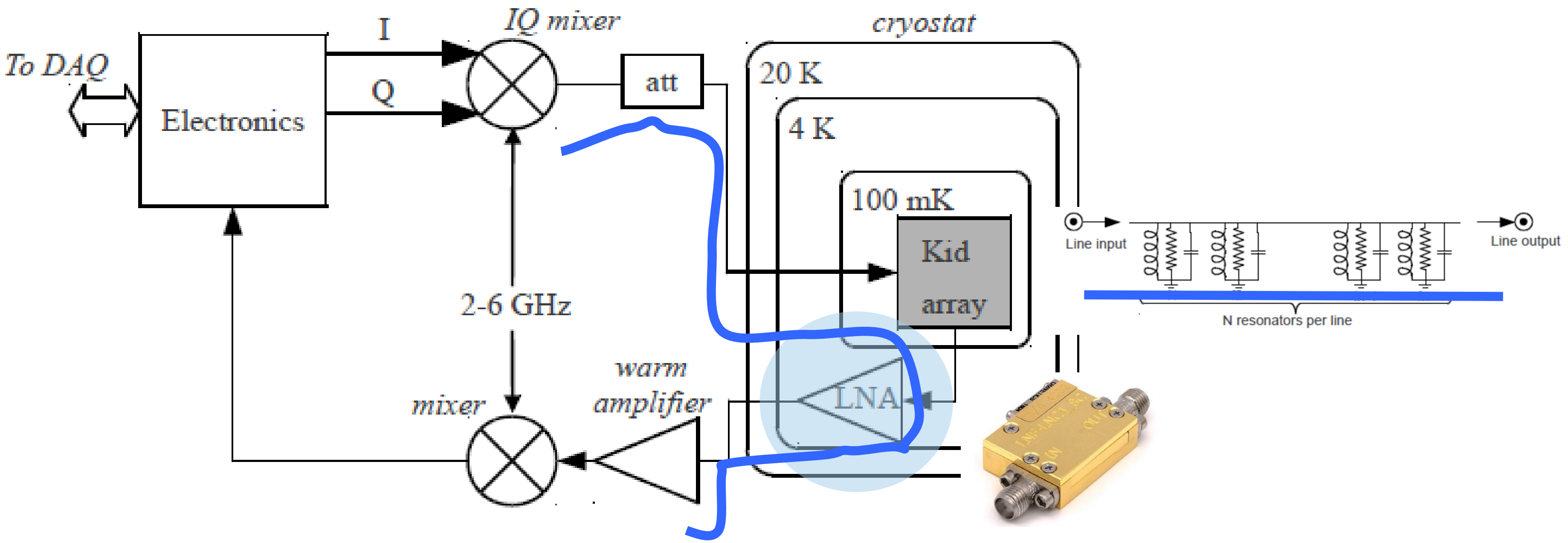

MKID 5

Most of the time the LNA limits the resolution that can be reached. However, it does a great job starting at 4.2 K, or even below.

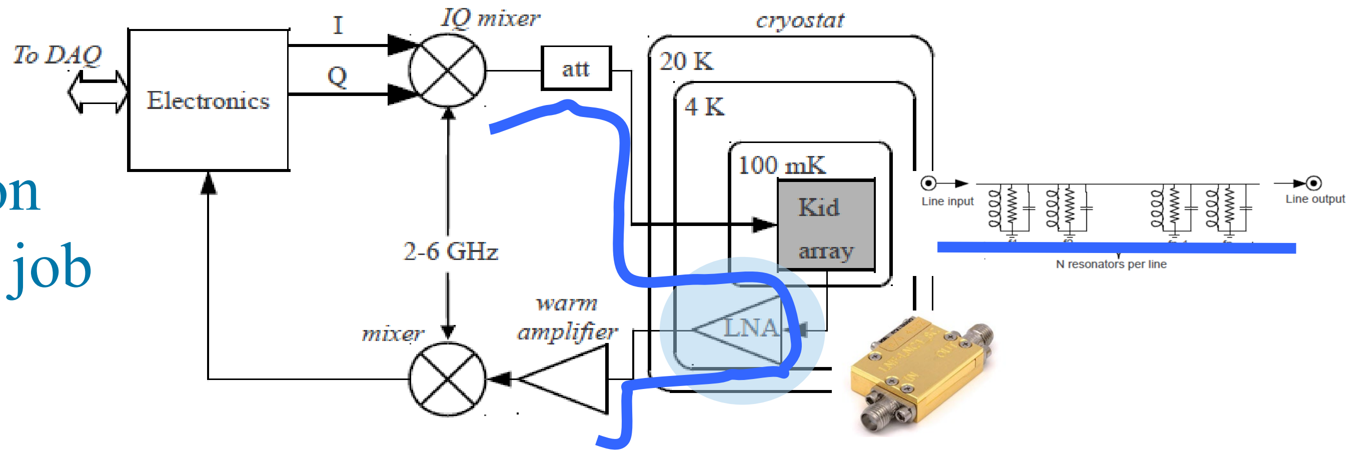

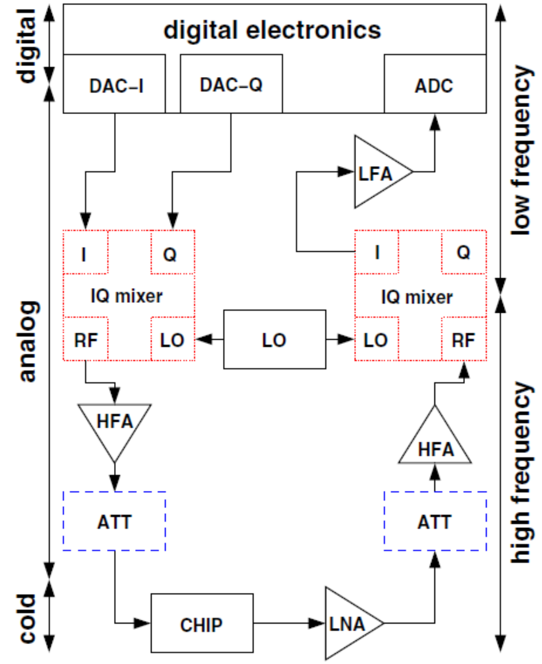

At high operating frequencies, LNA noise increases due to loss of matching and gain.

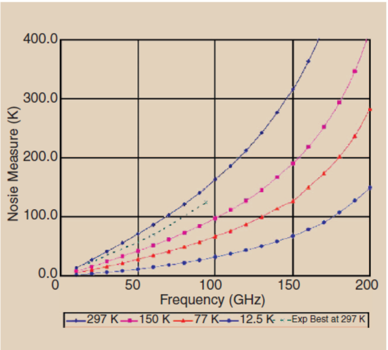

Figure 14. *A minimum noise measure of 0.1-µm gate length AlInAs/GaInAs/InP HFET [38]. The best experimental results from different laboratories are also shown [72]–[74].*

IEEE Microw. Mag., Sep,2005

Active devices capable of operating around 4 K and below are those produced in III - V compounds such as HEMTs (InP, InGaAs, ...), MESFETs in GaAs and AlGaAs, and HBTs in SiGe and Si-MOS.

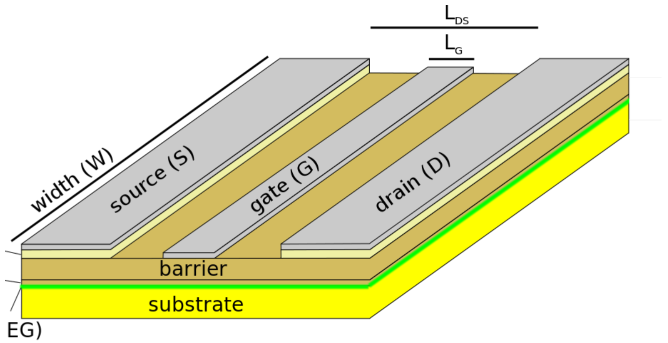

LNA technology 2

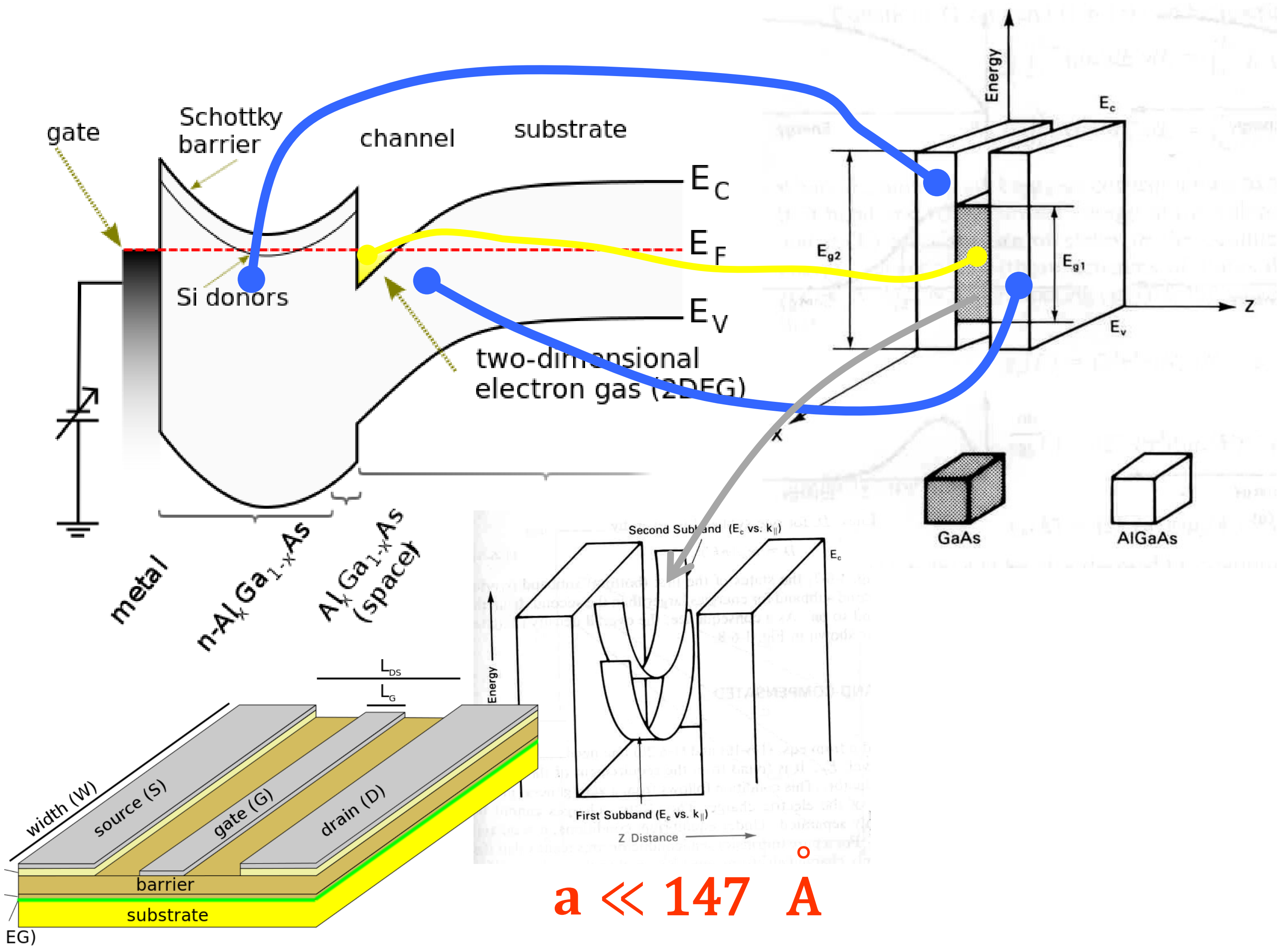

$a \ll 147\ \mathring{A}$

The HEMT is a "sandwich" between two semiconductors with a large bandgap and an undoped 2D sheet with a smaller bandgap.

Electrons driven into the sheet by the applied gate voltage are quantized and move within it at very high speed at any temperature, since there is no scattering.

LNA technology 3

The SiGe HBT has the smaller bandgap p-base than the emitter because a small percentage of Ge atoms is introduced to change its nature: *the base intrinsic concentration increases*

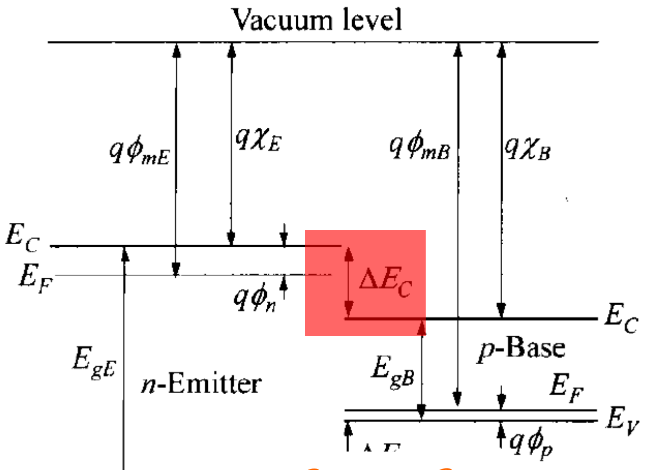

$n_{ie}^2 < n_{ib}^2$

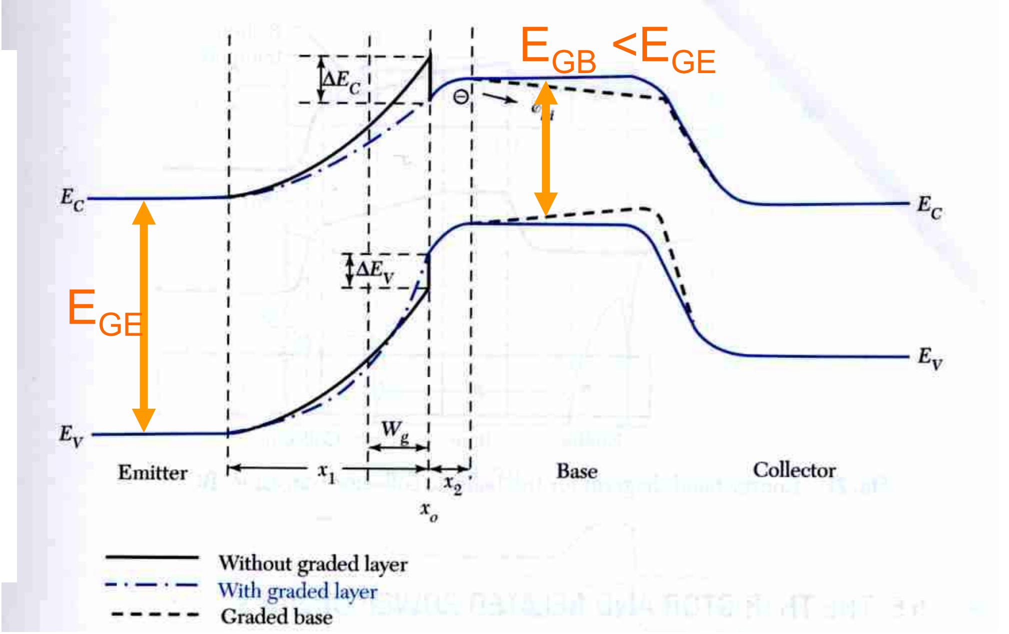

This metallurgical modification of the base allows a high dopant concentration level to be adopted, which improves speed, gain, and even low-temperature gain (not verified for all…): *this because the current gain is proportional also to the intrinsic concentrations of the base and the emitter.*

$$h_{FE} \doteq \frac{I_C}{I_B} \approx \frac{N_e}{P_b}\frac{n_{ib}^2}{n_{ie}^2} = \frac{N_e}{P_b}\exp\left(\frac{\Delta E_C}{K_B T}\right)$$

LNA technology 4

We should not to forget that Si-MOS are able to work at deep cold because the electric field applied between the gate and channel is very intense, especially when the oxide thickness is small.

The electric field is then able to extract charges that would otherwise be severely frozen, thus forming the conduction channel.

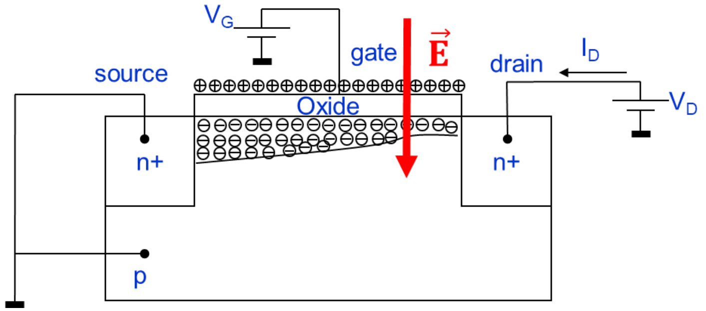

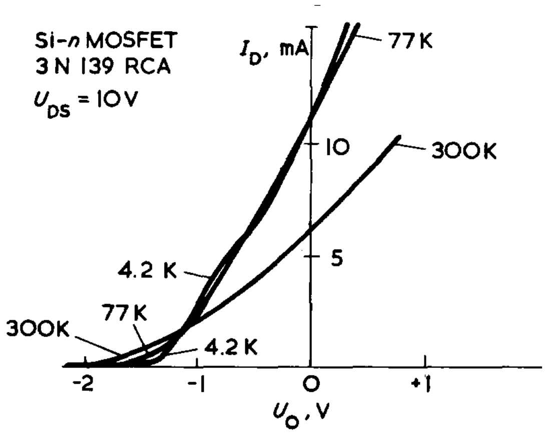

Fig.13 Output characteristic and transfer curve of *n*-channel MOSFET (3N 139 RCA) at 300, 77 and 4.2 K

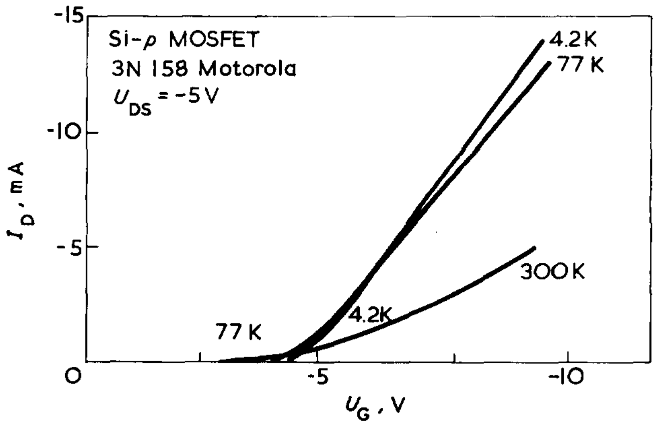

Fig.14 Output characteristic and transfer curve of *p*-channel MOSFET (3N 158 Motorola) at 300, 77 and 4.2 K

LNA technology 5

This is a 28 nm CMOS monolithic LNA operated at 20 K in a bandwidth from 50 GHz to 115 GHz.

Dissipation is 38 mW.

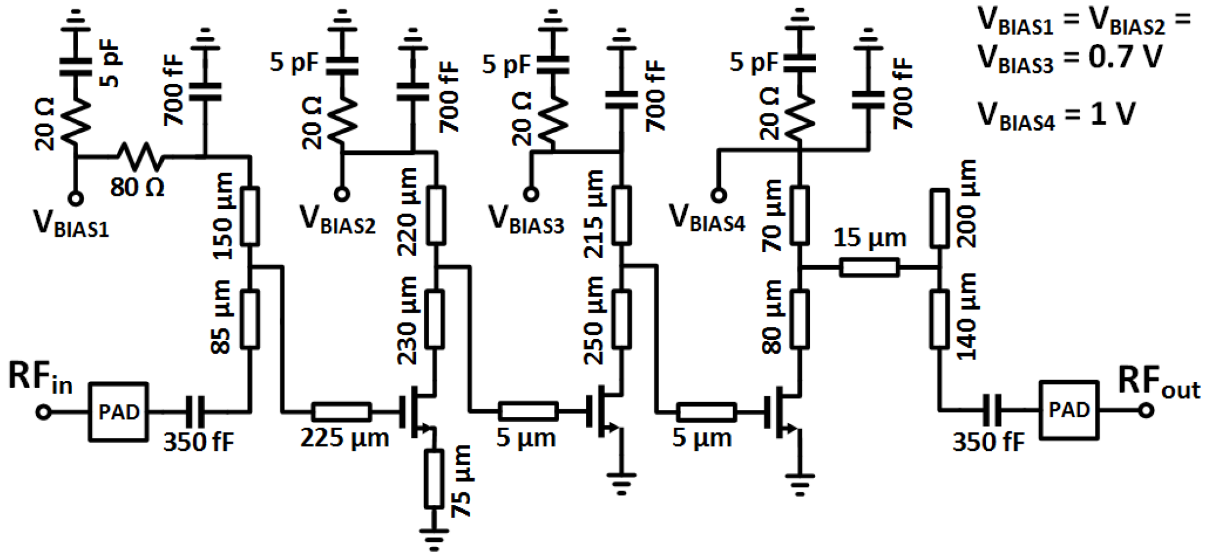

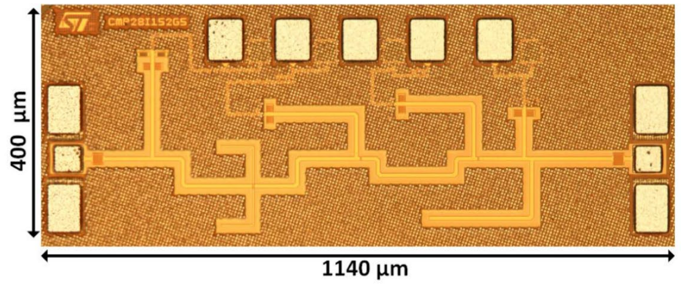

This is a 40 nm CMOS monolithic LNA operated at 4.2 K in a bandwidth from 4 GHZ to 8 GHz.

Working operation at 4.2 K is V=1.4 V, input stage current of 19 mA, following stages 8.6 mA in total.

transformer matching

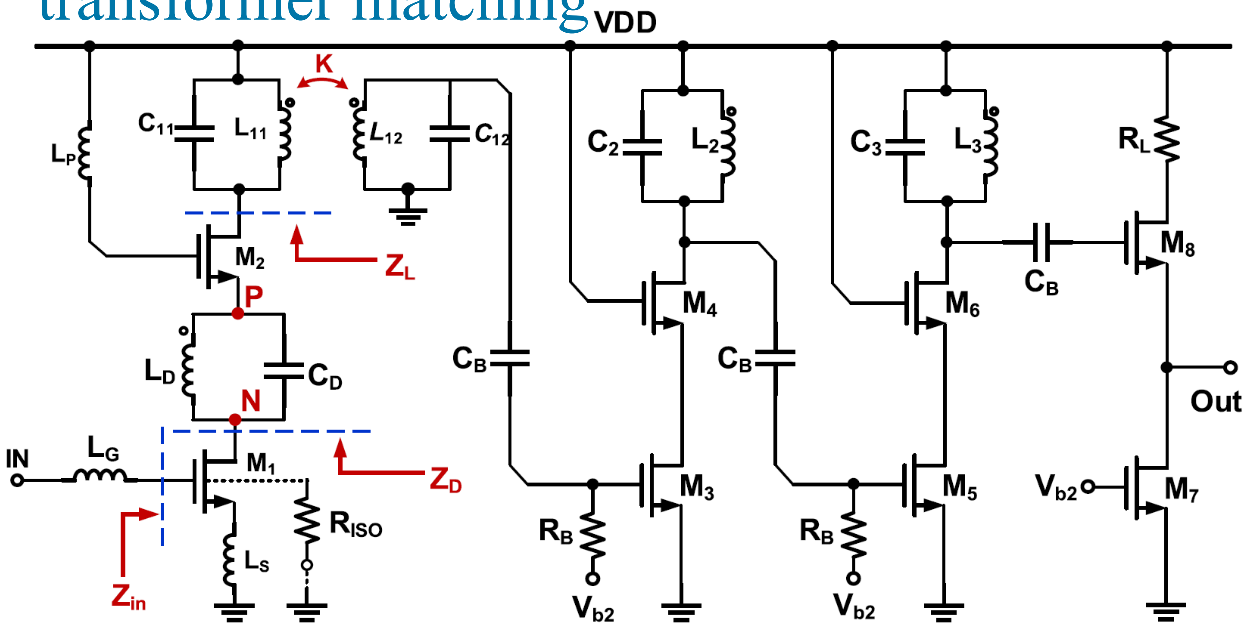

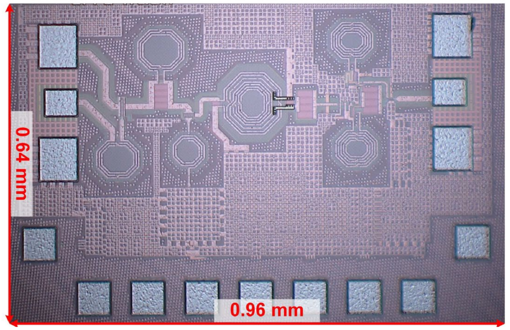

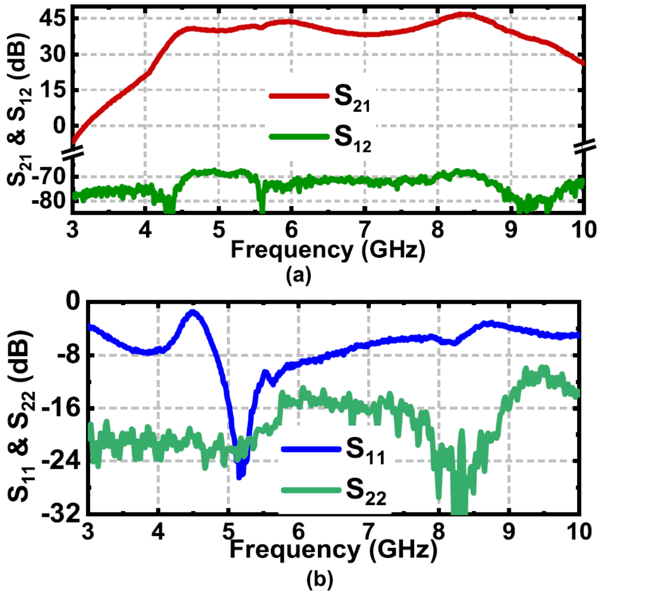

Fig. 16. S-parameter measurement results of the LNA at 4.2 K. (a) S_{21} and S_{12}. (b) S_{11} and S_{22}.

LNA technology 7

Design and implementation of microwave amplifiers must follow well-defined rules about both the geometry of all the connections for obtaining proper terminations and the stability of the transistors that are otherwise prone to oscillate at high frequency.

Here HEMTs at work.

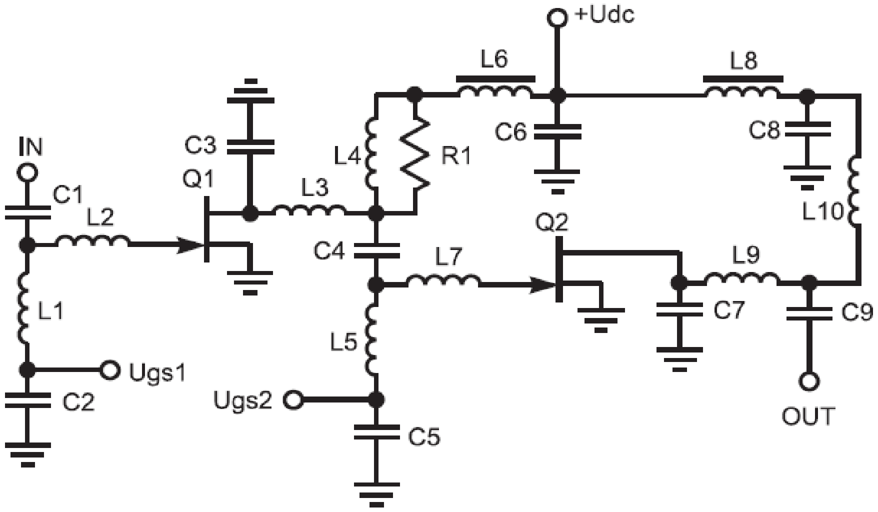

Fig. 2. The amplifier schematic. Q1, Q2 – ATF-36077.

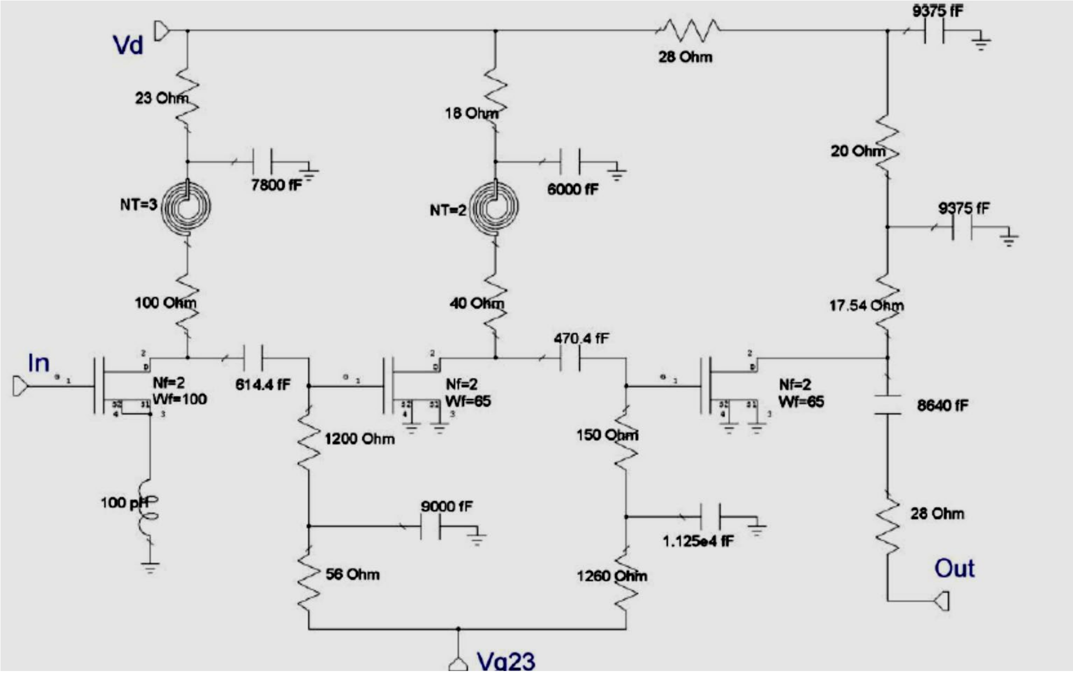

LNA technology 8

Cryogenics 60 (2014) 76–79

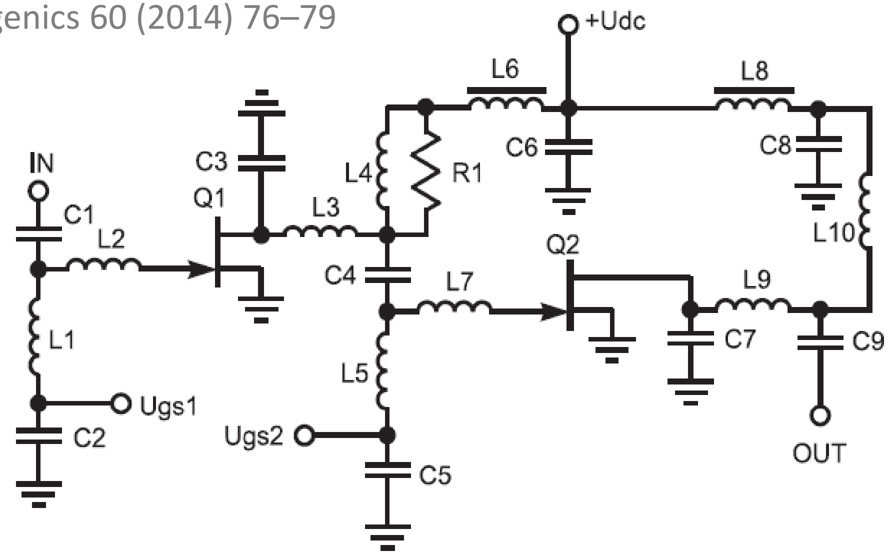

Fig. 2. The amplifier schematic. Q1, Q2 – ATF-36077.

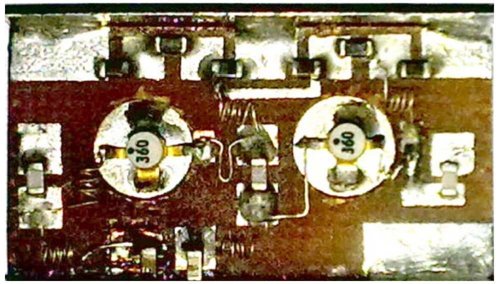

The amplifier is a multistage common-source or common-emitter amplifier, operating in open loop.

It is a 3-stage common source with inductance at the source of the input HEMT for line matching.

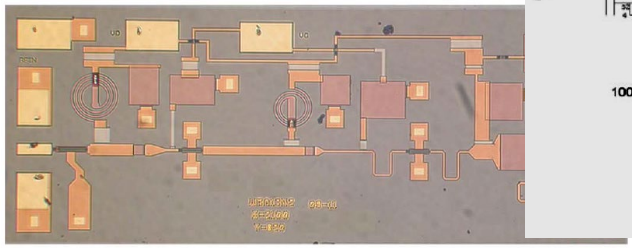

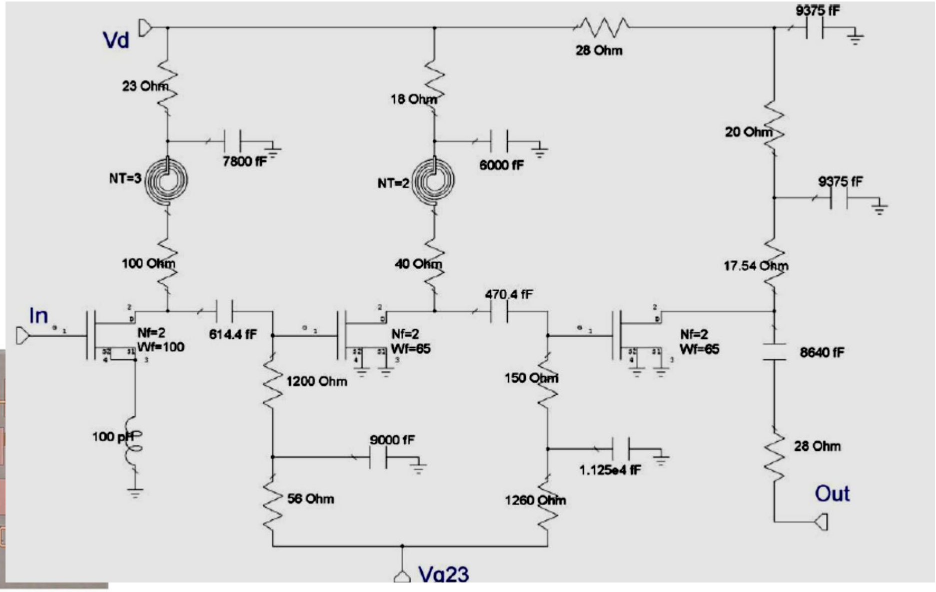

IEEE Tran. on Micr. Th. and Tech, 2013, 61 3285

Monolithic SiGe amplifier composed of a cascade of 2 common-emitter stages. DC bias is implemented with DC-coupled current mirrors, AC isolated with inductances.

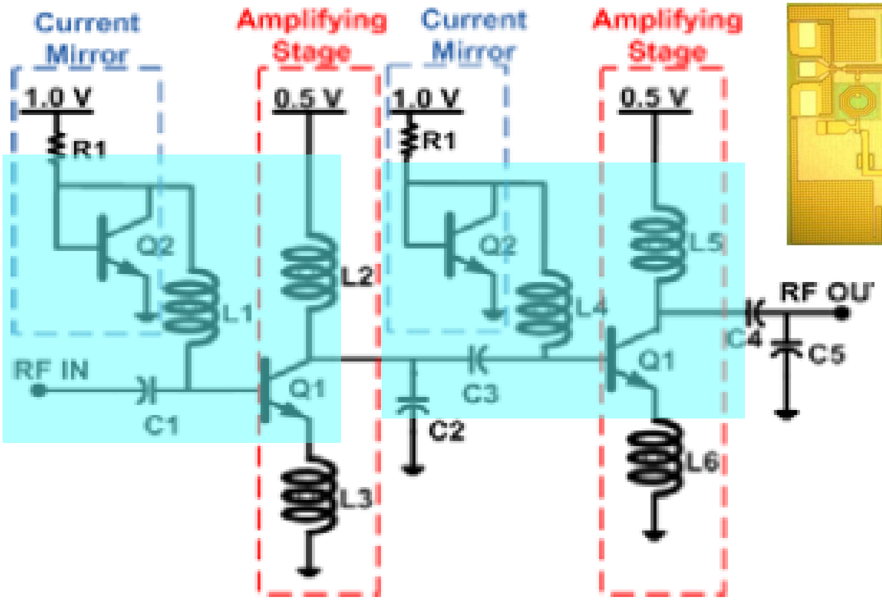

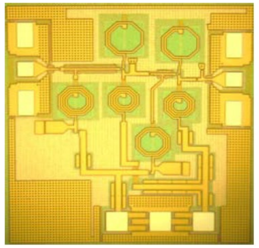

Cryogenic microwave amplifiers are capable of showing less than 100 pV/√Hz in the center of the passband, around a few GHz.
This corresponds to a noise temperature of less than 4 K of a 50 Ω resistor.

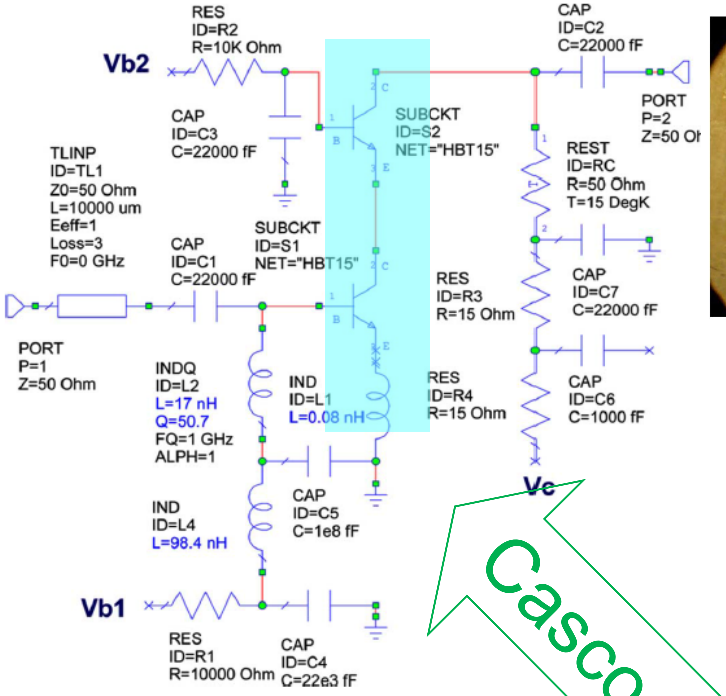

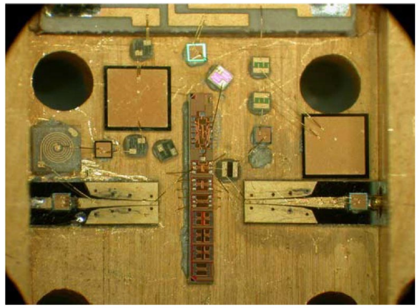

Fig. 12. Schematic of cascode 0.5–3-GHz amplifier modeled with circuit simulation software [7] and implemented as shown in Fig. 13 with bond-wire connections of small MIC components.

Cascode SiGe.

One question might be: why aren't microwave amplifiers used for dc-squid readings, or, in general, not modulated detectors?

III-V compounds are heterostructures obtained by joining dissimilar materials. At their interfaces, defect sites can be formed that act as capture centers for charge carriers.
The 1/f noise is a problem if the signal duration is comparable to that of the capture time constant.

$$I = e(N_{TOT} - 1)\mu\frac{V_{BIAS}}{L^2}$$

$$I = eN_{TOT}\,\mu\frac{V_{BIAS}}{L^2}$$

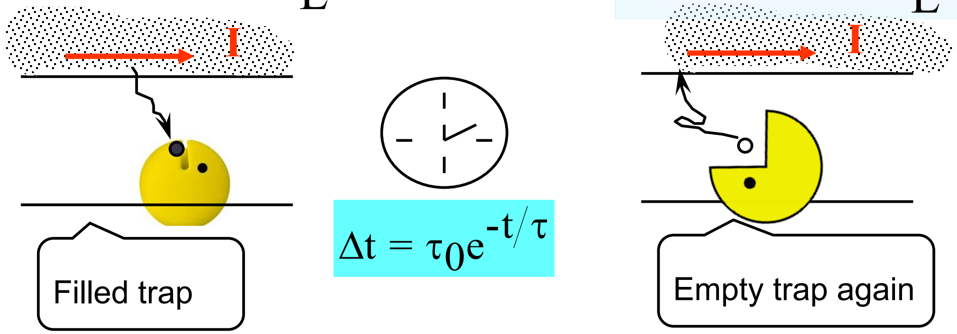

$$\Delta t = \tau_0 e^{-t/\tau}$$

Carrier generation-recombination in trapping centers generates low-frequency noise that worsens the S/N for dc-squids.

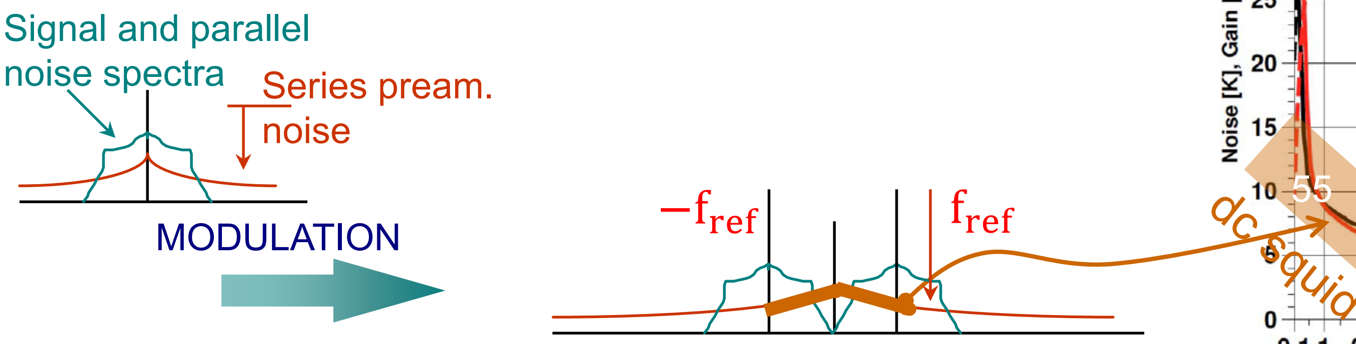

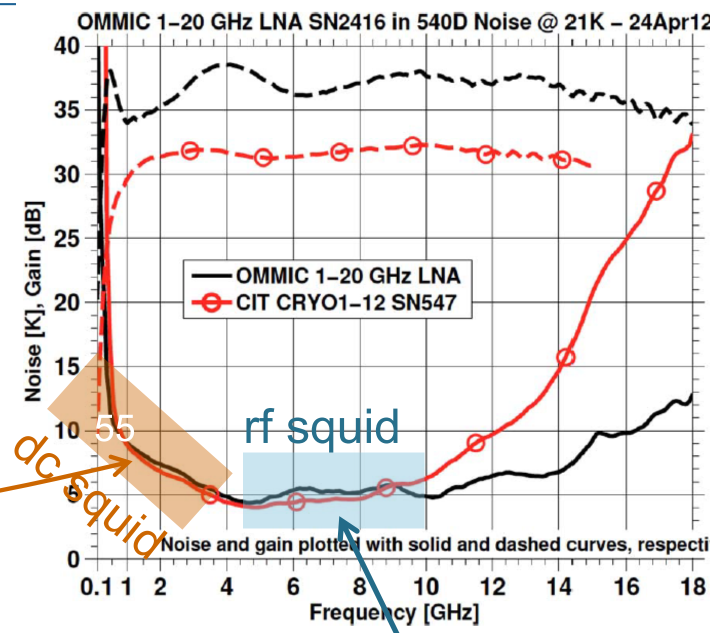

Modulation frequency for dc-squid is small and micro-wave devices still show large 1/f noise: the frequency shift is not enough to override 1/f noise.

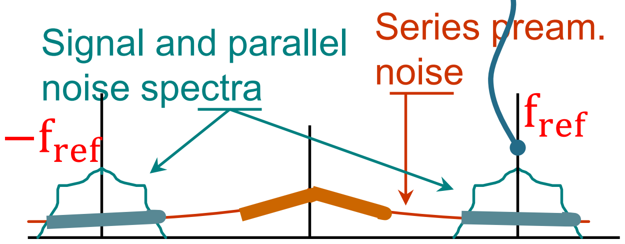

However...low-frequency noise is not an intrinsic source of noise, and technological processes could be optimized to achieve low noise.

With this cryogenic SiGe amplifier, the noise was very low. The authors stated a level of less than 8 × 10-8 $\Phi_O/\sqrt{Hz}$! The SiGe adopted was the NESG3031.

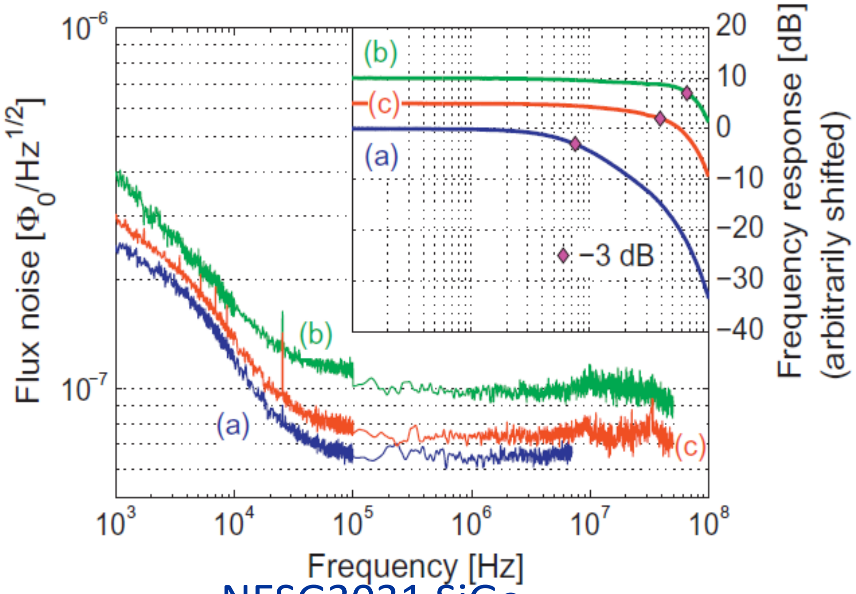

NESG3031 SiGe

A cascode differential input pair with output buffer and open-loop operation.

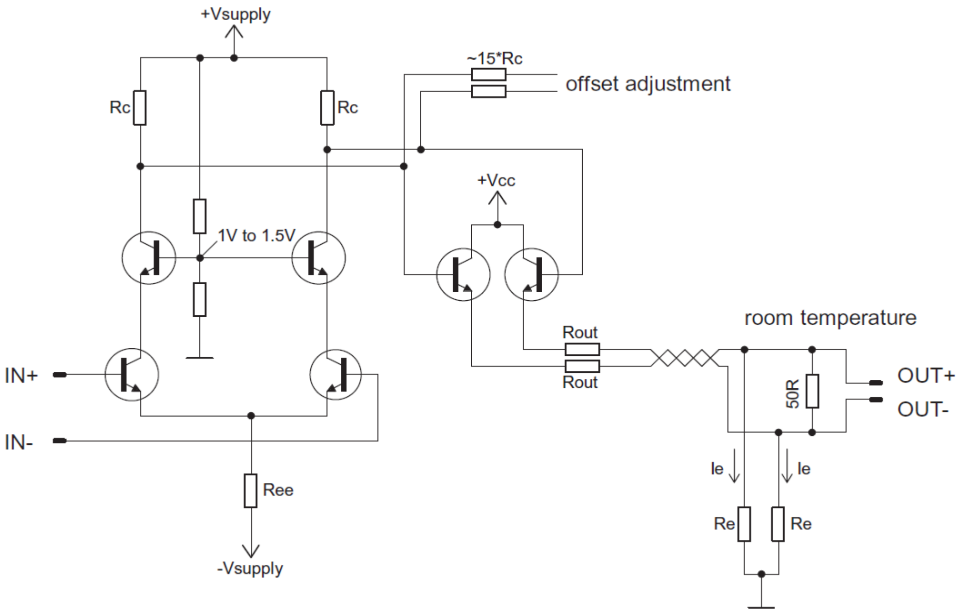

A cryogenic family of low 1/f HEMTs has been developed at CNRS/C2N, France.

The best performance is obtained at 4.2 K, with an HEMT with an input capacitance of 250 pF.

The noise is about 5 nV/√Hz at 1 Hz, and about 0.2 nV/√Hz is the minimum value at 4.2 K.

The HEMT is capable of operating up to 1.5 GHz, although it is optimized for low-frequency operation.

C_{Input}=240 pF

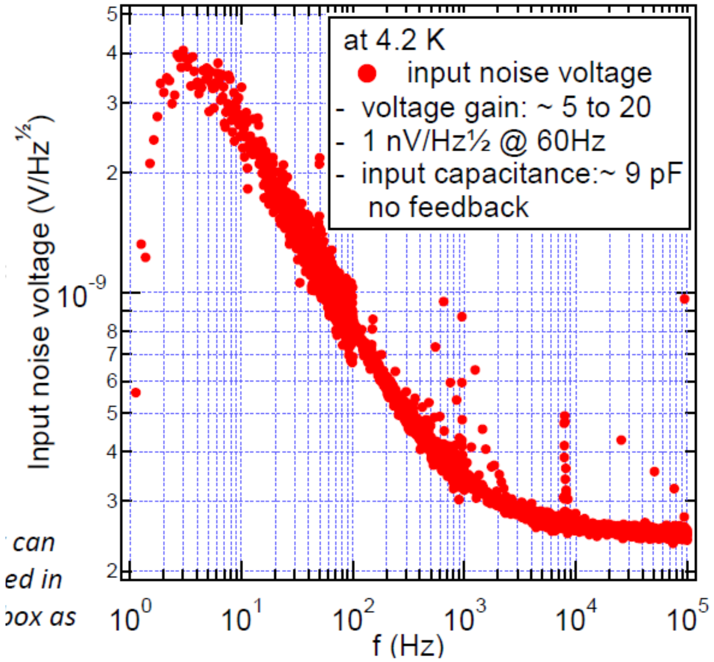

APP. PHY. LET. 2014, 105, 013504

The factor of merit $C_A A_f$ for this HEMT family is 3×10^{-27} J, a rather good feature.

To compare: a standard HEMT/Si-MOS device has order of 10^{-23} J, while a good Si JFET operated at room temperature has 2×10^{-29} J.

C_{Input}=240 pF

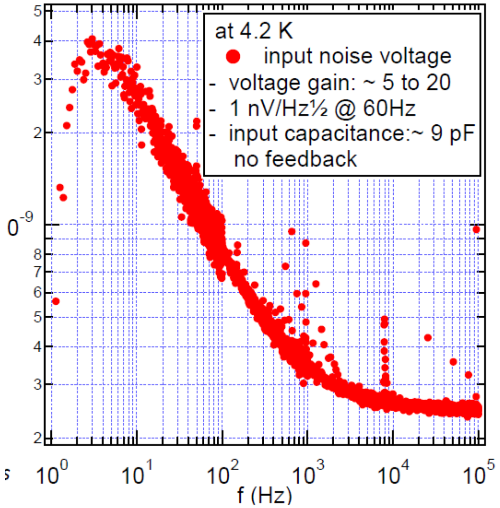

Name		200pch	100pch	30pch	5pch	1pch
L_gxW (μm^2)		1.5×10^5	6.4×10^4	2.0×10^4	2.0×10^3	4.0×10^2
C_{gs} (pF); C_{gd} (pF)		236; 8.9	103; 8.9	33; 3.5	4.6; 1.0	1.8; ~0.6
V_{ds}(mV); I_{ds}(mA)		100; 1.0	100; 1.0	100; 1.0	100; 1.0	100; 0.5
g_m (mS); g_d (mS)		52; 0.4	40; 1.2	115; 1.3	44; 1.3	15; 0.8
$ft = g_m/(2\pi C_{gs})$ (Hz)		3.5×10^7	6.2×10^7	5.5×10^8	1.5×10^9	1.3×10^9
e_n (nV/Hz^{½})	@1Hz @10Hz @100Hz @1kHz	5.4 1.7 0.52 0.24	6.3 2.1 0.76 0.34	14 4.5 1.5 0.57	30 12 4.5 1.4	100 30 10 2.7
$e_{n\text{-white}}$ (nV/Hz^{½})		0.18	0.22	0.12	0.21	0.4
i_n (aA/Hz^{½})	@1Hz @1kHz	21 6.8×10^2	15 5.1×10^2	9.1 2.4×10^2	2.2 70	3.6 57
R_n (Ω)	@1Hz @1kHz	2.6×10^8 3.5×10^5	4.2×10^8 6.3×10^5	1.5×10^9 2.2×10^6	1.4×10^{10} 2.0×10^7	2.8×10^{10} 3.7×10^7
T_{nt} (mK)	@1Hz @1kHz	4.1 5.9	3.4 6.2	4.6 5.0	2.4 3.6	13 5.6

APP. PHY. LET. 2014, 105, 013504

DEEP CRYOGENIC MEDIUM TO HIGH IMPEDANCE SENSORS

We consider now the case the sensor is from medium to high impedance: a semiconductor thermistor.

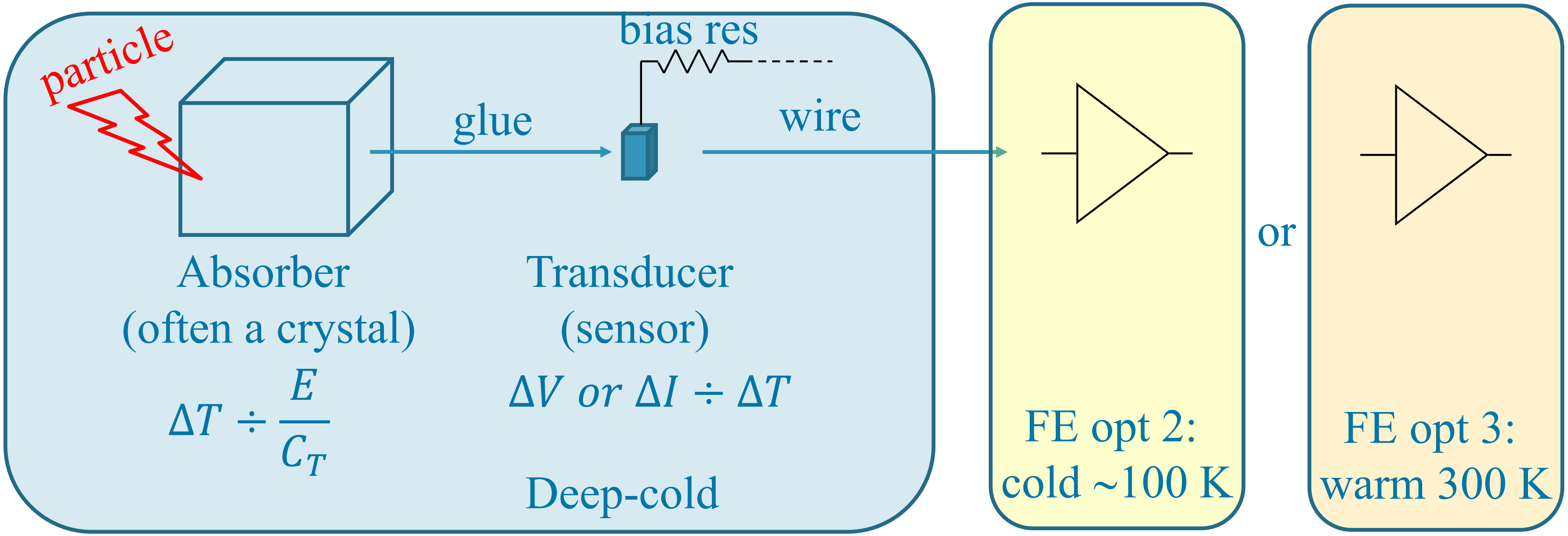

<u>REMEMBER</u>: Since the operating temperature is below 0.1 K the environment is a Dilution Refrigerator, wet or dry.

Deep cryogenic medium to high impedance sensors 2

High and medium impedance sensors are coupled to medium and macro absorbers. What do we mean by these two definitions?

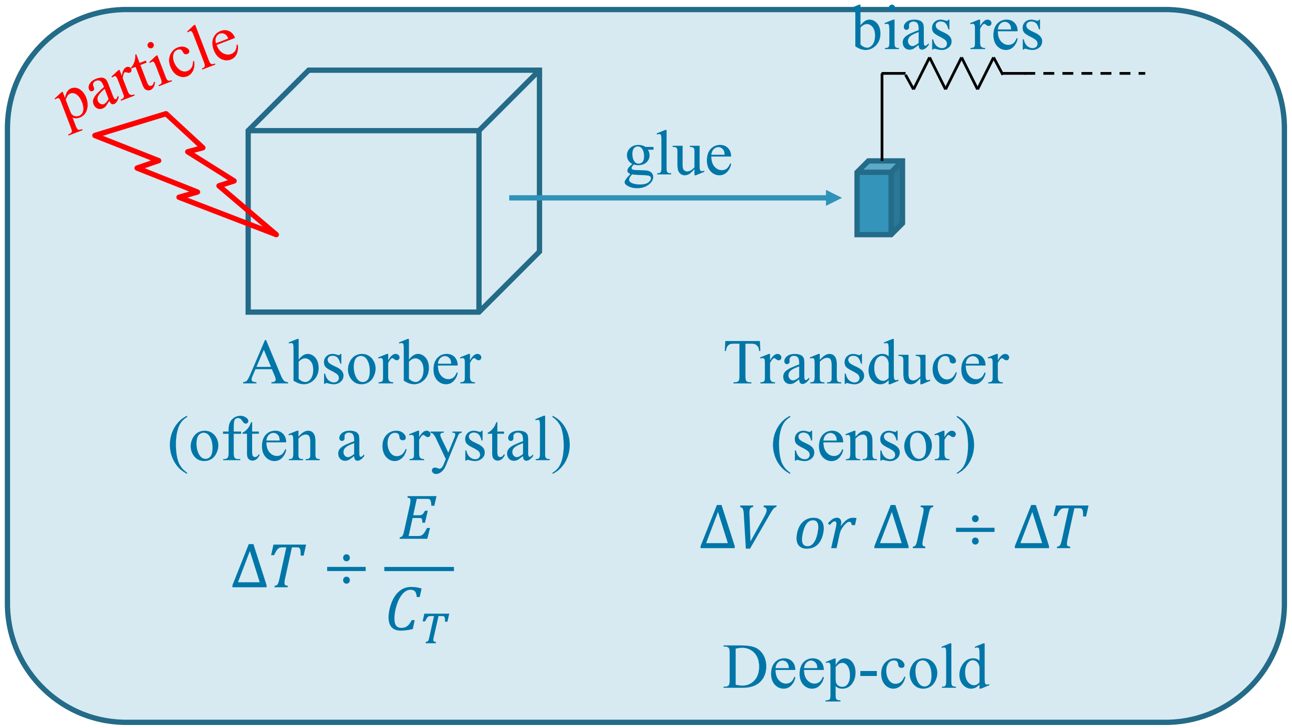

A medium-absorber is a crystal with a mass around grams and below.

Macro-absorbers are crystals with masses from tens of grams to hundreds of grams.

The reason thermistors are widely used in these applications is simplicity of implementation.

In recent years an additional feature has been exploited: some absorbers generate light, photons, in addition to heat, phonons.

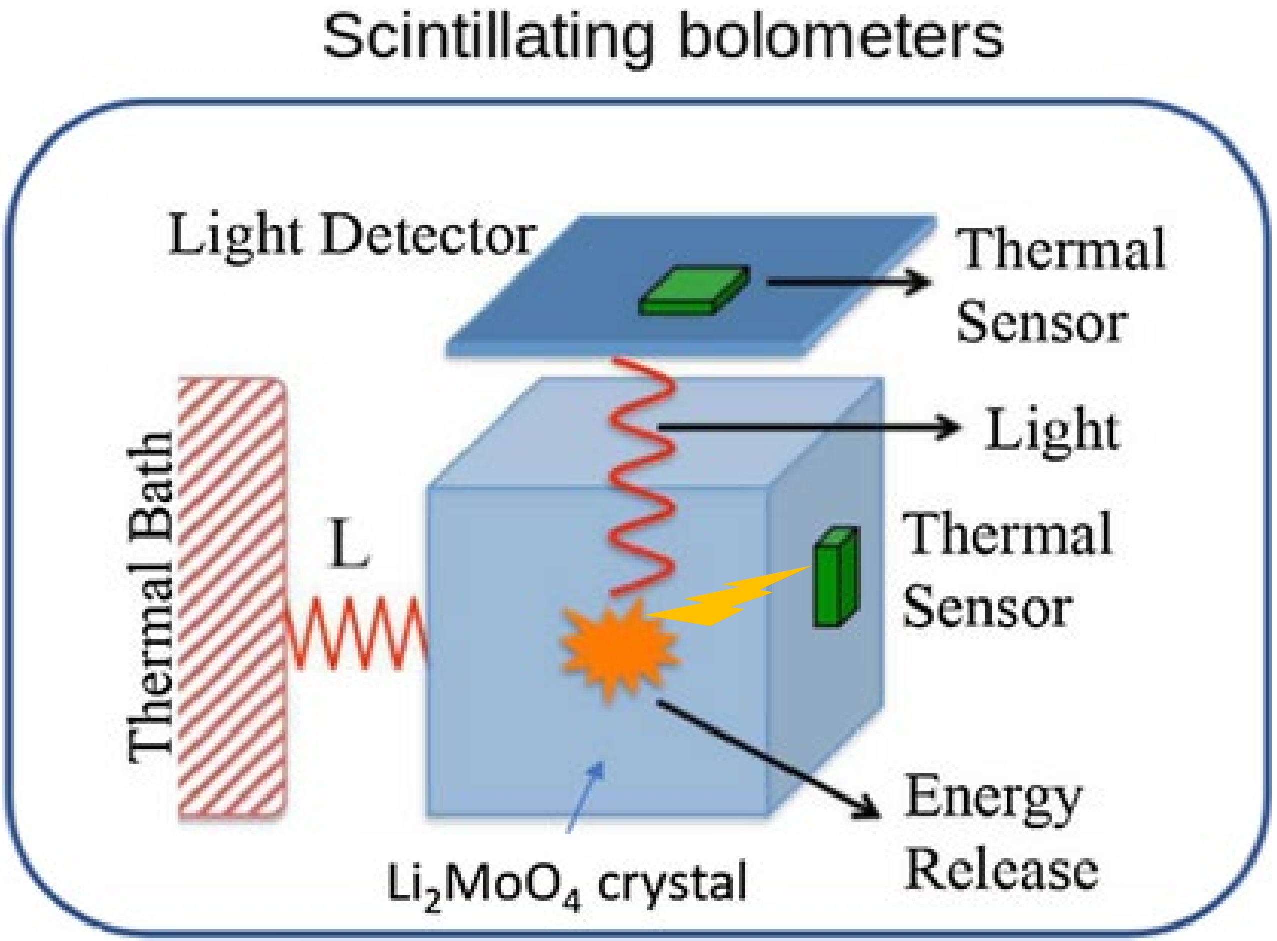

The photons are pushed toward an absorbing slab, ultra-pure Ge or Si, where they are converted to phonons.

An additional thermistor glued to the slab converts the heat into an electrical signal.

This additional channel is very useful for particle discrimination (light output is different between gamma rays and α–particles) and for timing, since the sheet absorber, being of very low mass, is much faster than the main absorber.

Deep cryogenic medium to high impedance sensors 4

Medium or high impedance thermistors mean values ranging from a few hundred KΩ to a few hundred MΩ.

An important aspect is the bias resistance of the thermistor. It must have a value of about ten times that of the thermistor in order not to lose signal amplitude, but it is almost impossible to find stable high values resistors capable of working at deep cryogenic temperatures.

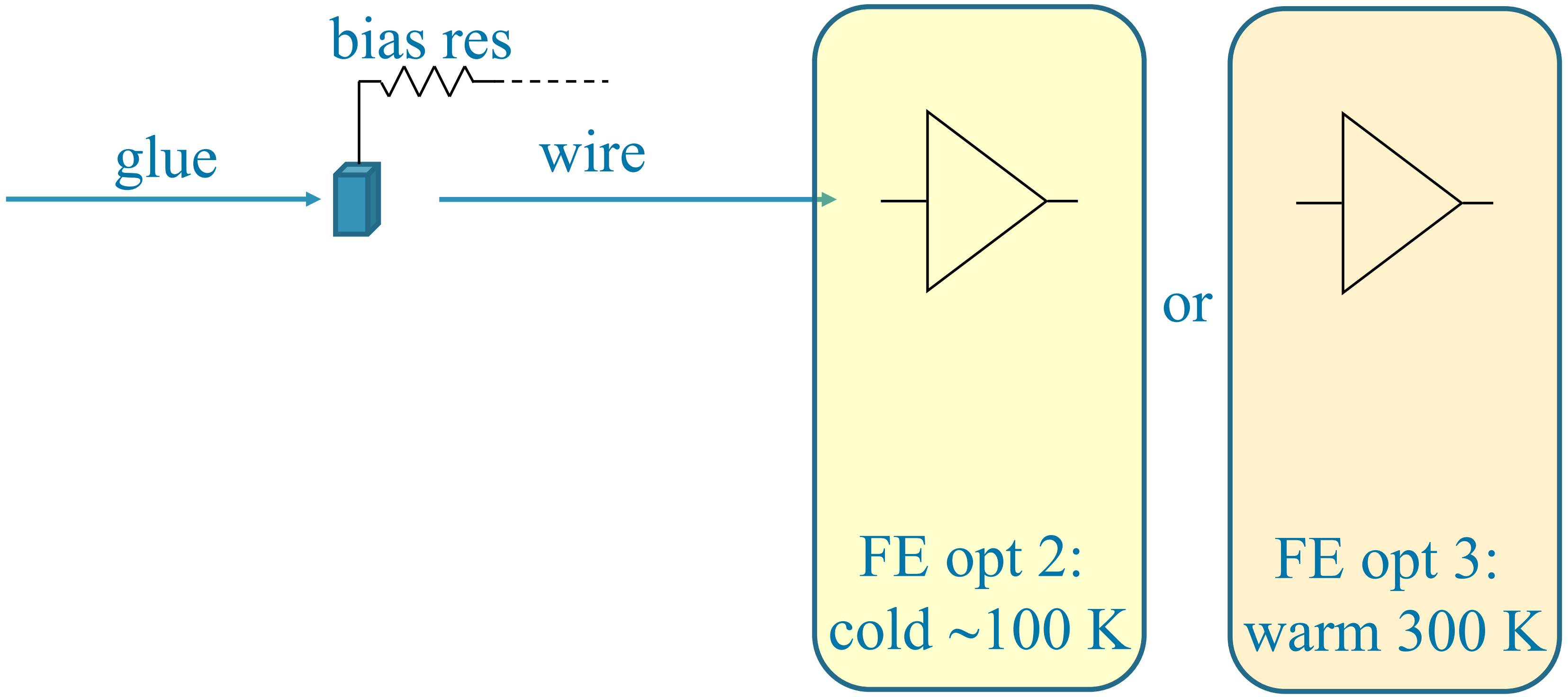

Medium or high impedance thermistors mean values ranging from a few hundred KΩ to a few hundred MΩ.

An important aspect is the bias resistance of the thermistor. It must have a value of about ten times that of the thermistor in order not to lose signal amplitude, but it is almost impossible to find stable high values resistors capable of working at deep cryogenic temperatures.

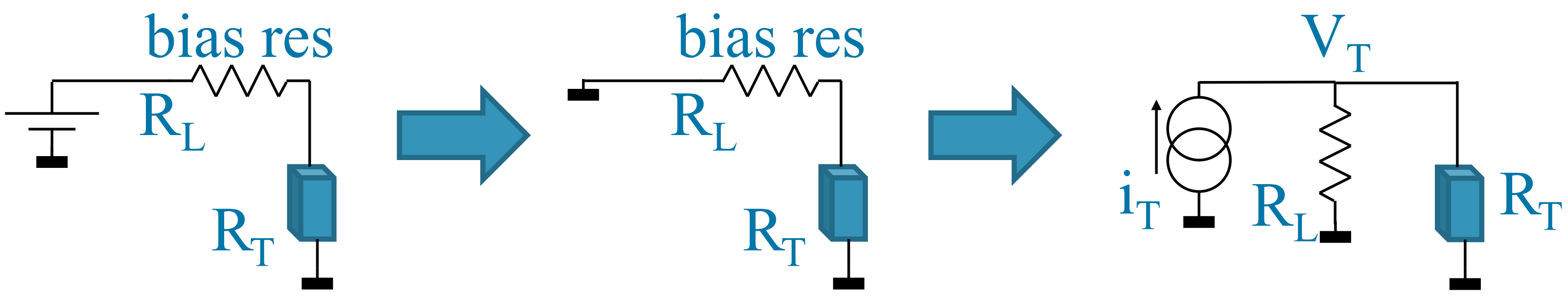

$$V_T = \frac{R_T R_L}{R_T + R_L} i_T \underset{R_L=10R_T}{\approx} 0.9\ i_T$$

Deep cryogenic medium to high impedance sensors 6

If the bias resistor is used at higher temperatures, its value must be much higher so as not to add noise:

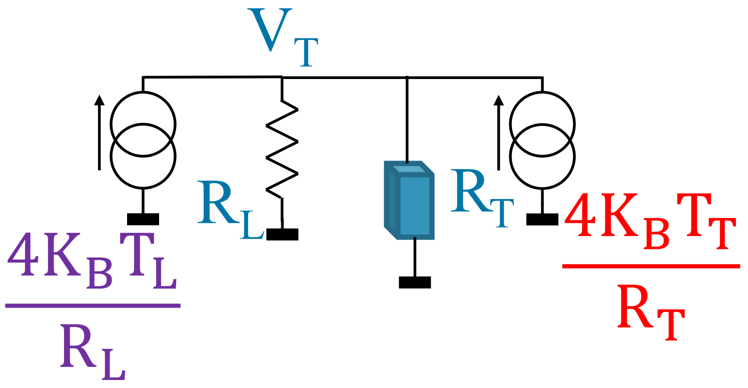

$$\frac{4K_B T_{thermistor}}{R_{thermistor}} \gg 4K_B \frac{T_{biasresistor}}{R_{biasresistor}}$$

thermistor noise   bias resistor noise

$$\Rightarrow \quad R_{biasresistor} \gg \frac{T_{biasresistor}}{T_{thermistor}} R_{thermistor}$$

For example, if $T_{biasresistor}$=300 K and $T_{thermistor}$=10 mK you get $T_{biasresistor}/T_{thermistor}$=30000, or 30 GΩ when $R_{thermistor}$ is 1 MΩ.

This means that very often the bias resistor operates mismatched and is the main source of noise.

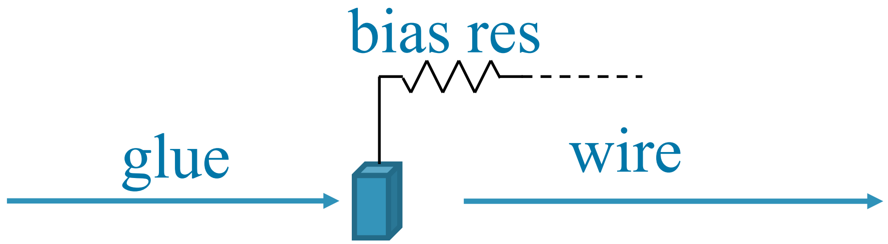

Signals from medium and large absorbers range from a few tens of Hz to a hundred KHz.

The 1/f noise must be low, which precludes the adoption of III-V devices operated at cold, with few exceptions.

The common solution is Si-JFETs operated at their optimum temperature, around and above 100 K, or Si-JFETs operated at room temperature.

The discrimination between cold or warm input stage is given by the bandwidth / wire capacitance relation.

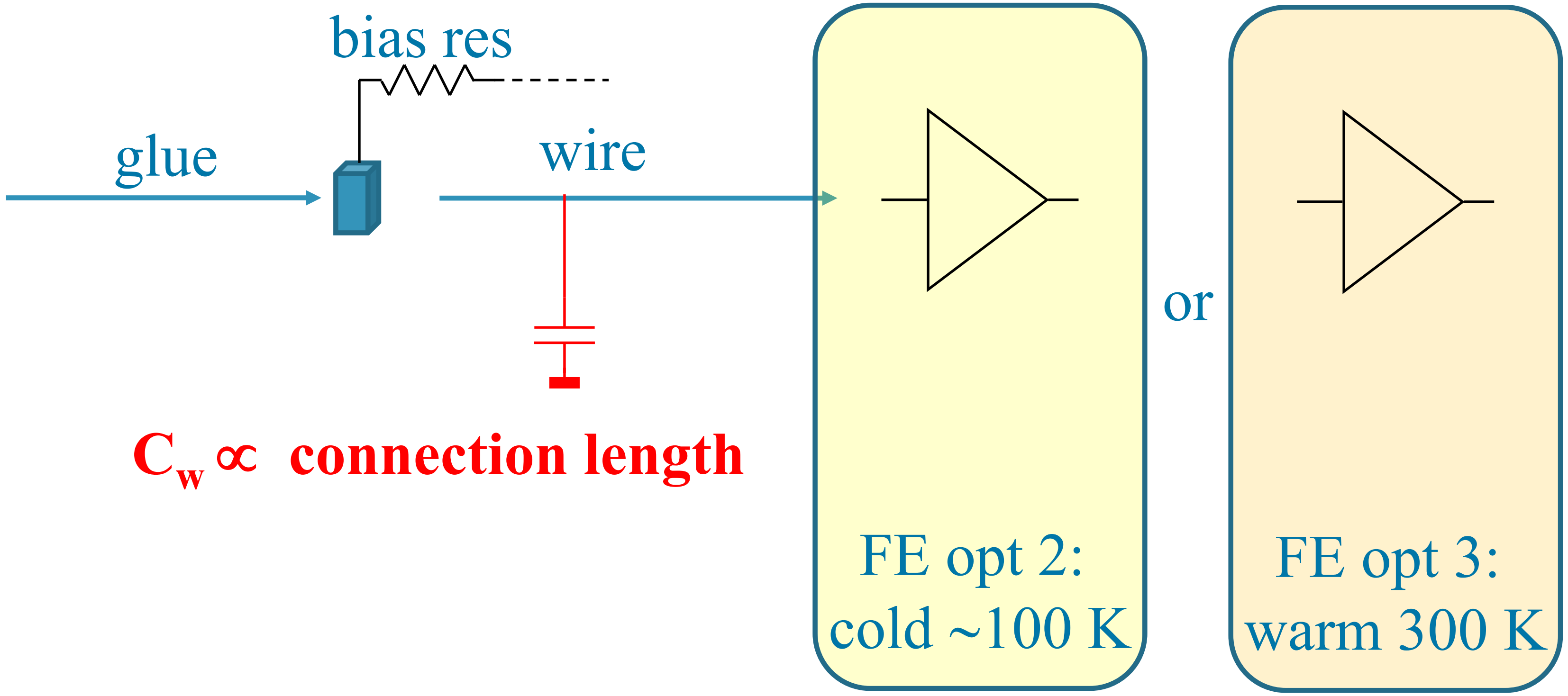

Front-end for medium and large impedance thermistors must shows low parallel noise.

Series noise must be low especially for medium value impedances.

In all cases, 1/f noise must be small.

$$\overline{e_A^2} = \overline{e_{White}^2} + \frac{A_f}{f}$$

$$\overline{i_A^2} = 2qI + \frac{I_f}{f}$$

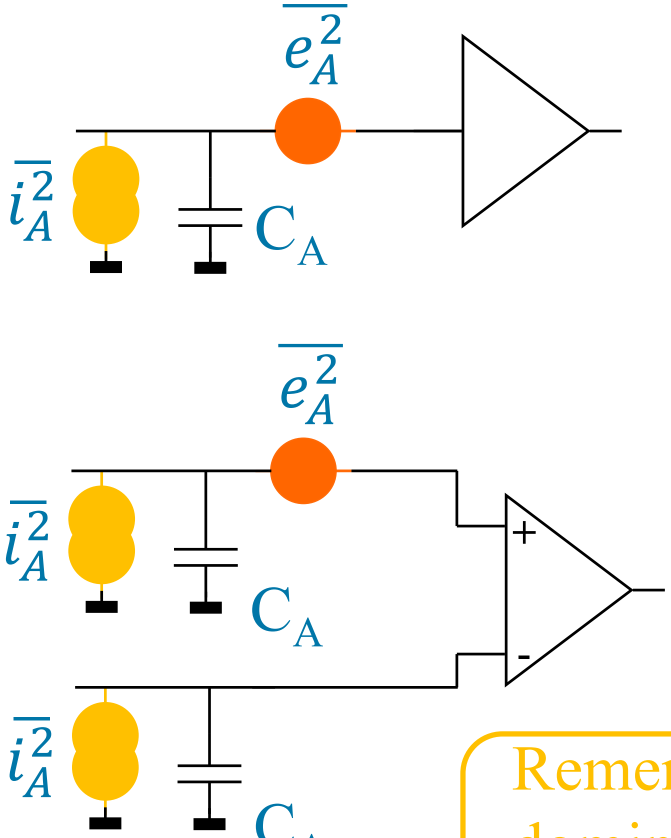

Very very often the solution is for a cryogenic input stage, single ended or differential:

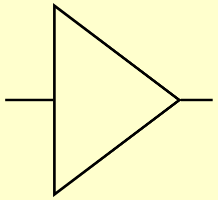

FE opt 2: cold ~100 K

Remember: an important, if not the dominant, source of (parallel) noise is the detector bias resistor:

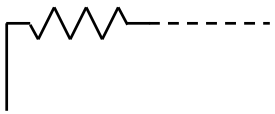

FRONT-END FOR MEDIUM VALUES THERMISTORS AND ABSORBERS

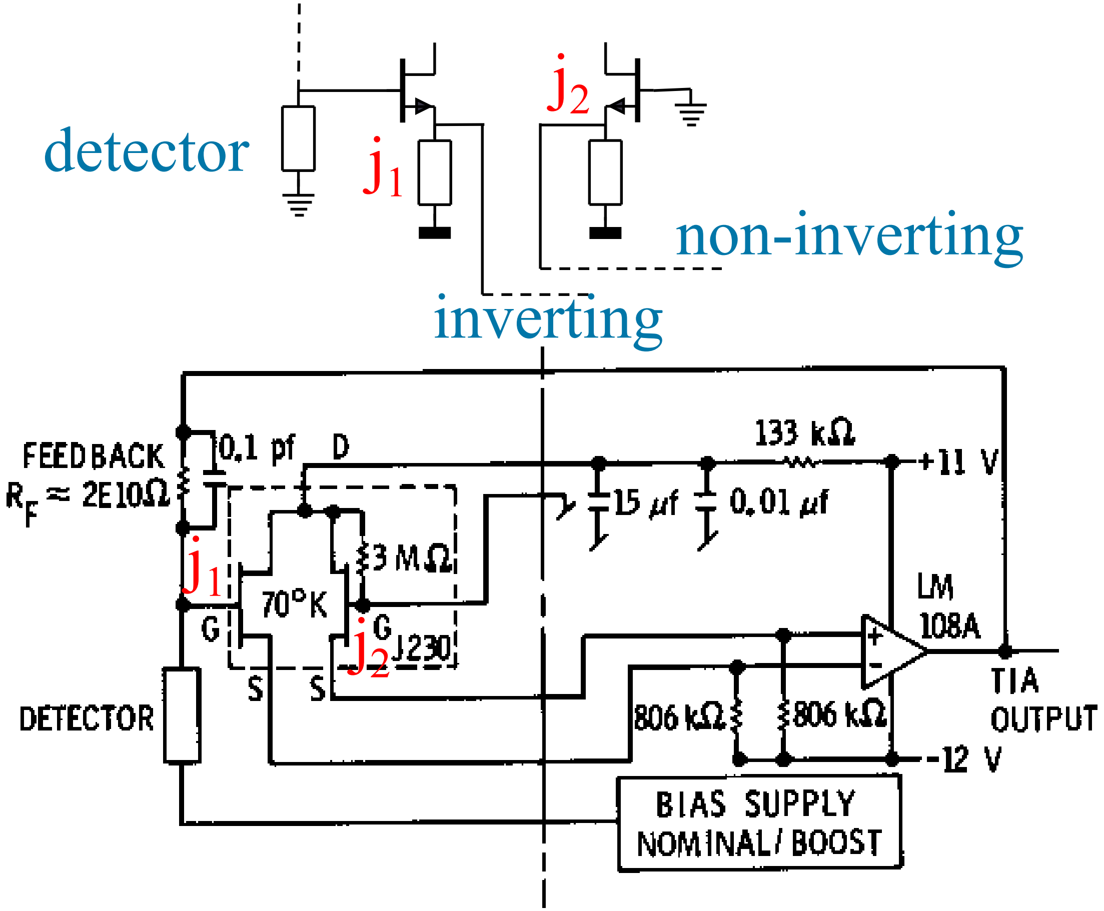

https://lambda.gsfc.nasa.gov/product/iras/docs/exp.sup/ch2/C5.html#tabC6 and Proc. SPIE 0445, Instrumentation in Astronomy V, (9 January 1984); doi: 10.1117/12.966154

According to Dan McCammon, the first use of a cryogenic configuration was with the IRAS (NASA) infrared satellite. The readout was for photodetectors read by a thermistor.

A pair of Si-JFET, J_1 and J_2, (in follower configuration) was placed at cold, “close” to the detector. J_2 is there only to generate an offset.

A second warm stage implemented a trans-impedance feedback with a 20 GΩ feedback resistor (Eltec model 102 metal film) maintained at 2 K.

Front-end For Medium Values Thermistors And Absorbers 2

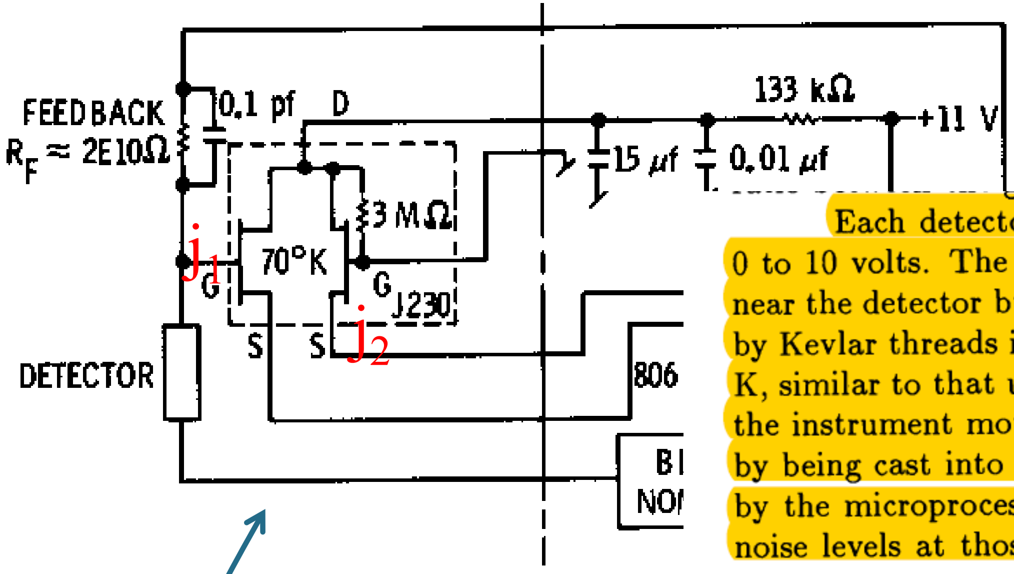

J.C. Mather, at al, Event: SPIE's 1993 International Symposium on Optics, Imaging, and Instrumentation, 1993

Each detector is biased through a load resistor of 40 MΩ by a low noise DC voltage supply, adjustable from 0 to 10 volts. The detector voltage is measured through a JFET source follower amplifier (gain ~ 0.995) mounted near the detector but thermally isolated from it. The amplifier uses dual JFETs connected in parallel, and suspended by Kevlar threads inside a copper can, so that the JFET bias power can heat it to an operating temperature of ~ 70 K, similar to that used for the *IRAS* detectors. Each amplifier has its own copper cooling strap directly attached to the instrument mounting flange. Wires into the bolometer housing are filtered against radio and microwave energy by being cast into an iron-loaded epoxy disk. Nevertheless, the detectors were sensitive to radio frequency emitted by the microprocessor clocks (~ 4 MHz), and beat frequency signals between different clocks were seen as excess noise levels at those frequencies despite efforts to provide additional external decoupling. Fortunately, these beat

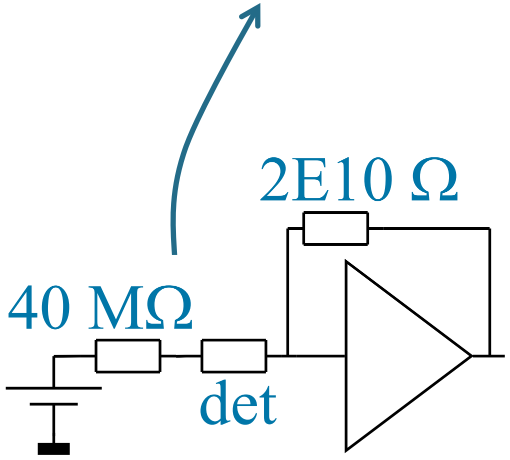

Note that the JFETs were operated at 70 K and special precautions were taken on the wiring so as not to inject thermal energy to the detector.

IRAS was the first spectrometer that used bolometers and cold-buffered first stage. Interesting: the clock noise of the μ-processor aboard the rocket was 4 MHz (1993).

Note that the J_2 generates only an offset, but add noise: this setup is not well optimized in this respect.

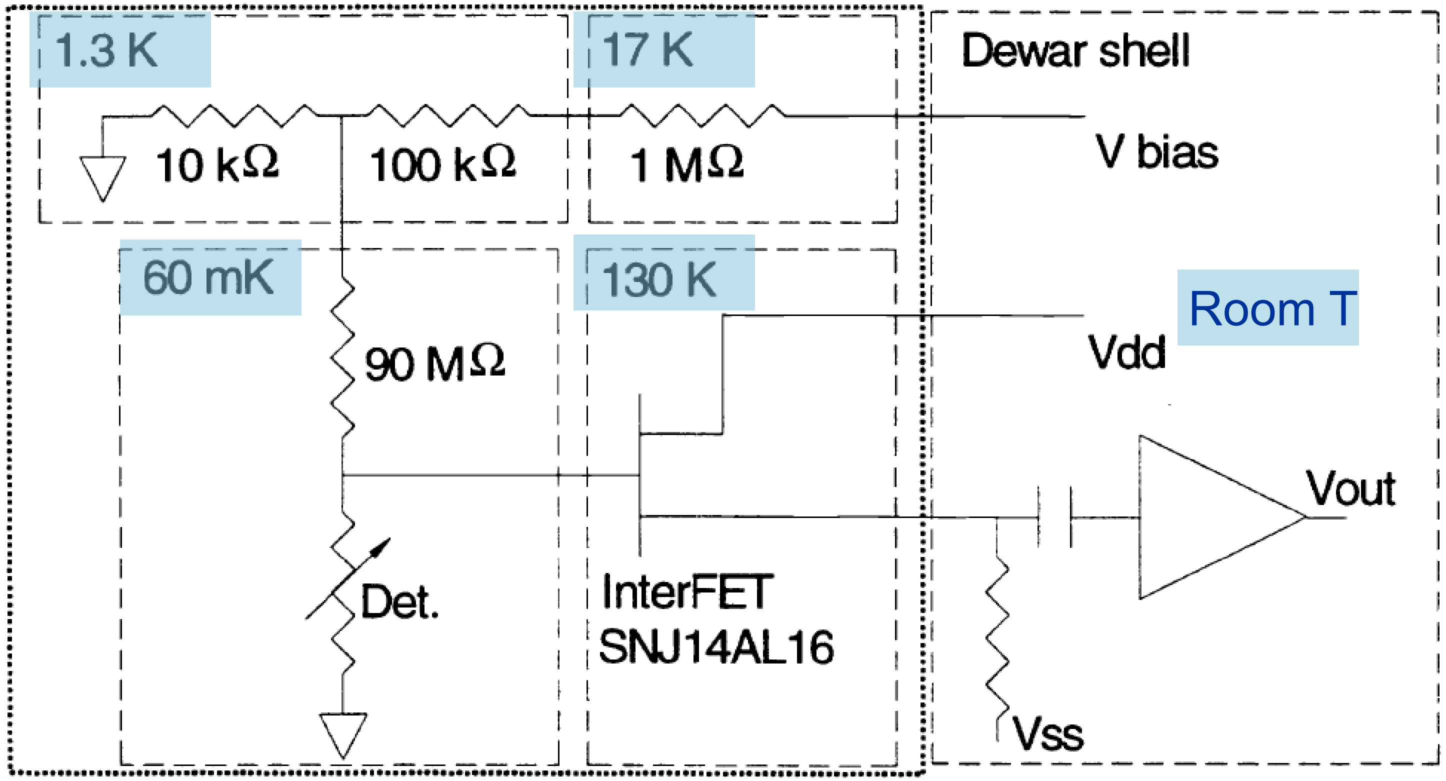

One of the first subsequent applications on cold reading is this one. Some of the details are interesting…

Proc. SPIE 7732, 2010,
doi: 10.1117/12.857888

Front-end For Medium Values Thermistors And Absorbers 4

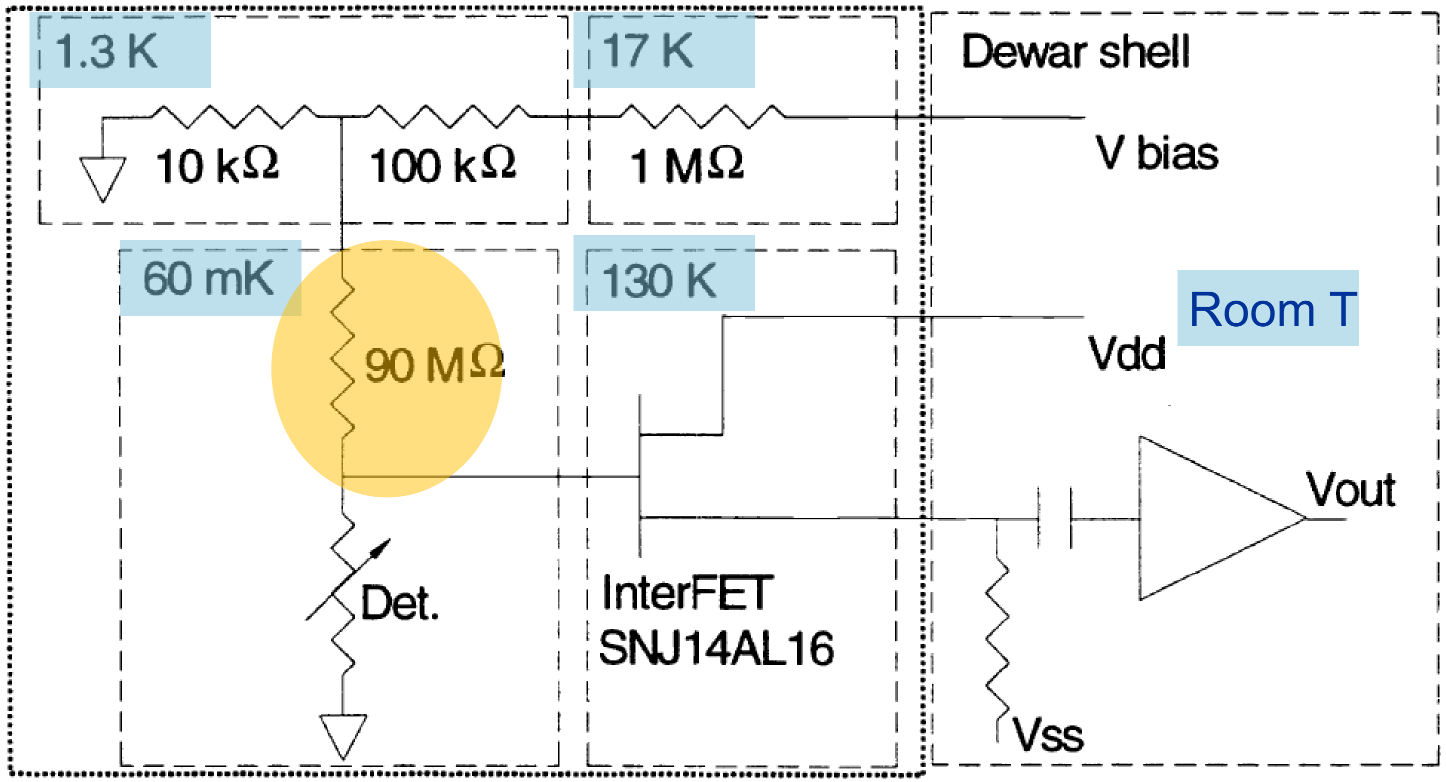

The setting minimizes parasitic capacitance by placing the load resistor at the same temperature as the detector and closed to it.

To work at low temperature, the load resistor must be metal film to ensure stability, and its value cannot be very large..

Proc. SPIE 7732, 2010,
doi: 10.1117/12.857888

Front-end For Medium Values Thermistors And Absorbers 5

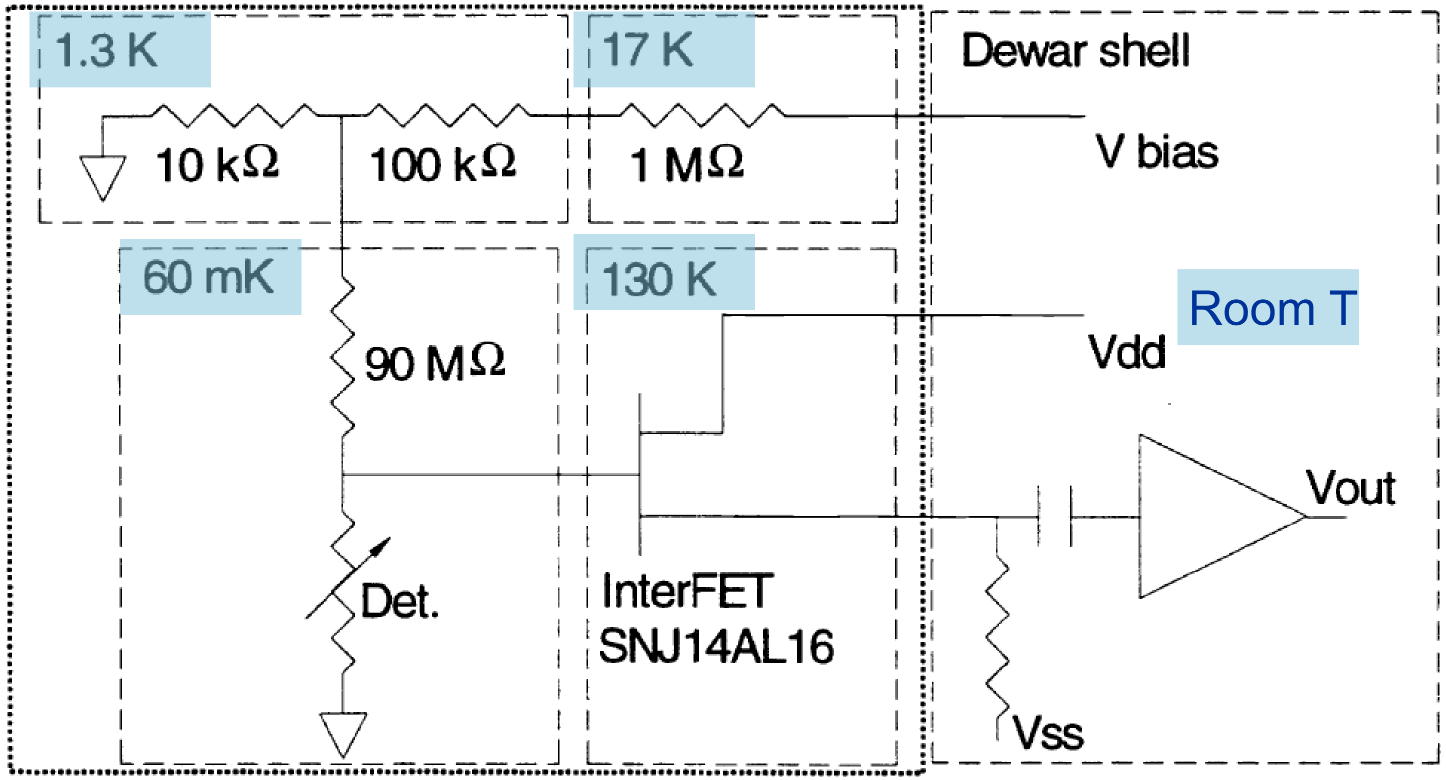

This configuration was used for readout detector arrays with an average resolution better than 5 eV_{FWHM} (see ref. below).

Proc. SPIE 7732, 2010, doi: 10.1117/12.857888

Proc. SPIE 3765, EUV, X-Ray, and Gamma-Ray Instrumentation for Astronomy X, (22 October 1999); doi: 10.1117/12.366556

Front-end For Medium Values Thermistors And Absorbers 6

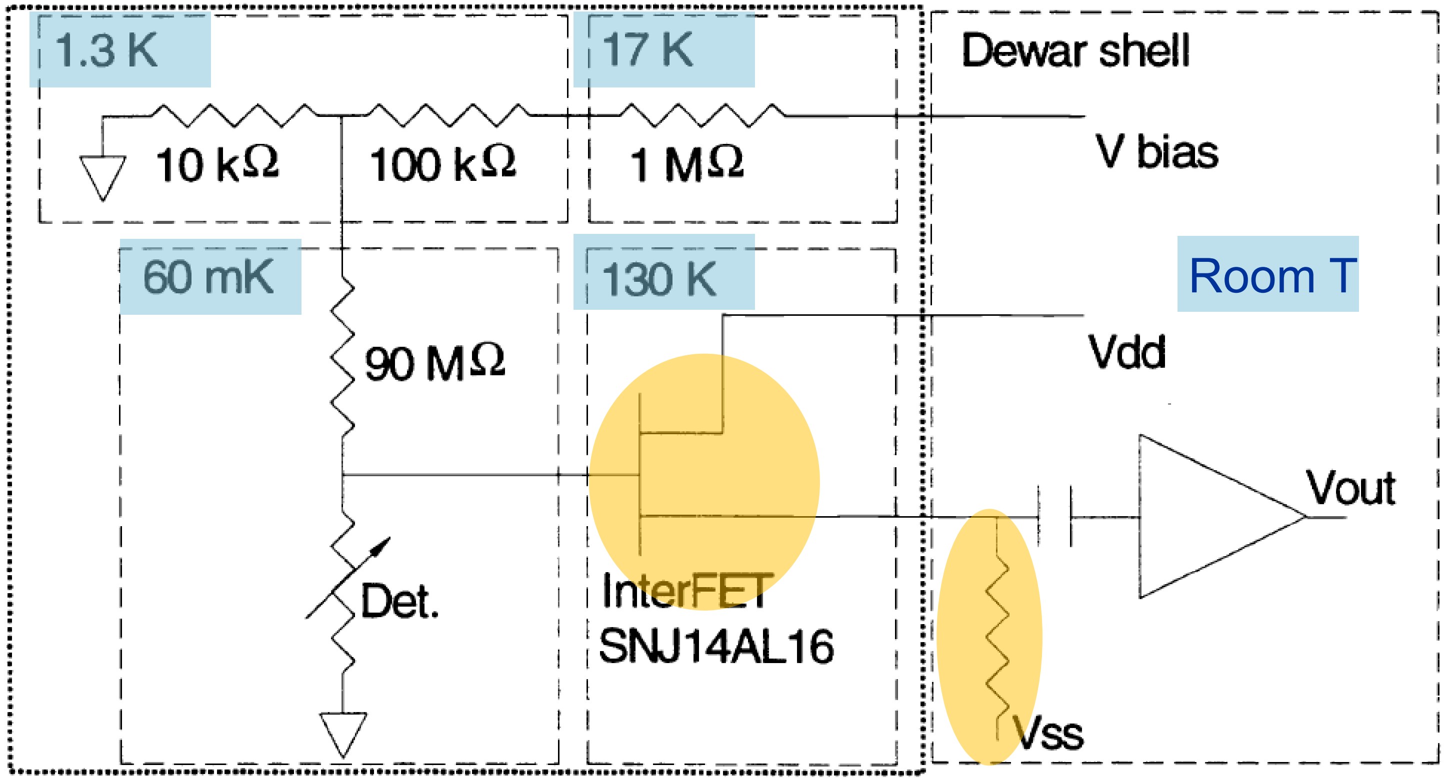

The detector signal is slow and III - V and Si-MOS compound devices have low-frequency noise that can be a limitation; Si-JFET transistors are most often used at their optimum temperature between 120 K and 150 K. They are normally configured common-source, unity-gain (to avoid a long feedback path from room temperature to the inside of the refrigerator) with their bias resistor at room temperature to minimize cold power dissipation.

TIP: The value of the bias resistor connected to the source terminal must be large enough, otherwise its thermal noise is not negligible.

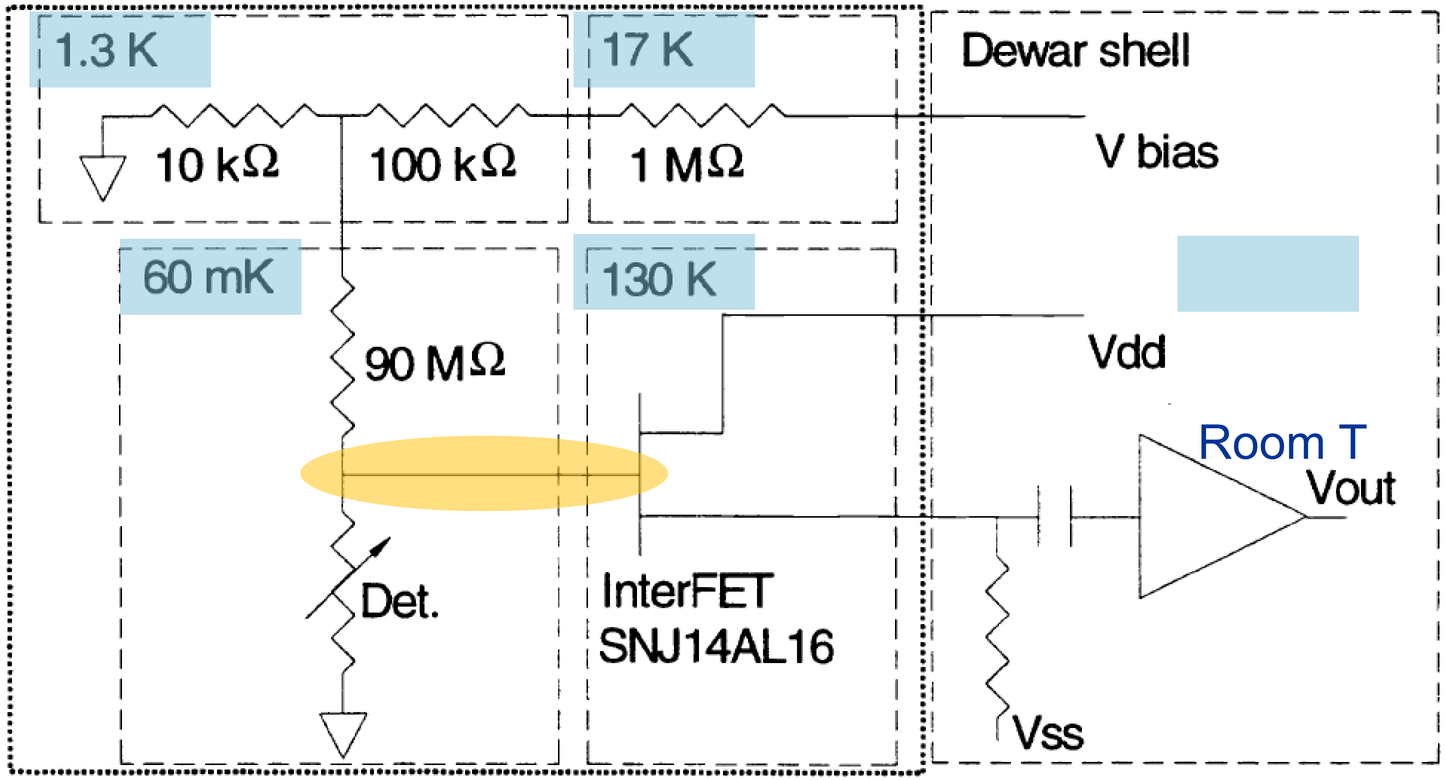

The connection between the JFET and the detector must be short, and the connection must ensure negligible heat injection from the large thermal gradient.

The JFETs are in a box, suspended, for example, with Kevlar cables, to minimize thermal conductance to the bath and create their working environment.

Often a heater is placed near them to give an initial temperature rise, then their dissipation is able to maintain the operating temperature. The connection to the detector should also minimize microphonic effects.

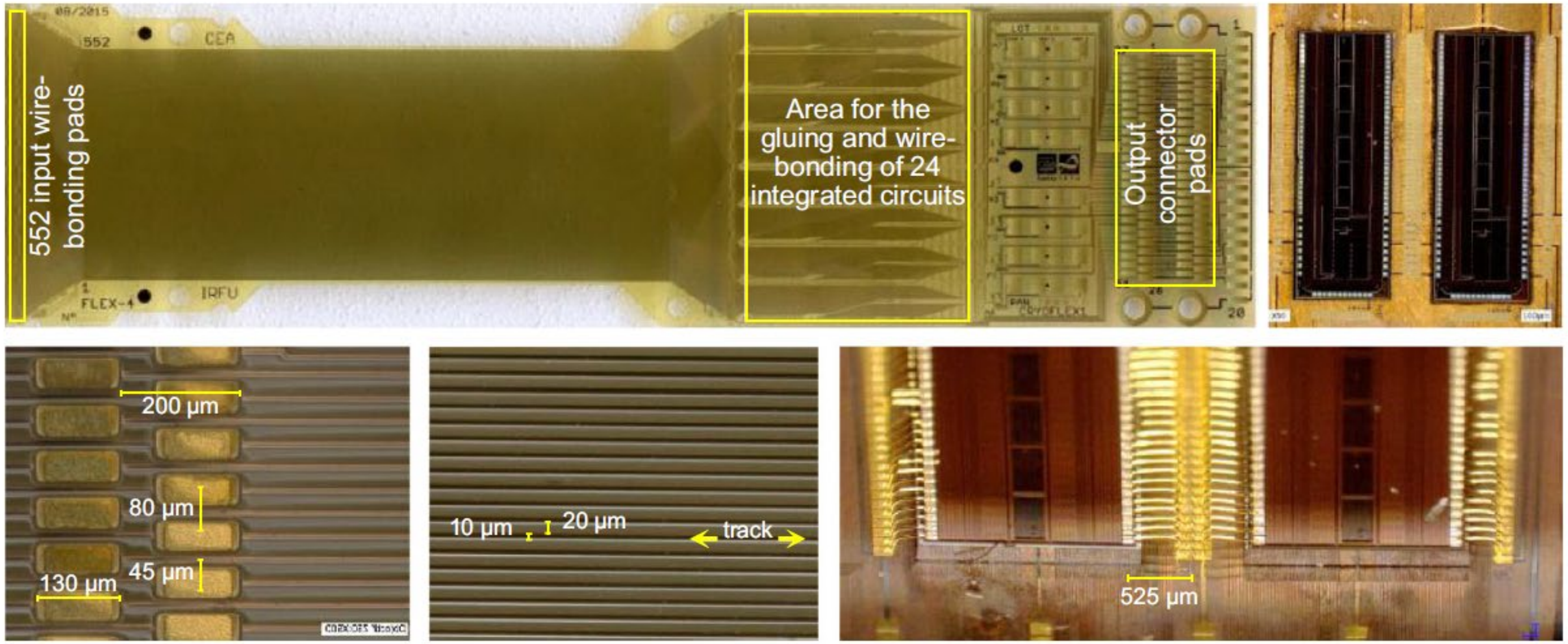

Here is an example of a very dense connection made with superconducting tracks and polyimide substrate to maximize thermal insulation in the readout of a high impedance TES sensor array.

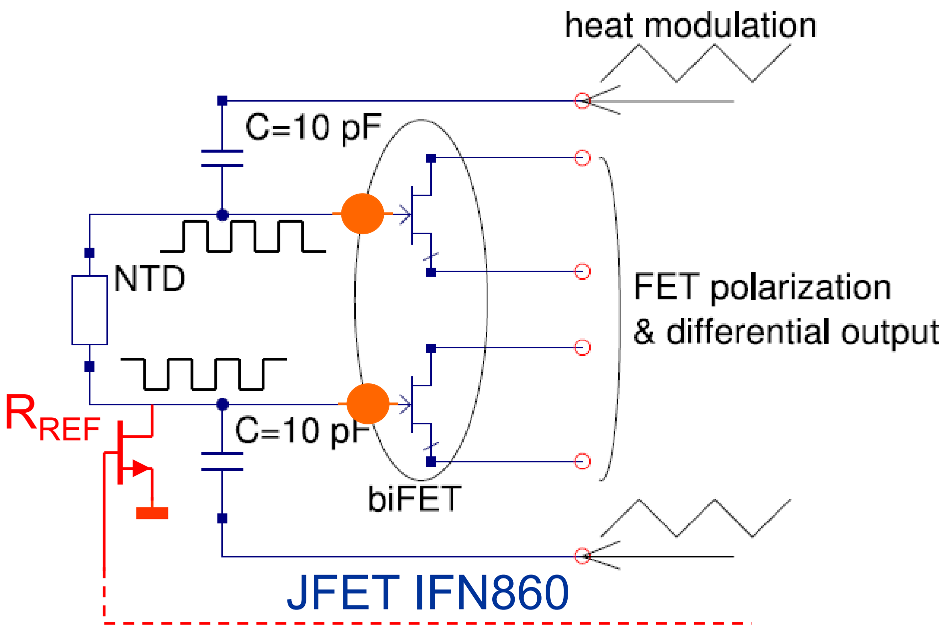

The EDELWEISS experiment attempted to mitigate the low-frequency noise in series at the JFET gate held a coled with an AC bias: the detector signal modulates the AC bias while the noise in series does not, so that its contribution is that at the modulation frequency, where there is no low-frequency noise, just as we saw with dc-squid.

To maintain symmetry the bias is differential given through 2 small capacitances: the AC bias is triangular and integrated across the capacitances in order to become a square signal.

Remember:

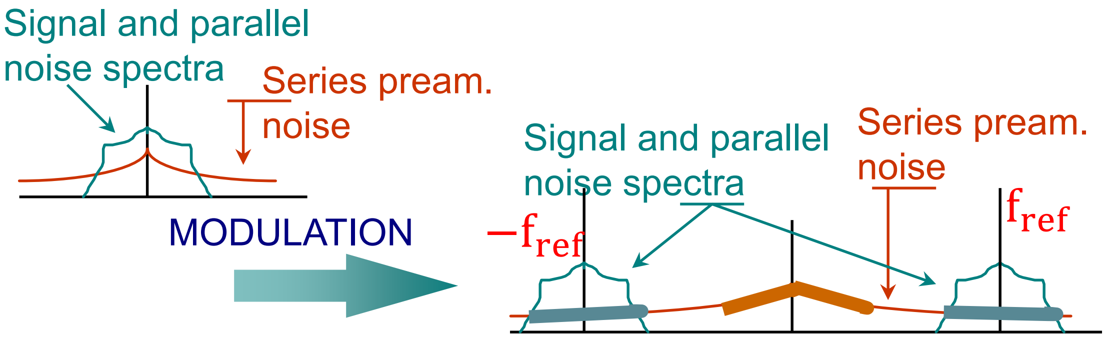

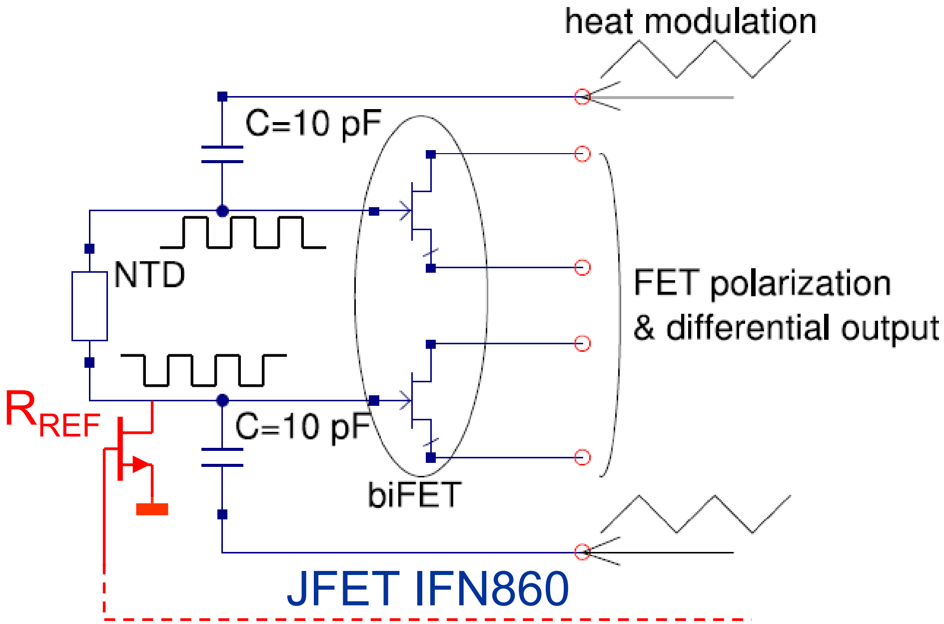

A reference resistor is required to establish the ground reference, but it does not have to be accurate and stable.

To maintain symmetry, they used a cut-off biased JFET obtaining a resistance value above 10^{12} to 10^{13} Ω.

Front-end For Medium Values Thermistors And Absorbers 11

JINST 2017 **12** P08010

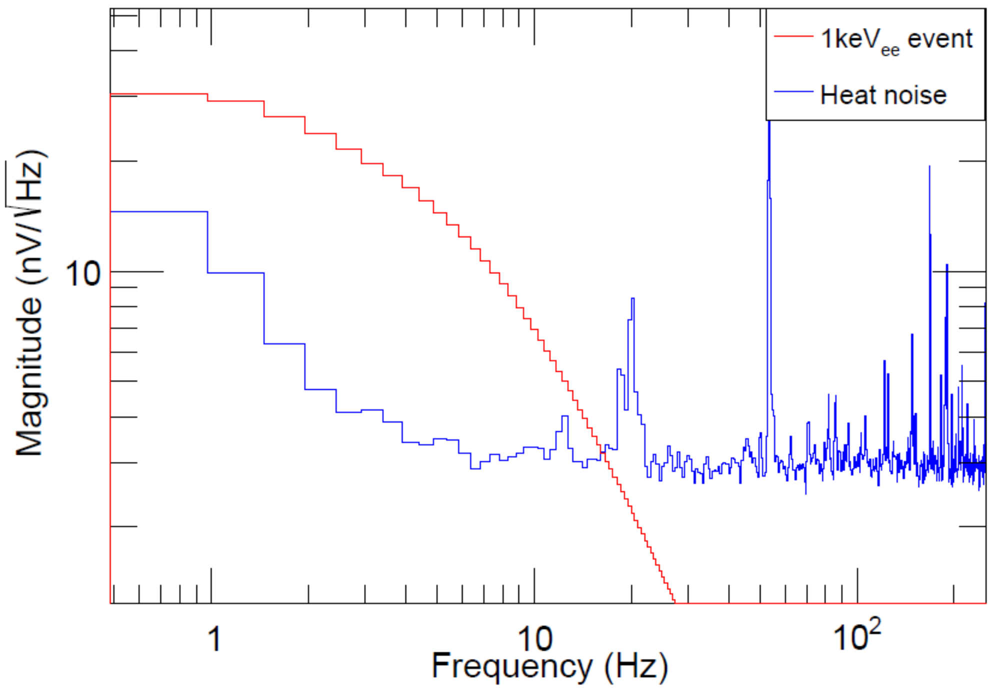

The noise result is quite good. The bias frequency is between 500 Hz and 1 KHz (I do not know the value adopted for the measurement of this plot).

The low-frequency noise mitigation seems efficient: the signal spectrum is shown for comparison.

The residual low-frequency noise could result from the friction of the detector and the vibration of the wire, that is, the parallel noise that is not mitigated by modulation. This residual effect limits the final resolution in various applications.

In this situation, the solution adopted is often the front-end operating at room temperature, especially for large detector arrays.

The connection between the detector and the front-end is long, a couple of meters and more, and the parasitic capacitance is large.

There is no matching impedance, and the signal bandwidth is generally small, at most a few KHz..

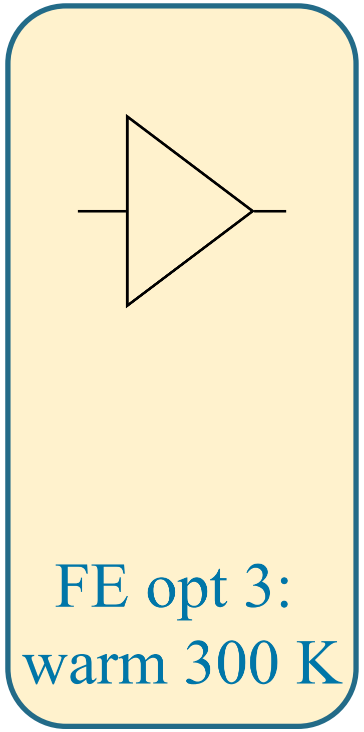

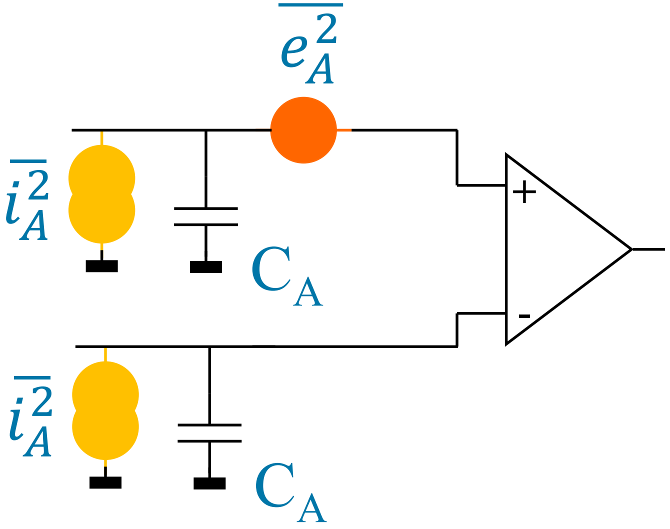

The preamplifier is differential voltage input (mitigation of cross talk for array readout).

Front-end for large values thermistors and absorbers 2

- ✓ The reasons for tolerating large impedances and also large parasitic capacitances are several:

- ✓ A very large dynamic range of signals, typical in neutrino physics studies, which extends from a few KeV up to a few tens of MeV asks for thermistors that can handle large signals;
- ✓ Low background, if required, finds benefit if the front-end is operated far from the detector;
- ✓ The detector is composed of a large-mass crystal to which the thermistor is glued: to reduce its heat capacity to a minimum, the temperature must be as small as possible, less than 10 mK;
- ✓ Crystals are large and several: heat injection must be minimized;
- ✓ …

Effective choice for front-end location: room temperature, very safe for background.

Possible location of the front-end, mixing chamber and above the lead scield.

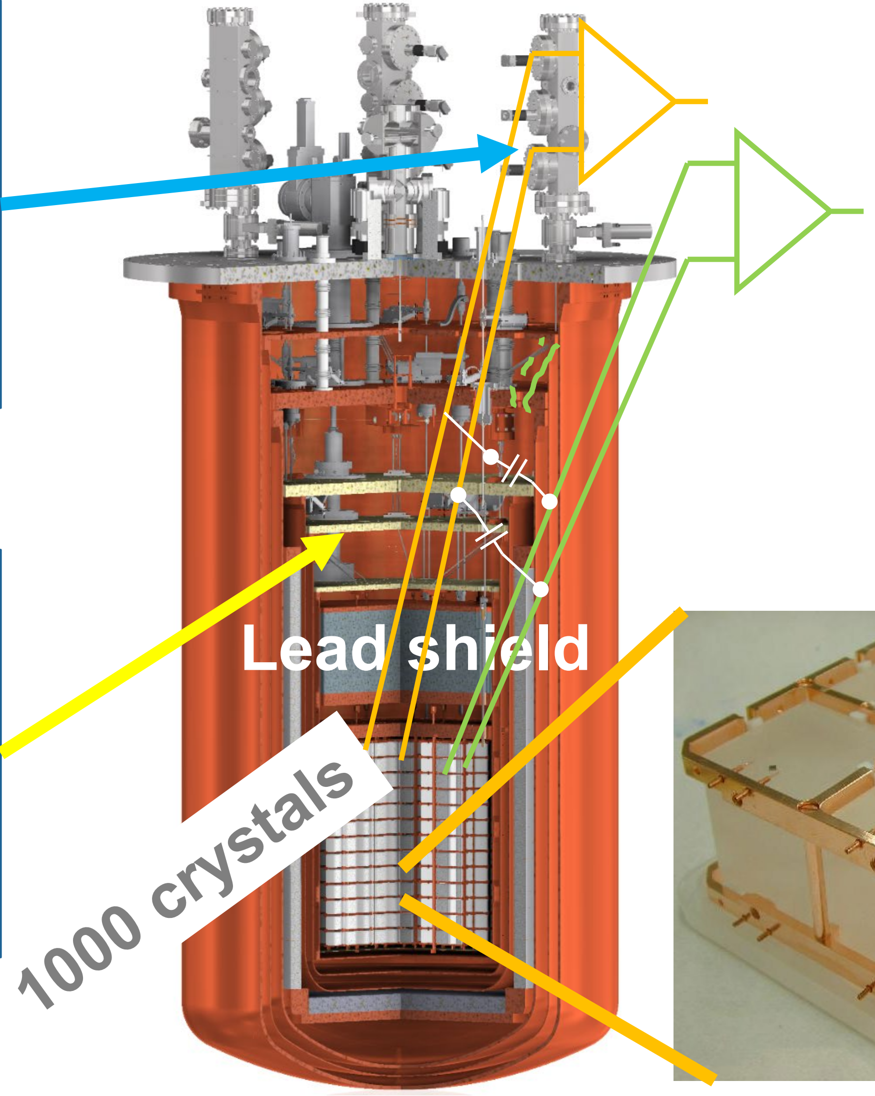

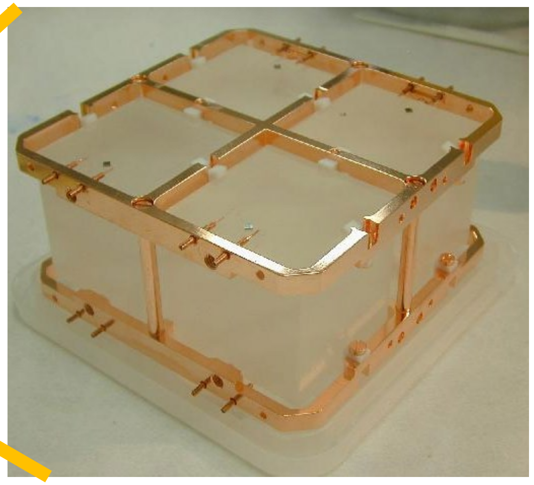

CUORE is an example of a rigorous requirement of low background.

It consists of 1000 TeO_2 crystals with a mass of 750 g each.

The thermal sensors are NTD thermistors with high resistance values.

Front-end for large values thermistors and absorbers 4

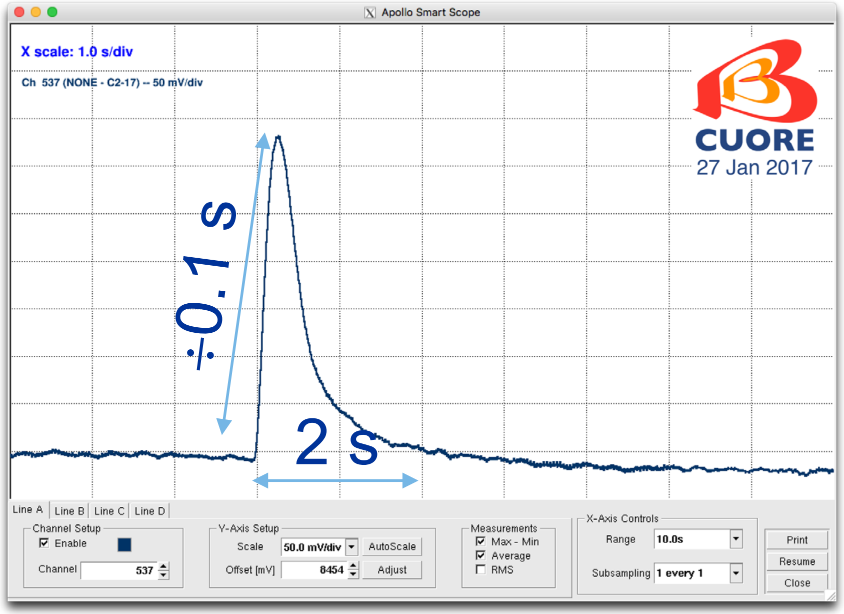

To meet the background, everything in CUORE is macroscopic:

- ✓ The BW of the signal is less than 5 Hz;
- ✓ The value of thermistor impedances are a few hundred MΩ on average;
- ✓ Load resistances at room temperature are 60 GΩ to attenuate parallel noise;
- ✓ Input capacitance is about 500 pF;
- ✓ Very tight stability of the front-end baseline.

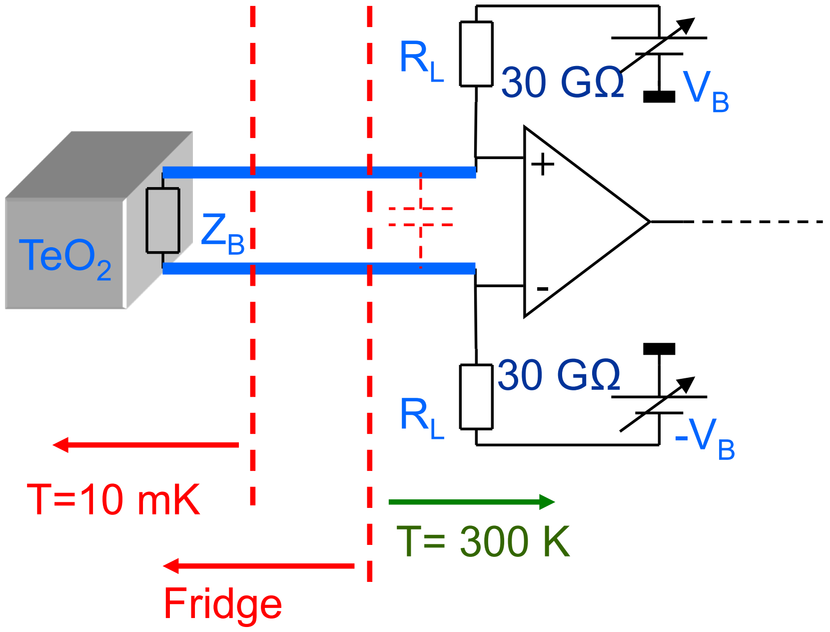

Parallel noise from load resistors is the dominant:

$$\sqrt{\overline{i^2_{\mathrm{LoadRes}}}} = 0.5\ \mathrm{fA}/\sqrt{\mathrm{Hz}}$$

Parallel noise from preamplifier input JFET is:

$$\sqrt{\overline{i^2_{\mathrm{Gate}}}} = 0.18\ \mathrm{fA}/\sqrt{\mathrm{Hz}}$$

Front-end for large values thermistors and absorbers 6

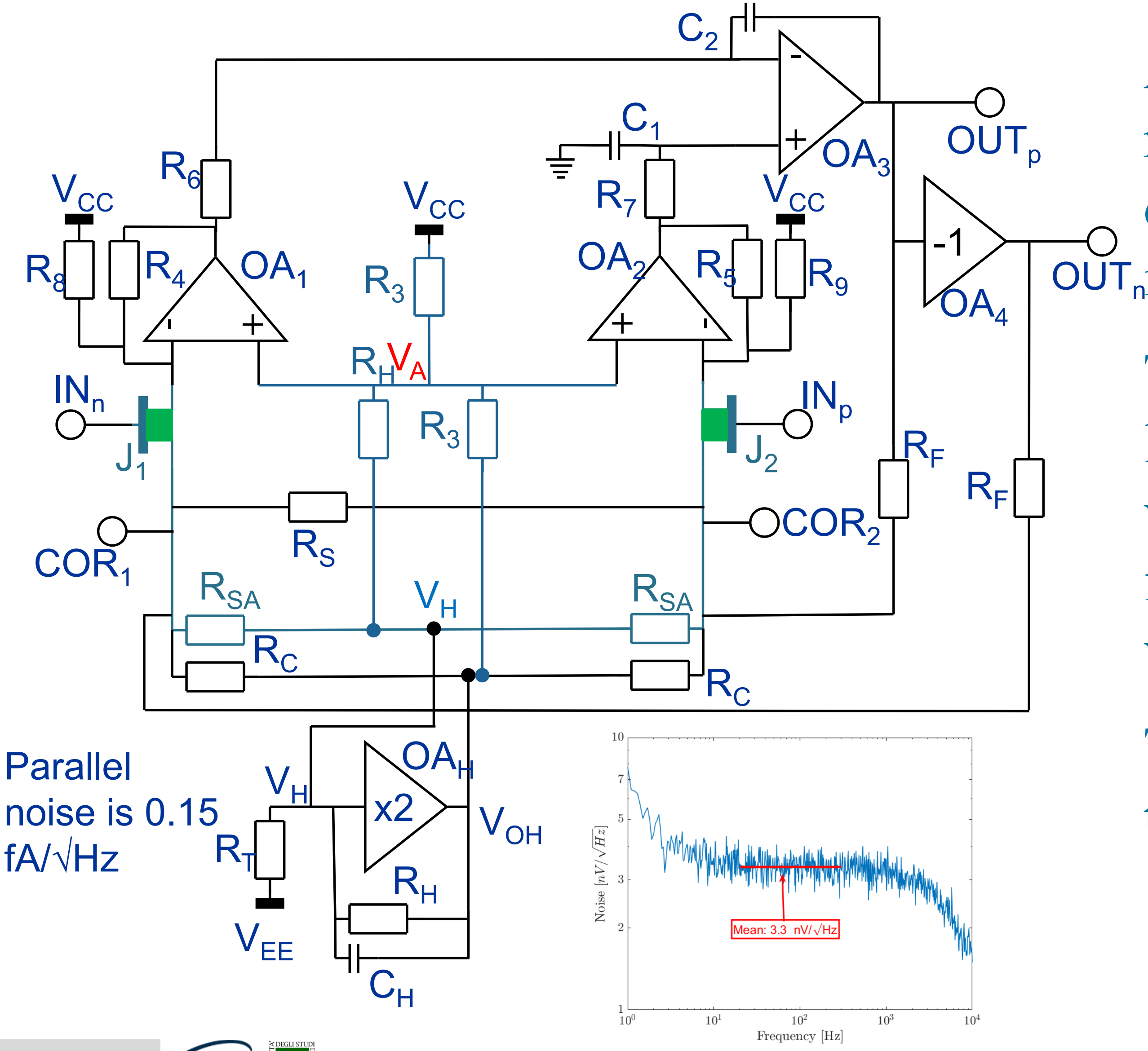

Parallel noise is 0.15 fA/√Hz

An example of a preamplifier operating at room temperature is this: the configuration is differential with only 2 JFETs, J_1 and J_2, at the input.

The circuit is designed to have a large open-loop gain (extensive use of OAs), to achieve a very precise large closed-loop gain, and to force the JFETs to work at constant current and voltage.

The circuit is thermally compensated, with a thermal drift of less than 1 μV/°C.

The preamplifier is not the only element of the setup to be contemplated.

For cryogenic arrays of detectors several parameters must be considered to be met:

- often, the spread in the energy conversion of every detector is compensated by biasing each detector individually;
- the base temperature must be maintained stable;
- residual temperature fluctuations over long periods affect the energy conversion and to mitigate this 2 strategies are considered:
  1) the baseline drift is monitored;
  2) stabilization pulses are sent periodically;

Electronics system 2

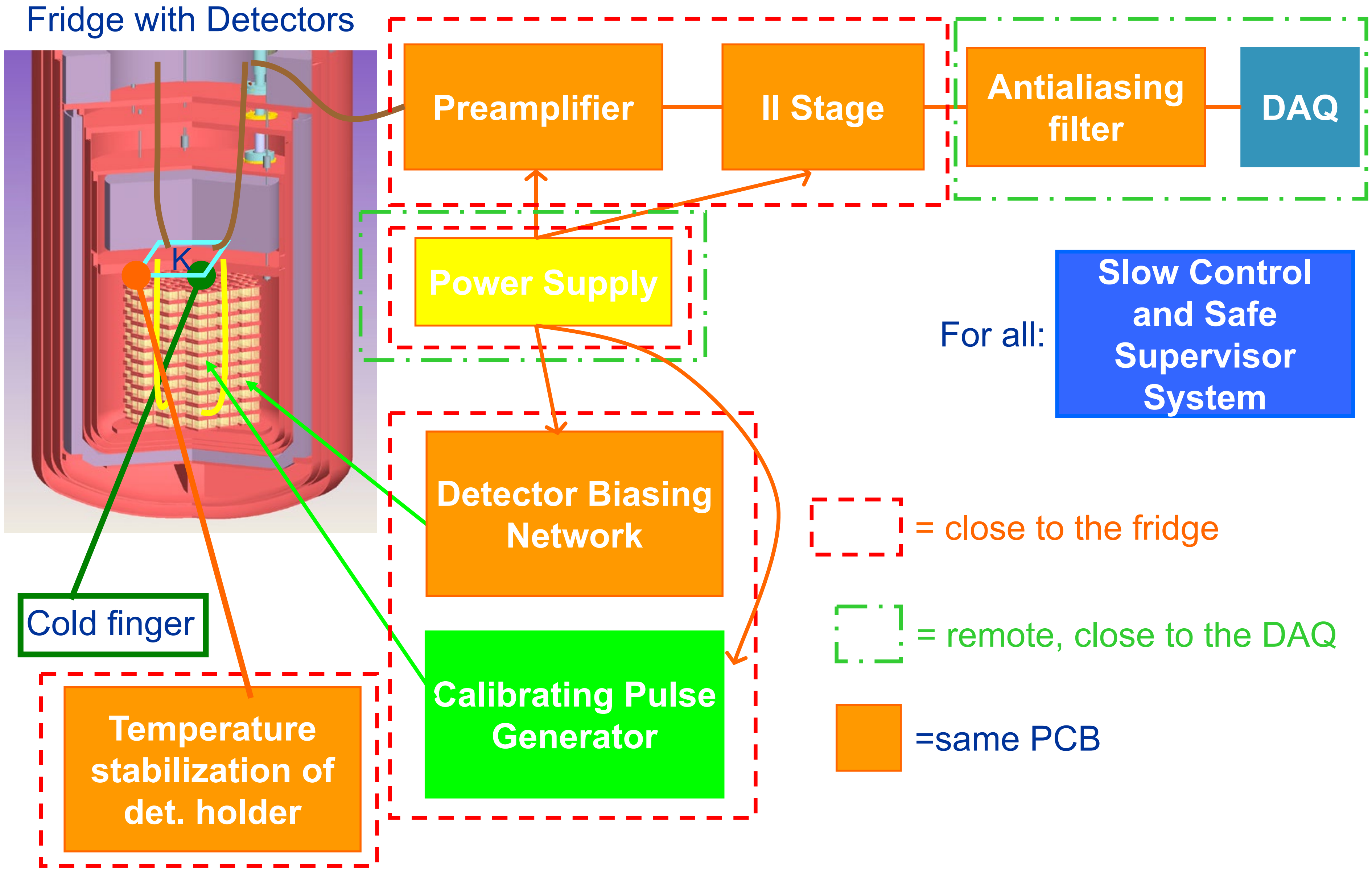

Here the electronic system organization of the CUORE experiment.

2018 JINST 13 P02026

Electronics system 3

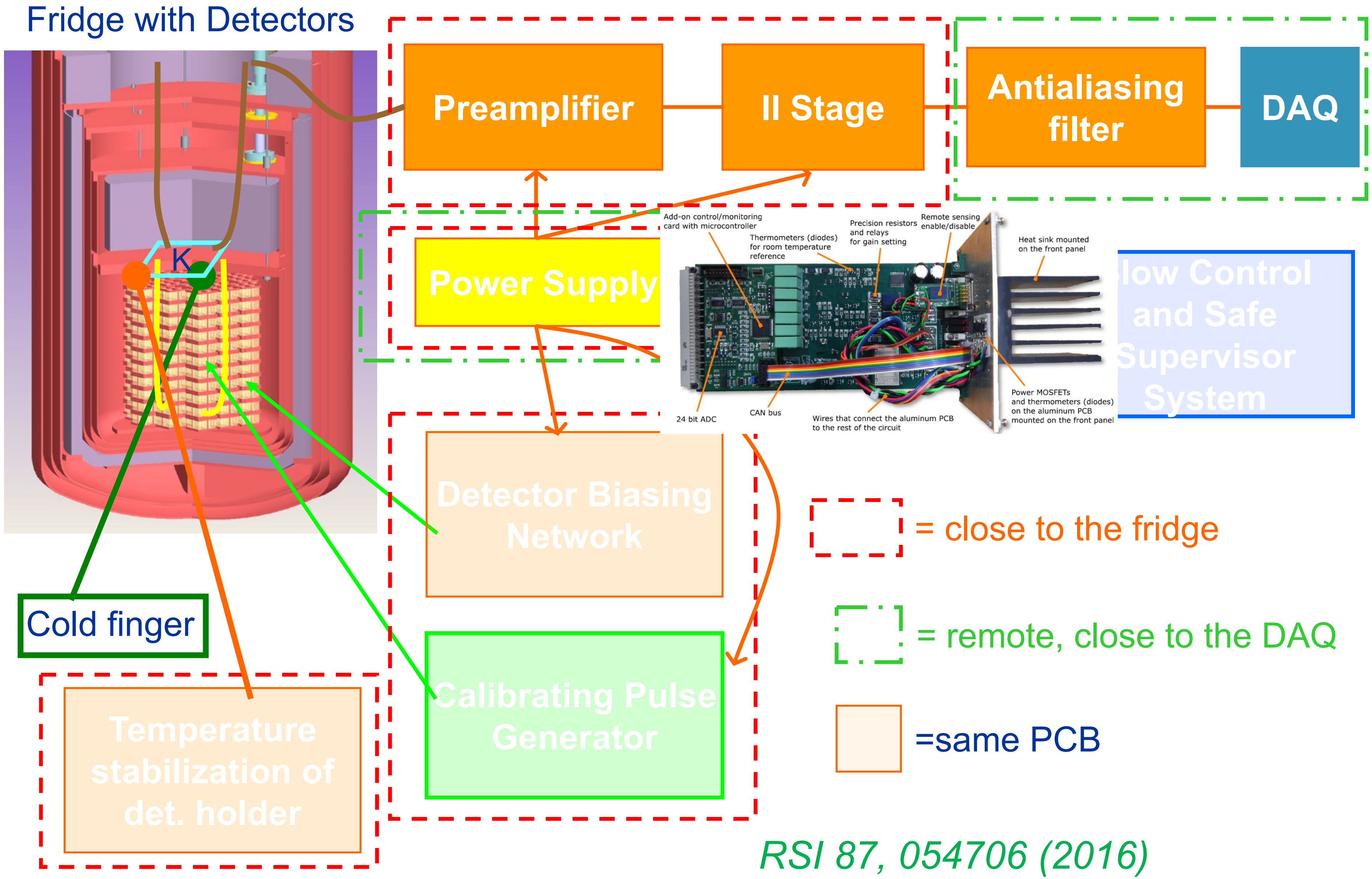

The amplification chain has the gain stable at a few ppm/°C, while the thermal drift of the preamplifiers is trimmed for being smaller than 1 μV/°C. This has been possible thank to the **power supply system** that operate as a low noise and 1 ppm/°C reference voltage.

RSI 87, 054706 (2016)
RSI 86, 124703 (2015)

Electronics system 4

Fridge with Detectors

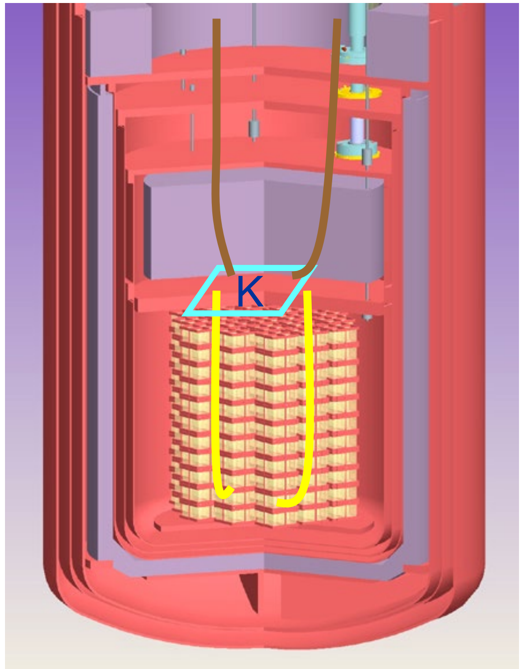

Power Supply

Power supply chain (one unit)

Commercial power supply

Low pass /protecting filter

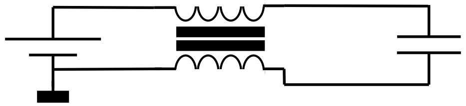

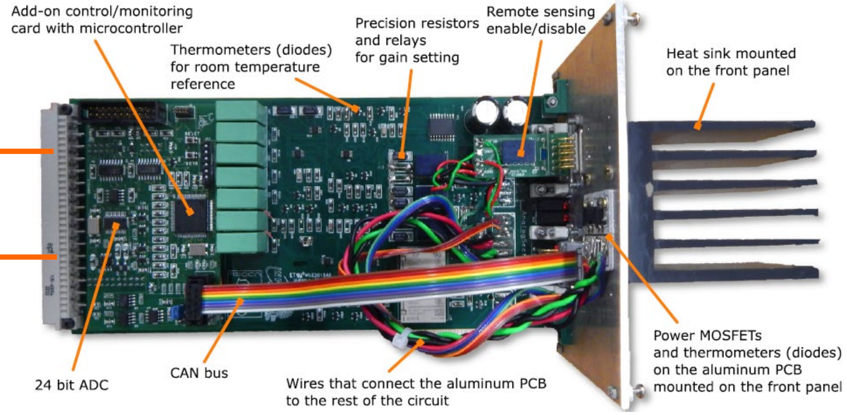

Electronics system 5

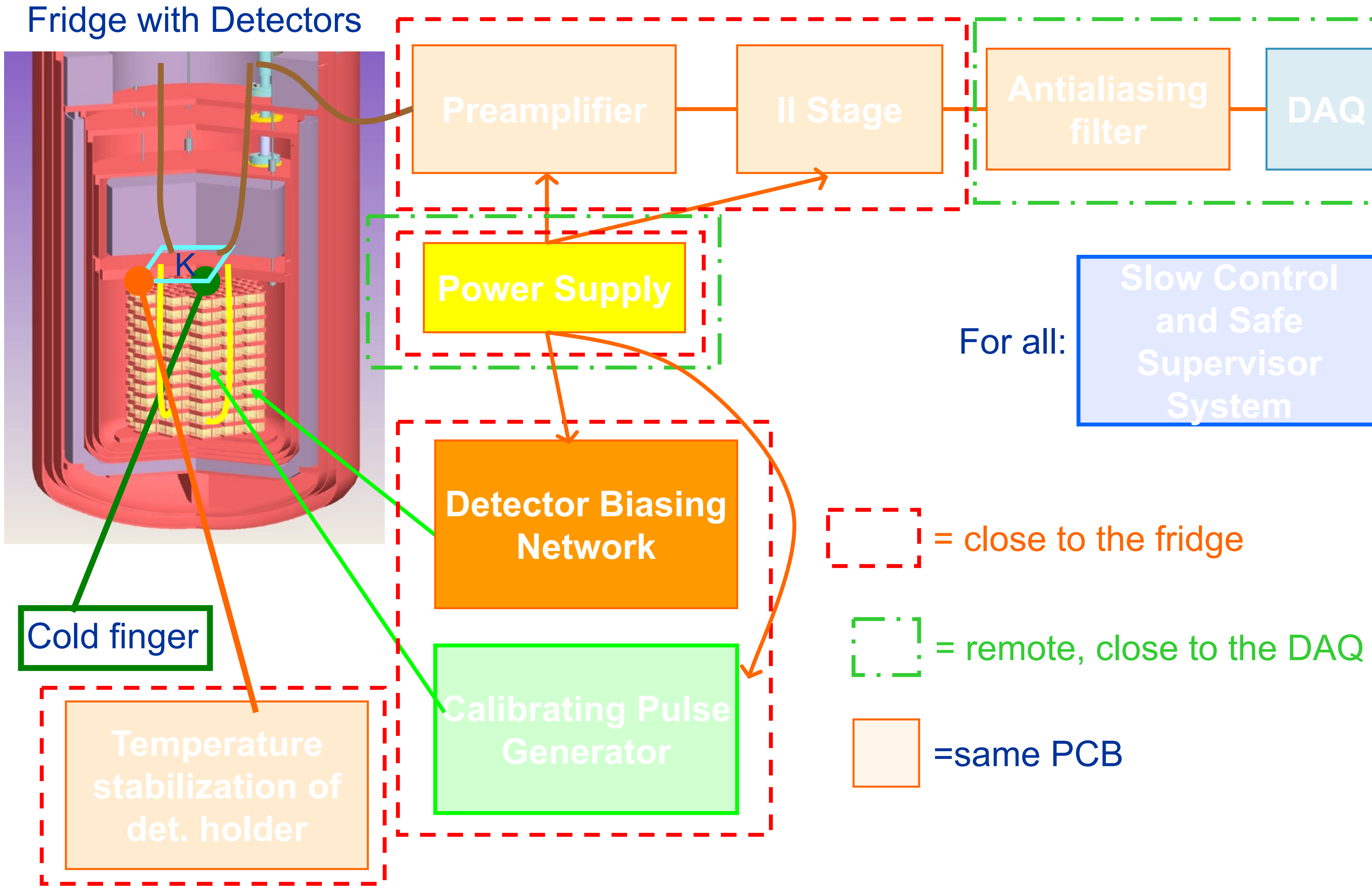

The detector biasing system was also designed to be stable below 50 ppm/°C and is able to generate up to 50 V (±25 V) of voltage to allow for the adoption of very large value load resistors (placed at room temperature).

Electronics system 6

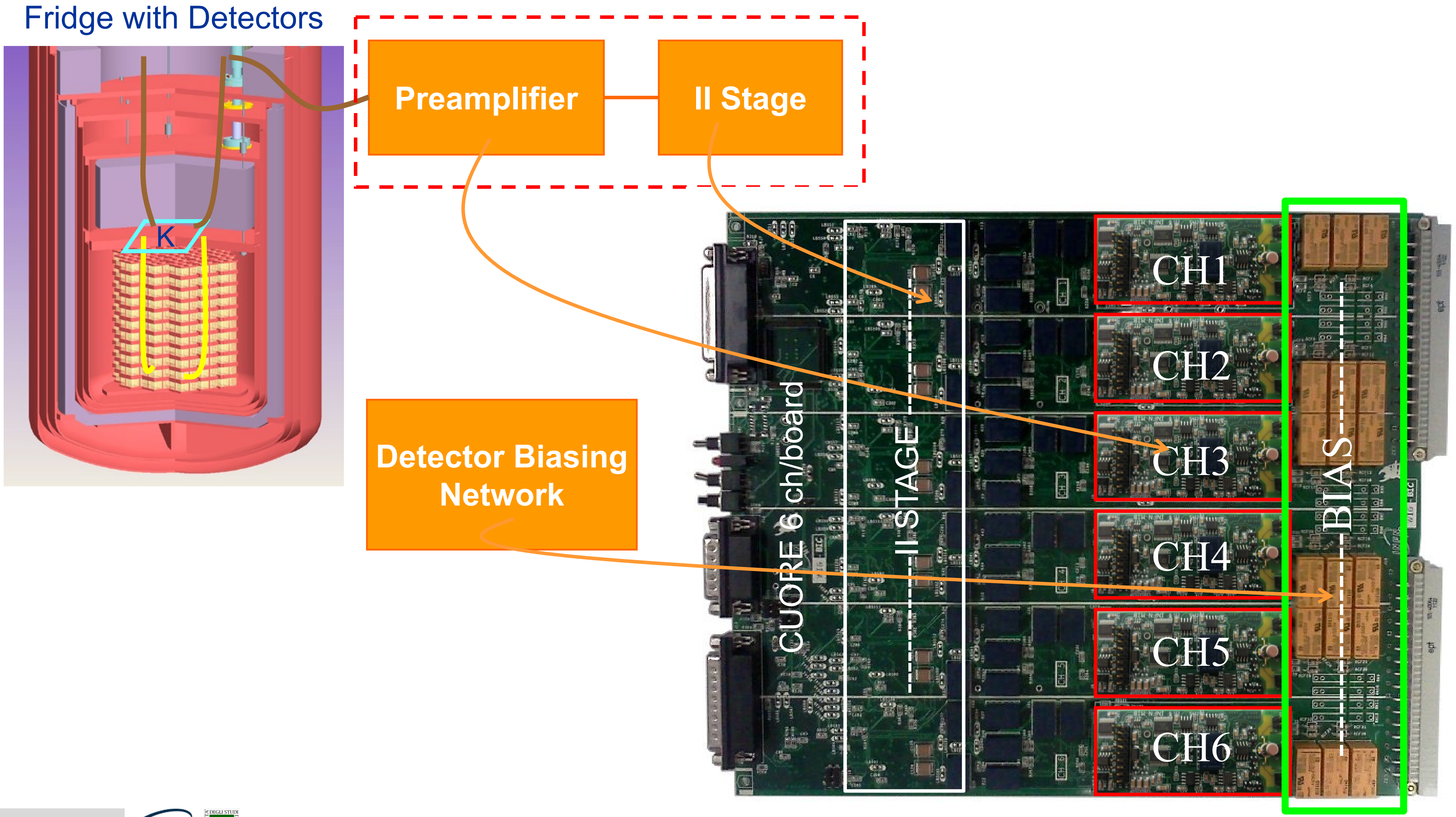

Electronics system 7

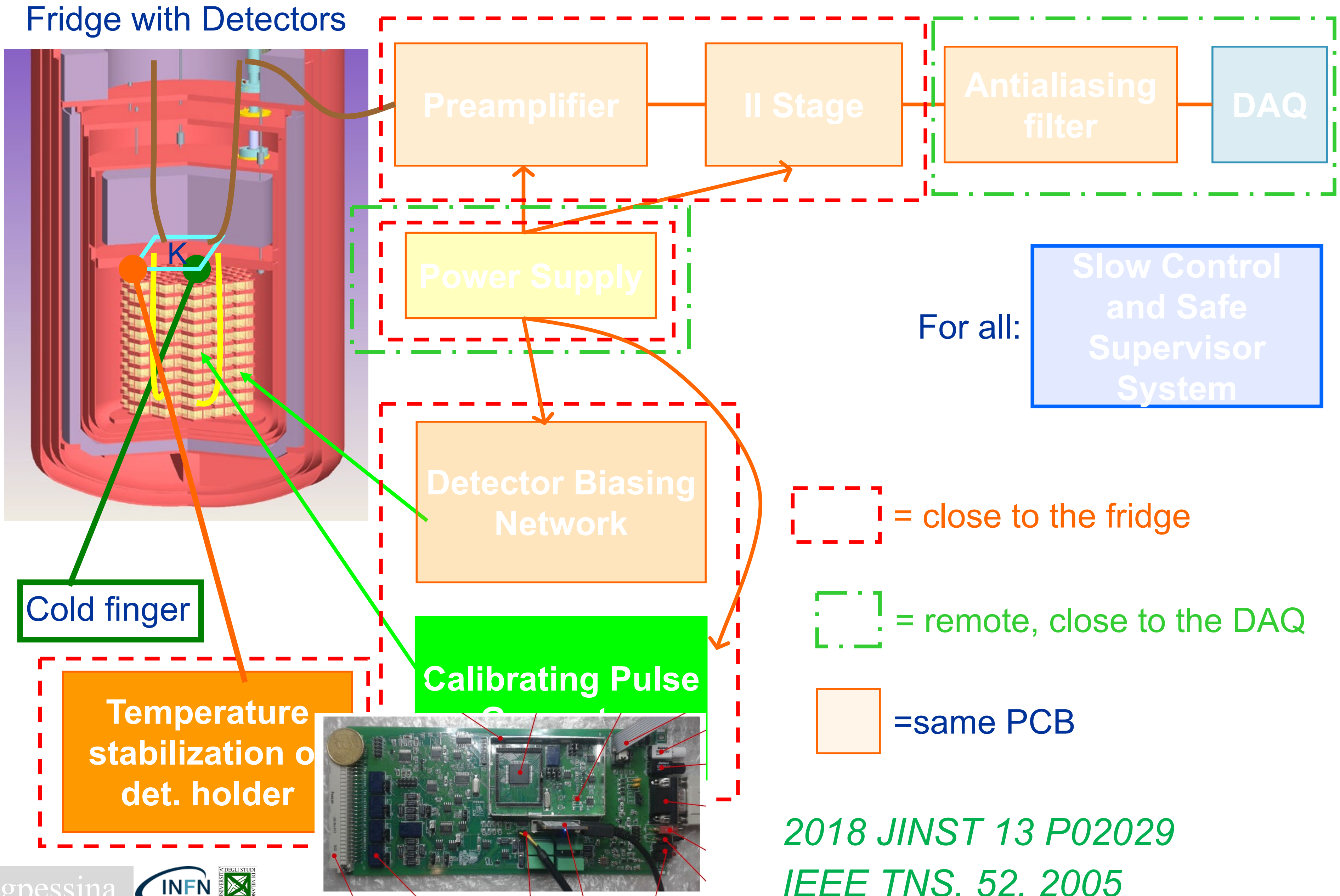

2018 JINST 13 P02029

IEEE TNS, 52, 2005

For detector stabilization a voltage pulse is sent to the crystal heaters. **The pulse** emulates a particle energy and is precise at better than 1 ppm/°C in both amplitude and width. The pulser is also able to generate a DC signal and this is exploited to **stabilize the baseline** temperature with a PID algorithm.

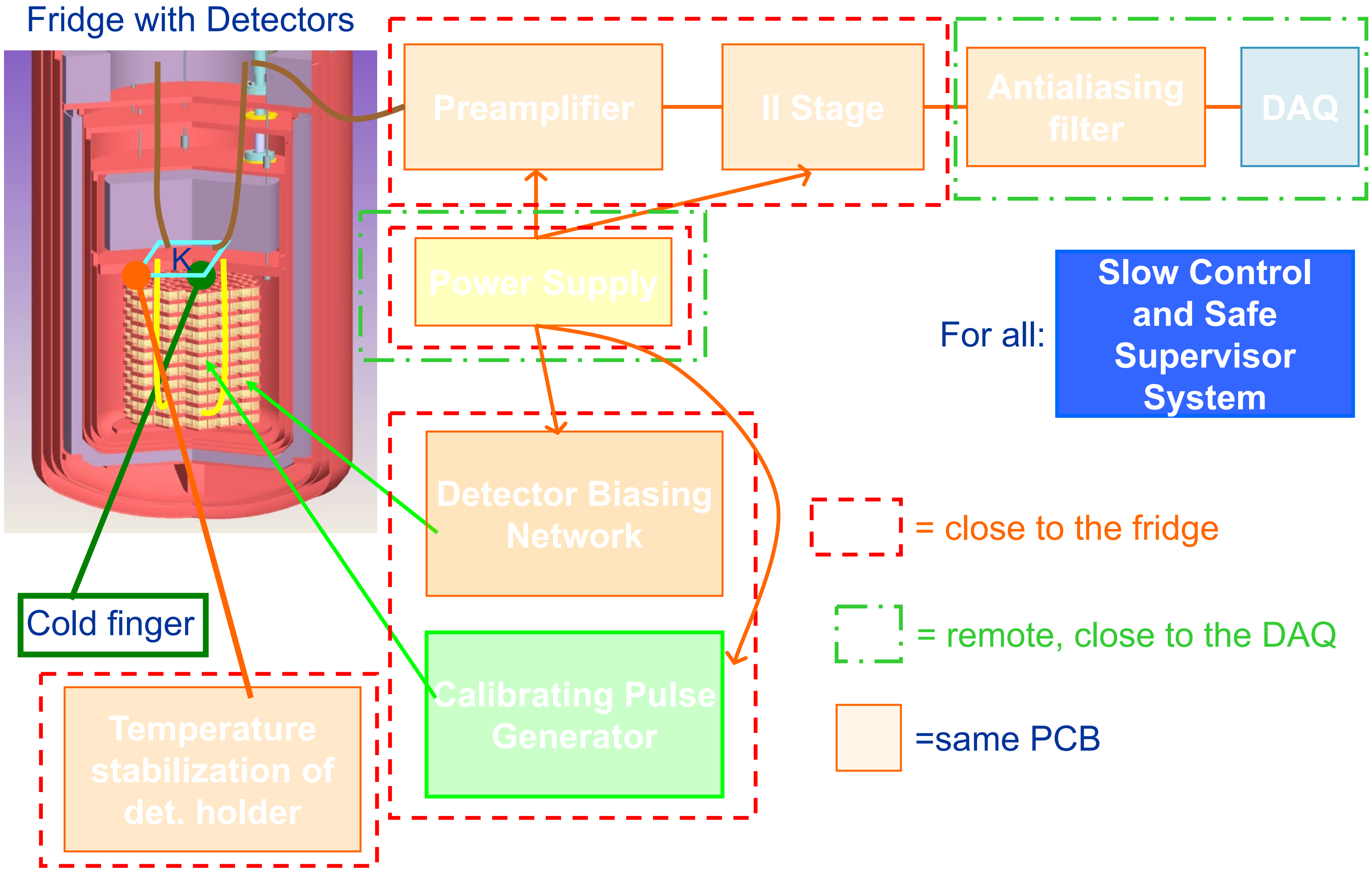

The Electronics system is completely **programmable** in its parameters via fibre optic.

Electronics system 9

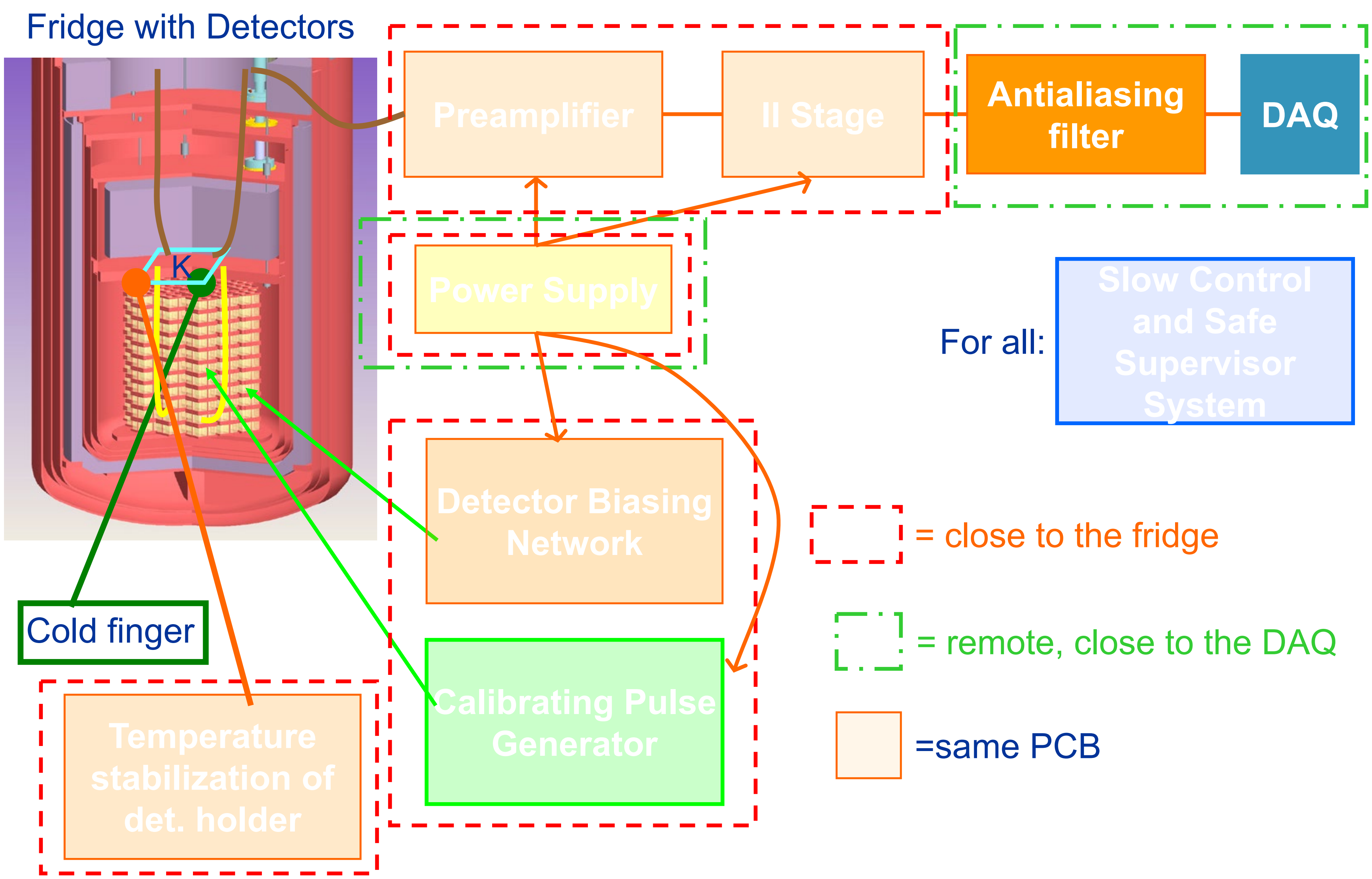

DAQ needs a resolution of at lest 18 bit, and a small input noise.

We have developed a 24 bit DAQ with embedded the antialiasing filter that is programmable in the roll-off frequency.

Electronics system 10

Fridge with Detectors

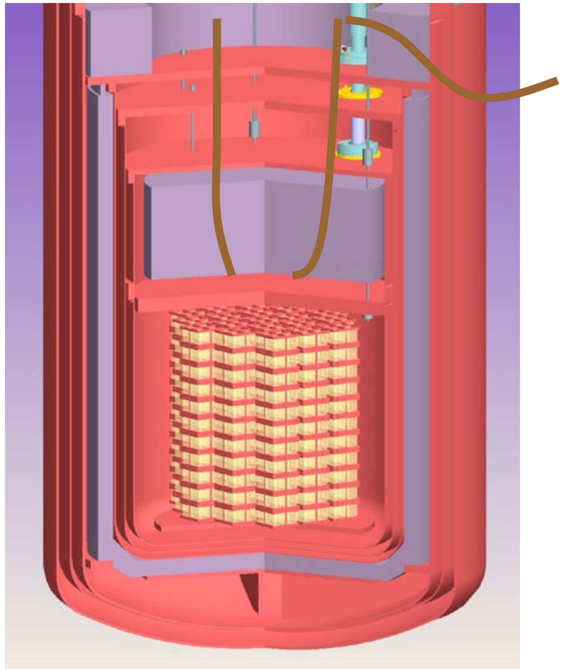

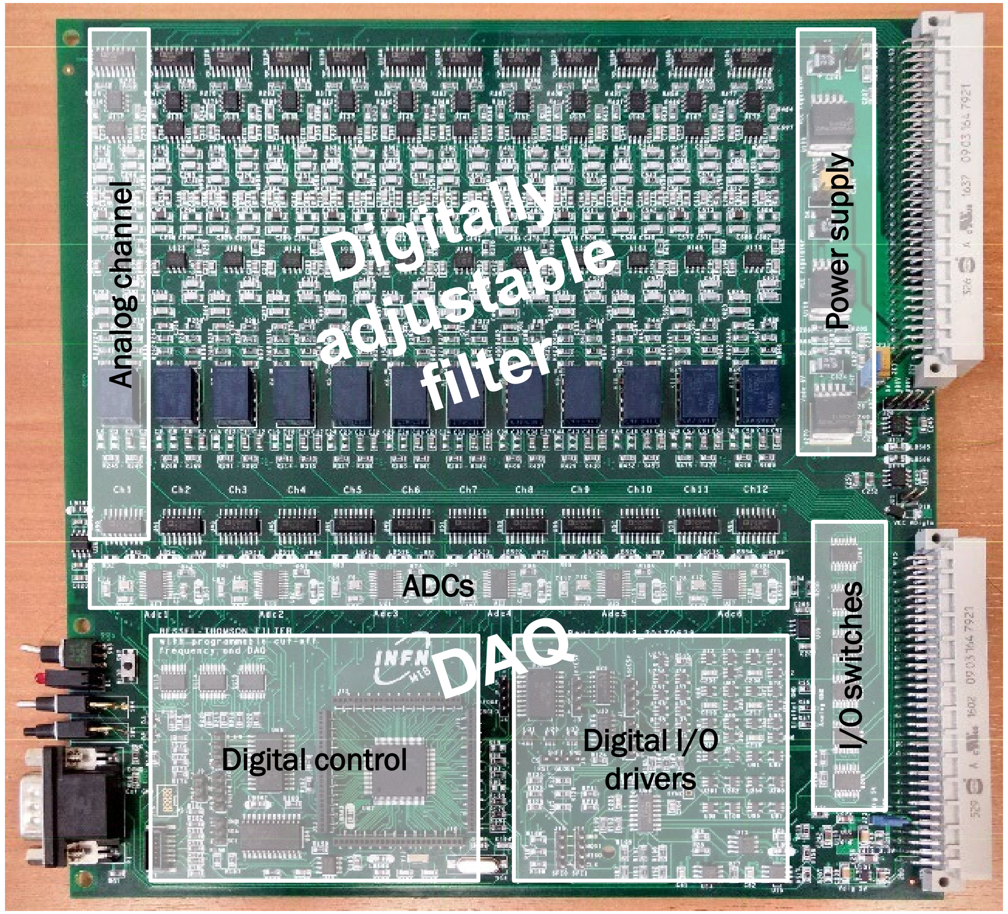

BIBLIOGRAPHY

L. Fleischmann et al, Metallic Magnetic Calorimeters for X-Ray Spectroscopy, IEEE Transactions On Applied Superconductivity, 19, 63, 2009.

S.H. Moseley et al, Thermal detectors as x-ray spectrometers, J. Appl. Phys., 56, 1257, 1984.

P. D. Mauskopf, Transition Edge Sensors and Kinetic Inductance Detectors in Astronomical Instruments, Astronomical Society of the Pacific, 130:082001, 2018, https://doi.org/10.1088/1538-3873/aabaf0.

R. L. Fagaly, Superconducting quantum interference device instruments and applications, Review Of Scientific Instruments 77, 101101, 2006.

R. Bosisio et al, Parasitic effects in superconducting quantum interference device-based radiation comb generators, Journal Of Applied Physics 118, 213904, 2015.

H. Kim et al, Cryogenic particle detection based on magnetic microcalorimeters for rare event searches, Eur. Phys. J. Plus,138:518, 2023.

Y. Zhang, H. Dong, H.J. Krause, G. Zhang, X. Xie, SQUID Readout Electronics and Magnetometric Systems for Practical Applications, Wiley-VCH, 2020.

Bibliography 2

B. A. Mazin, Microwave Kinetic Inductance Detector, Thesis, https://thesis.library.caltech.edu/3910/

K. Chang et al, A simple SQUID system with one operational amplifier as readout electronics, Supercond. Sci. Technol. 27 115004, 2014.

S Henry et al, The 66-channel SQUID readout for CRESST II, JINST 2 P11003, 2007.

D. N. Seitz et al, SuperCDMS Detector Readout Cryogenic Hardware, AIP Conference Proceedings 1185, 282, doi: 10.1063/1.3292334, 2009.

D.S. Akerib et al, Design and performance of a modular low-radioactivity readout system for cryogenic detectors in the CDMS experiment, NIMA 591, 476–489, 2008.

F.Fontanelli et al, The front-end electronics of the LSPE-SWIPE experiment, Proc. of SPIE Vol. 9904, doi: 10.1117/12.2232859.

D.F. He et al, High-Tc dc SQUID readout electronics with low noise and high bandwidth, Physica C, 445–448, 982–985, 2006.

R.D. Penny et al, Wideband Front End for High-Frequency SQUID Electronics, IEEE Transactions On Applied Superconductivity, 7, 1997.

F. Foroughi et al, A micro-SQUID with dispersive readout for magnetic scanning microscopy, Applied Physics Letters 112, 252601, 2018.

Bibliography 3

Appl. Phys. Lett. 92, 023514 2008.

Eur. Phys. J. C (2015) 75:112.

A&A 609, A115 (2018).

APL 107 (2015) 093508.

JINST, 2011,6 P06012.

JINST, 2011,6 P06012.

Eur. Phys. J. C (2015) 75:353.

Cryogenics 60 (2014) 76–79.

IEEE Tran. on Micr. Th. and Tech, 2013, 61 3285.

DOI: 10.1109/BCTM.2011.6082758.

IEEE TR. ON MICR. TH. AND TECH., 2007, 55, 2306

Cryogenics 57 (2013) 129–133.

Journal of Low Temperature Physics 211(5-6), DOI:10.1007/s10909-022-02909-3, 2022.

Bibliography 4

Journal of Low Temperature Physics 211(5-6), DOI:10.1007/s10909-022-02909-3, 2022.

D. Karaca, A 53–117 GHz LNA in 28-nm FDSOI CMOS, IEEE Microwave And Wireless Components Letters, 27, 171, 2017.

M. Varonen et al, Cryogenic Millimeter-Wave CMOS Low-Noise Amplifier, 2018 IEEE/MTT-S International Microwave Symposium, 1503.

D. Kang et al, Cryo-CMOS design-technology co-optimization of low noise amplifier for silicon qubit readout, Microelectronic Engineering, 262, 111837, 2022.

Y. Peng et al, A Cryogenic Broadband Sub-1-dB NF CMOS Low Noise Amplifier for Quantum Applications, IEEE Journal Of Solid-state Circuits, 56, 2040, 2021.

Proc. SPIE 10699, 2018 : doi: 10.1117/12.2312532

J Low Temp Phys (2018) 193:578–584

PH. REV. LET. 120, 132501 (2018)

2018 JINST 13 P02026

Eur. Phys. J. C (2018) 78:388

Eur. Phys. J. C (2018) 78:388

Bibliography 5

NIMA 591 (2008) 476–489.

M. D'Incecco et al, Development of a Very Low-Noise Cryogenic Preamplifier for Large-Area SiPM Devices, IEEE Transactions On Nuclear Science, 65, 1005, 2018.

V. Radeka et al, Cold electronics for "Giant" Liquid Argon Time Projection Chambers, Journal of Physics: Conference Series 308 (2011) 012021 doi:10.1088/1742-6596/308/1/012021.

G. De Geronimo et al, Front-End ASIC for a Silicon Compton Telescope, IEEE Transactions On Nuclear Science, 55, 2323, 2008.

The Large Enriched Germanium Experiment for Neutrinoless Decay, LEGEND-1000 Preconceptual Design Report, LEGEND-1000 Preconceptual Design Report, Date: July 27, 2021, arXiv:2107.11462v1 [physics.ins-det] 23 Jul 2021.

L. Bombelli et all, "CUBE", A Low-noise CMOS Preamplifier as Alternative to JFET Front-end for High-count Rate Spectroscopy, 2011 IEEE Nuclear Science Symposium Conference Record, N40-5